An Improved Methodology for Seismic Capacity Assessment of Reinforced Concrete Buildings using System Identification and Numerical Simulation

システム同定と数値解析を用いた鉄筋コンクリート建物の耐震性評価法の改善

A Doctoral Dissertation

by

Chaitanya Krishna Gadagamma
ガダガンマ　チャイタニャ　クリシュナ

(Roll No. 37-137006)

Under the supervision of

Prof. Kimiro Meguro

DEPARTMENT OF CIVIL ENGINEERING
THE UNIVERSITY OF TOKYO–JAPAN
January, 2017

This thesis is dedicated to my family as a sweet outcome of all the sacrifices and hardships they had to go through for my career

Abstract

There is a huge threat to mankind in the context of increasing risk of earthquakes in many countries in the world, and the consequences are deeper especially in the case of developing countries; because of their social and economic development limitations, the exposure levels are increasing. Also, due to rapid increase in the built environment and lesser frequency of earthquakes, the communities have become complacent with the currently existing poor quality of dwellings. However, with current emphasis on mainstreaming disaster risk reduction, it is now very important to assess and improve the disaster resilience capacity of our communities. The built environment is comprised of many components but dwellings and lifelines are the most important ones to be improved and therefore this research focuses on the damage or condition assessment of buildings. Typological studies suggests that Reinforced Concrete (RC) buildings are amongst the most common and most vulnerable to earthquakes.

In order to assess the vulnerability of buildings there are many parameters to be addressed, however due to limitations on field restrictions and priorities, this research assesses the stiffness of a building by simplifications and reasonable assumptions of other parameters such as strengths, reinforcement detailing, etc. based on experience and RVS (Rapid Visual Screening) of buildings. The three major components of this study which combine to address the vulnerability of buildings are: 1) a numerical tool for accurate modelling of buildings 2) an identification methodology for estimating the material properties 3) a reliable capacity quantification scheme for judging the vulnerability of buildings.

Firstly, the numerical tool for carrying out modelling of RC buildings used in this study is Applied Element Method (AEM). To verify the capability of AEM to carry out inelastic analysis and study the properties of plastic hinges corresponding to different damage states, a validation of rectangular RC columns was required. In the process of validation, certain compression failure issues were identified and solved with a proposal

of new compression material models for the tool.

Secondly, to identify the material properties of the building, a method based on vibrational characteristics of the building was needed. In this stage, the natural frequencies and mode shapes are identified through Operational Modal Analysis (OMA). Further, a two-step identification methodology is developed which includes 2 steps of estimation of stiffness, in which the first step consists of a conventional mode shape and natural frequency based stiffness estimation from an assumed based line. Using the output of this first step and an optimization problem based on minimizing the error between natural frequencies and mode shapes, can overcome the limitations of insufficient modal values to estimate the stiffness accurately.

Thirdly, in this study the capacity of the buildings is assessed based on estimating deformation based damage indices for each member of the structure. The global damage states are further estimated as a weighted sum of these local damage indices, where the weights are considered as inter storey drifts of the structure.

To check the implementation of this methodology, a field study was conducted in Nepal on a selected building, and a series of incremental dynamic loading were applied to the numerical model. Further, a fragility function is developed based on the analyzed building in Nepal with varying non-structural masses. This method of capacity assessment of buildings could be reliable as it uses the actual measured and surveyed parameters from the field to develop a numerical model. This method could be useful in pre-earthquake assessment, for making decisions on strengthening of structures, judging the vulnerability of a geographic region and even for post-earthquake assessment.

Although there are a few improvements required such as improving the estimations of contributing masses, estimating accurate mode shapes, and validation of damage indices for the estimation of capacity of the structure, this methodology is helpful for achieving vulnerability assessment with in the limitation of uncertain masses and inaccurate mode shapes of the structure.

Contents

List of Tables

List of Figures

Acknowledgments

I would like to express my deepest gratitude to my advisor Prof. Kimiro Meguro, who had been a tremendous mentor in making me a researcher. I would like to thank him for motivating me in saving lives of people against disasters, having an insight of learning positives and negatives, teaching me to use innovative research ideas to solve social problems and mainly his advice on research and my career are invaluable to me. I would also like to thank my committee members, Prof. Nakano, Prof. Ozawa, Prof. Nagai and Prof. Muneyoshi Numada for giving me extremely useful suggestions in appropriate completion of my dissertation.

I am grateful to Dr. Hideomi Gokon for supporting me academically and also motivating me at hard times. Also, I would like to thank all my fellow lab members stimulating fruitful discussions and helping me with my experiments and had made me feel being with a family. I would also like to thank all the secretaries and ICUS members who have helped me with various documentations in the university.

I would like to thank my master's supervisor Prof. Ravi Sinha for his support, guidance and suggestions with my research and career. I indebted to Dr. Saurabh Shiradonkar for the technical discussions and sleepless nights of working together in the laboratory in IIT Bomabay.

I would like to thank my friends who have supported me at tough times and I am grateful to Harish, Bhargav, Niveditha, Dr. Yasmin, Dr. Shanthanu and Srividya who have consistently supported me and inscented me to strive towards my goal. A special mention of gratitude to all my friends, faculty members of the university and the hospital staff who have supported my during my accident.

I would like to thank all the staff in the university, Civil Engineering Department, Foreign Student Office, Host Family Members and Japanese language teachers for helping me in my survival in Japan.

A mention of appreciation to the Japanese government and the MEXT scholarship for providing me with an opportunity to study in University of Tokyo and Japan.
Last but not the least; I would like to thank my family members for all the sacrifices they made in letting me take up a career of my choice. A special thanks to Smt. Padmavati, my mathematics teacher, who I would also thank all the school teachers and university faculty members for identifying the potential in me for higher studies.

Date: _____ Chaitanya Krishna Gadagamma
ガダガンマ　チャイタニャ　クリシュナ

Chapter 1

Introduction, Review and Proposed Methodology

1.1 Introduction

Earthquakes are considered amongst the most severe forces of nature and due to the poor construction practices, there have been massive earthquakes in the past which have disturbed many countries at different levels. One of the most efficient ways of understanding the impact on the society or a building is to understand its *risk* first. Estimating this could actually give very useful information for characterizing a building or components depending on its damage/deterioration. Seismic risk is most efficiently explained as:

$$Risk = Hazard \times Vulnerability \times Exposure \tag{1.1}$$

This scientific representation of the earthquakes is definitely in-numerous in various aspects but however, the reliability factor plays a major role in its acceptance as the uncertainties involved in estimating the independent parameters of equation 1.1. Seismic hazard plays a major role but it could neither be controlled nor predicted, and therefore in the prevailing amelioration of science the effect is being estimated based on probabilistic patterns from past earthquakes, estimated strain accumulations from shallow faults, etc. Seismic exposure is a socio-economical parameter which governs the increase or decrease in the population and corresponds to the infrastructure needed for the change. Seismic vulnerability is the capability of infrastructure to resist damage due to a hazard; herein the socio-economic as well as socio-technical factors plays a major role in governing the vul-

nerability of the infrastructure. This research is motivated in the development of a sound methodology for damage assessment of Reinforced Concrete (RC)buildings especially for developing countries in South East Asia and therefore it was affianced to improve the built environment of Nepal, India and other countries in the Indian sub continent. Thence the seismicity and built environment has been discussed in the forthcoming sections of this chapter.

1.2 Background

1.2.1 Seismicity of Indian Subcontinent

Indian subcontinent comprising of countries, India, Nepal, Pakistan, Myanmar is under huge threat due to earthquakes and this causes the countries in the mentioned region, subjected to huge risk especially along the mountain ranges called *Himalayas*. Even this day the Himalaya are rising to a height of 1cm every 100 years due to the thrusting which confirms the activity of plates.

It has already been observed that great earthquake ($M_w > 8.0$) is concentrated in the Himalayan zone. Detailed observation of the zone shows relatively less activity in the last 100 years. Hence a huge amount of stress is being developed along the Main Boundary Thrust. The geography of Himalaya is prominently classified into two parts Northern Himalaya and Southern Himalaya [68]. The northern Himalaya constitutes the Tethiyan Himalaya or the Tibetan Himalaya. The Southern Himalaya is divided into Higher, Lower and Sub-Himalaya. According to the work of [20]; the Southern Himalaya structurally comprises the Main Central Thrust (MCT), Main Boundary Thrust (MBT) and Main Frontal Thrust (MFT). Many workers [68], [69] have carried out research on these faults and observed that Main Boundary Thrust (MBT) which separates Outer Himalaya and Lesser Himalaya is reasonably more seismically active. The rupture of major earthquakes Shillong(1897), Kangra (1905), Bihar-Nepal (1934) and Arunachal Pradesh (1950) are believed to have ruptured along the MBT. The recent earthquake in the Himalayan belt is the 2015 Gorkha earthquake which occurred on 25 April 2015 had occurred in the valleys of Nepal. This earthquake was a moderate to big earthquake with a magnitude Mw= 7.8, which had damaged a number of non engineered and masonry buildings; which also caused a death toll of about 9000 people. This earthquake is of particular importance as

Nepal was chosen as the field study for carrying out building damage assessment which is discussed in later chapters.

The actual observation of stressed zone in Himalayan region is a challenge for the geologists to study from the available data and make use of seismographs and ground acceleration measuring devices. An anticipated damage can be immeasurable aid to the disaster management organizations to plan emergency forces after the quake, to provide with the protocols for relief operations, to measure the volume of relief supplies to the affected places and to plan the routes and rescue teams to proceed. However, the prior prediction is not possible and hence it is intended to prepare with mitigation measures by understanding the built environment and it vulnerability to potential earthquakes.

Table 1.1: Major earthquakes on Indian sub-continent

Date	Name	Deaths*	Magnitude	Phase
16 June 1819	Gujarat	2,000	8	Phase II
12 June 1897	Assam	1,500	8.3	
04-Apr-1905	Kangra	19,000	7.5	
15-Jan-1934	Bihar	10,700	8.1	Before strong motion data was recorded
15-Aug-1950	Assam - Tibet	1,526	8.6	
10-Dec-1967	Koyna	177	6.3	
20-Aug-1988	Nepal–Indian border	1,000	6.8	Phase I
19-Oct-1991	Northern India	2,000	7	
29-Sep-1993	Latur–Killari	9,748	6.2	
21-May-1997	Jabalpur	38	5.8	
26-Jan-2001	Gujarat	20,085	7.6	After strong motion data was recorded
08-Oct-2005	Pakistan	86,000	7.6	
18-Sep-2011	Sikkim	75*	6.9	
25-Apr-2016	Nepal G.orkha	8,900+	7.8	

1.2.2 Built Environment in Indian Sub-Continent Countries

According to the building typology in Indian context [2], which is similar with other developing countries in the region including Nepal, the dwellings in the built environ-

ment are extensively classified into 54 types of structures, and is broadly classified into 5 types, among them it is intended to focus on various types of *structural concrete* types of constructions. There are 12 different types of structural concrete configurations in the typology report and is enlisted in table 1.2; here from the general understanding A-G of the sub typologies are considered to be the most common practice in India.

There are various non-engineering practices in the built environment as summarized in

Table 1.2: Different types of structural concrete systems in Indian subcontinent[2]

Sub Typology	**Loading System**
Designed for gravity loads only (predating seismic codes i.e. no seismic features) (A)	Moment Resisting Frame (MF)
Designed with seismic features (various ages) (B)	
Frame with unreinforced masonry infill walls (C)	
Flat slab structure (D)	
Precast frame structure (E)	
Frame with concrete shear walls (dual system) (F)	
Open ground storey structure (G)	
Walls cast in-situ (H)	Shear Wall Structure (SW)
Precast wall panel structure (I)	
With load bearing masonry (J)	Mixed Structure (MS)
With composite steel (K)	
With timber, bamboo or others (L)	

[6], and has also mentioned the intricate structural parameters. In a RC building; the seismic configuration, lateral stiffness, lateral strength and overall ductility properties in RC buildings are the major governing parameters in a structure, and under these interests, it has been understood that the buildings are not seismically sound enough due to various technical reasons. Firstly, the existing limitations in the seismic code doesn't allow buildings to be constructed as earthquake proof since seismic code provisions are only meant to design the structure for a reduced response to provide life safety, mainly due to the effect of cost of construction upon earthquake frequency, (i.e the investment on stronger houses is not worthwhile where the number of earthquakes are lesser and infrequent); in addition, the seismic hazard threat is also not uniform across the coun-

try whereby not enabling a strict guideline to be followed for constructions everywhere. Secondly, non-engineered design and construction are being practiced everywhere causing various problems. Thirdly, in this country the ductile detailing needed for seismic safety is cumbersome, due to the common practice to employ unskilled labor for constructions. Finally, architectural demand is another major problem which causes highly vulnerable construction practices such as geometric irregularities, vertical irregularities etc.

1.3 Statement of the Problem

The fundamental objective of this research is to develop a well defined simple, practical, comprehensive and flexible damage assessment procedure to estimate damage of individual existing/damaged Reinforced Concrete (RC) Buildings against earthquakes using Applied Element Method based numerical approach and operational modal analysis.
It is intended to have the following properties

- Simplified implementation process
- The practical ability to be applicable on any RC building
- Provides with detailed information of damage states for each building
- Be able to be upgraded or extended to 3D or more instrumental information can be complemented to the procedure

1.4 Literature Review

There are many existing methodologies for carrying out damage assessment and they can be categorized with respect to the flow as shown in the figure 1.2 and the the desired methodology is explained in the sections of this chapter.

1.4.1 Selection of Buildings

In damage assessment methodologies, there are many ways of selecting buildings for the damage assessment or condition assessment to represent vulnerability of a particular built environment, or to assess the damage to critical facilities, or to retrofit key structures

which have disaster prominence. Typically, the assessment of condition or damage of buildings for preparedness is focused on a group of buildings as it is easier to consider, computationally cheaper, easier to approximate and rather than carrying out assessment on a large number of buildings which is very inconvenient considering various social, economical and technical conditions. Therefore, the vulnerability assessment methods mentioned in the literature [45],[22],[25] and [32] have only been able to discuss the condition of a limited number of buildings only. There are also other interesting ways of building selection to carryout assessment for a large number of building such as through use of satellite information or remote sensing data to collect the building damage information and prioritize them as in literature [46] and [37], where an automatic methodology for the damage assessment of building after an earthquake has been explained. With further advancements of technology and science the quality of satellite information shall become more useful in the collection of more quantitative information of buildings. However, in order to be able to carry out assessment for every building, it is understood that the methodology has to be computationally cheaper and should be as rapid as it could be, meeting this requirement, the Rapid Visual Screening (RVS) method [7],[51], [4] has provided superiority over other methods because of its time efficiency factor in screening and analyzing as well as its wide spread usability even by people of limited engineering expertise. However, the accuracy and reliability of these methods are questionable.

In continuation with the last statement, the major objective of this study to be able to do a building wise assessment which hugely depends on the available and convenient methodologies for the assessment. Existing suitable methodologies are limited but reviewed bridges are less complicated as compared to bridges are shown in [65]. A methodology in the interests of this study is described by [**?**],[59] and [58]; which provide damage assessment methodology using an innovative non-contact type vibration measuring system called the U-Doppler for detecting the vibration of bridge viaducts and during damage assessment analysis with the aid of Applied Element Method (AEM). However, such a methodology on building is a complicated approach.

Therefore, from the literature it is understood that the the damage assessment of buildings shall be done one by one, and the selection of number of buildings largely depends on the methodology being used which has to be comprehensive but reliable, practical for engineers to implement in the field and compute on workstation in a reasonable CPU

time.

1.4.2 Identification of Material Properties

In order to assess anything from a building's condition, damage, vulnerability, residual capacity, to post-earthquake safety assessment, the identification of structural properties plays a very important role. The reliability, numerical accuracy, and practical applicability, depends on the extents of prediction or estimation of the material and geometric properties of a structure. The later one can be assessed by knowing the blueprint or CAD information or physical measurements of the structure if available but achieving material properties involves both aleatory and epistemic uncertainties. The concrete which is supposed to be a complicated property is theoretically idealized with many assumptions such as homogeneous and isotropic nature, however a real site condition can be contradictory. Also, the environmental conditions and aging makes it a time dependent parameter, which makes the predicting of material property difficult. Some structures show damage only in a few locations which could be due to the deterioration caused as result of poor construction practice, or intentional human error on the buildings. In the mentioned conditions, it is almost an unattainable feat to estimate the material properties of the structure by any expert based on engineering judgment. Thence, the current challenge is to have a reliable solution to identify the material properties to be used in numerical simulations. In existing studies, an expert opinion based identification have been done: [3],[45] have done assessments using various numerical approaches but the methodology used in the identification includes a few sets of assumptions, while in other literature [53], [48], [30] a parametric or random parameters study was implemented to compensate for the uncertainties-this is implemented by either randomizing the inputs or changing the assumed inputs by deviating the parameters. Some studies such as [47]consider the initial strength of the building either reported by the builder or the landlord to the local authority as the material properties for numerical simulations. A more recent trend is to consider some interesting remote sensing technologies such as IR thermal images and Xray to understand the internal structure of concrete and steel in RC buildings. This research recognizes vibration based damage assessment or material identification as a more reliable method and the previous research in bridges [65],[58] and the field of Structural Health Monitoring [63],[38],[1] have shown good reliability through this approach. However, the

practical applicability and completeness of these methods have not been well demonstrated adequately. Most of the methods rely strongly on sound modal parameters and the completeness is governed with both number of identifiable parameters and quality of the parameters.

1.4.3 Numerical Analysis

The choice of numerical assessment plays a major role in governing the ability, efficiency and reliability of the methods.The choice of analysis is regulated based on various factors such as desired accuracy, feasibility of computational time, available numerical tool, and the ability of the expert to carry out and understand the analysis. The quickest among the analysis is RVS [4] which involves no/least computational effort, where only a simple scoring correlating to a damage is used which would have been preliminarily evaluated based on past earthquakes or other numerical simulations. Second to this, are the analytical methods in assessing the vulnerability of the structures. [16], [32] However, these are considered very primitive as they use simple linear models for the assessment and the calculations are usually hand calculations. Among all the non-linear methods, the most widely accepted numerical simulations is non-linear static analysis as already cited in the literature [48],[19],[5],[30] and [35]. In these methods, the material properties are assumed to be non-linear at elements and usually the Finite Element Method (FEM) based discretization is considered and the dynamic ground motion is converted into equivalent static load or displacement and is applied on to the numerical model of the structure as target displacement to obtain the corresponding capacity of the structure. Many methodologies such as HAZUS [23] have considered this method more reliable subjected to the conditions of the limitations, availability of tools and computational time. However, there are also many researchers [50],[27],[28] and [**?**] who have considered non linear dynamic analysis to carry out assessment of structures. A comprehensive chronological review of the evolution of different methods are shown in [13]. However, the most promising is complete collapse assessment of structure which is considered to have more reliable information of damages to buildings subjected to lateral loading. The Discrete Element Methods such RBSM, AEM, EDEM have demonstrated these advantages, and among them AEM has been proven to be the most reliable one with high accuracy in non linear phase and reliable estimate in the collapse phase. [21] has used this analysis

to carry out collapse analysis on buildings in Nepal to develop fragility functions.

1.4.4 Capacity Assessment

The seismic capacity assessment is that component of a methodology which quantifies the damage or condition of the structure based on certain structural outcome parameters obtained from the numerical methods. This component is useful in various applications, functioning as a decision making index for disaster management agencies, development of damage probability matrix for vulnerability assessment, safety assessment index in the case of post earthquake damage assessment, and most importantly will quantify the relative damage/inadequacies of each members for making a call on retrofitting of buildings. Analogous to these applications, the primary intention would be to develop Local Damage Indices (LDI) and Global Damage Indices (GDI). In the literature this has been well established by many researchers [43], [29], [53], [40]. Here, the research of [52] proposes a damage index formulation based on the validation of intermediate damage states, LDI is developed based on measurable engineering parameters [41] and GDI based on drift ratios [23] and residual capacity [40] is under consideration. The current methodologies, however, have conservative modeling techniques in spite of using different numerical tools that do not have extensive modeling abilities like collapse. The approximations in material identification using Non-Destructive Tests (NDT), Rapid Visual Screening (RVS), Remote sensing, etc, have been very uncertain due to various problems. In case doing numerical assessment of building, usually it is intended to carry out such an assessment on a number of buildings to cater for the existence of variations from building to building, where computational expense prevails and is a major problem. The current finite element methods do not administer reliability in modeling already damaged components of the structure or, in other words, numerical inadequacy prevails to model already damaged buildings. In the seismic capacity estimation of buildings, the moderate damage states of members of the structure are inaccurate and are not sufficiently correlated to the real damage states of the structure due to inadequate validation with real damages.

1.5 Proposed Methodology

The comprehensive map of the proposed methodology is shown in the figure 1.3 and herein, a building selected in principal is expected to be a reinforced concrete (RC) building. The selection of the building is subjected to the choice of the administrative or decision making body to prioritize certain buildings and the approach used for a field study will be discussed in the later chapters. Each stage of the overall methodology shall be explained as follows:

Building Assessment As supposition a building is always vibrating due to various sources of loading, and corresponding response of the structure is measured by setting up the micro-tremor measuring devices and conducting the ambient vibration tests. In addition to this, the building condition is collected in the format of visual assessment forms developed by NDMA, India, for typological classification. The assessment forms also mandates to procure the geometric information of the structure. In the possibility of available instruments, further information such as thermal images of the structure and ferro-scanning of RC members could be complemented for better numerical simulations.

Operational Modal Analysis In the previous, measurements at different levels and locations are combined together based on the reference locations. Further, upon requirement the data is also corrected or smoothed and the natural frequencies and mode shapes are obtained mainly using two methods as recommended in this study:

- Frequency Domain Decomposition
- Stochastic Subspace Identification

Since, these methods follow the premise of using only output response for identification, therefore the mode shapes obtained are only operational modes and special techniques or considerations in the identification algorithms would be needed in the further steps for the identification of material properties of the structure.

Generate Baseline In the first stage, the geometric properties or the dimensions of the structure are collected. However, most of the buildings constructed in the target countries of this research are non engineered and do not have construction drawings,

or are very old, and therefore the drawings are likely to have been misplaced since a long ago. In such cases, an engineer's expertise in considering the geometric configurations of the structure is expected. The baseline state of the structure is designed using the existing configuration and required seismic capacity. Here, the seismic capacity is based on the expected seismic hazard levels or the seismic code expectations for that region, if available or the capacity based on deterministic/probabilistic seismic loads on the structure.

2 Step Identification The next step is to identify the member properties or damages of the structure and in this research a two step identification is described, to estimate the stiffness deviation of each member from the designed baseline of the structure. Step 1 uses manipulations on equations of motion to estimate the deviation from the baseline and step 2 further minimizes the error between measured and estimated modal parameters.

Material Properties Further, the material properties are distributed into the AEM model for each element by considering appropriate concrete and steel spring properties.

AEM Modeling In this step, incremental dynamic loading is applied to the numerical model until collapse of the structure.

Seismic Capacity Estimation The seismic capacity of the modelled structure is estimated by calculating the local damage indices and then combined to form the global damage indices which quantitatively represents the seismic capacity of the structure.

This complete methodology could be used in the both pre-earthquake condition assessment and post earthquake damage assessment. The following are the major outcomes of this study:

1. A simple, comprehensive and practical damage assessment procedure
2. A robust procedure for estimating the material properties of a structure
3. Improved Applied Element Method (AEM) for better capacity assessment

- Compression size effect
- Effects of confinement

4. Vulnerability assessment of select RC buildings in Nepal

1.5.1 Tools in the Research

In order to achieve the mentioned goals, verify and test the applicability of the proposed methodology, the various tools used in this research can be enumerated as:

- Miniature Experiments
    1. Laser Displacement Sensors (LDS), Accelerometers
    2. U-Doppler: Non-Contact Vibration Measurement System Frames
    3. Simple miniature models for verifying the sensors and for validating the methodology
- Numerical Analysis
    1. Applied Element Method: Modifications to accommodate different types of compression models
    2. Operational Modal Analysis: Frequency Domain Decomposition (FDD) and Stochastic Subspace Identification (SSI)
    3. Identification Procedures: Matlab and Fortran
- Field Study – Nepal RC Buildings
    1. Microtremors measuring devices to measure ambient response of buildings

1.6 Organization of the Dissertation

This dissertation is divided into This dissertation is divided into 7 chapters

Chapter 1: Introduction, Review and Proposed Methodology This chapter presents the purpose of this research based on the motivation and background of damage assessment of buildings for potential earthquakes in future. A thorough literature

review is substantiated for understanding the existing methods and its corresponding limitations. Furthermore, the problems in existing current methods and the need for an improved method to assess damage and seismic vulnerability are described, emphasising its corresponding applications.

Chapter 2: Numerical Simulation Tool used in the Study: AEM This chapter introduces a numerical tool called Applied Element Method (AEM) used to assess the capacity of a building. However, certain limitations are identified in compression effects in the modelling of concrete in AEM, which are then addressed by changing the compression modelling of concrete. After implementing these changes, the tool is validated for different cases, and the importance of this tool model in various aspects to the behaviour of concrete is discussed.

Chapter 3: Identification Methodology, Derivation and Evaluation This chapter develops a damage identification and the optimisation algorithm to estimate the material stiffness of a structure. Estimation of stiffness is done in two stages, first stage is the methodology, which is based on simple damage localization, and the second stage is optimisation problem to minimize the observed and estimated values obtained from the outcomes of the former step. Furthermore, the importance and various aspects of this methodology are discussed in this chapter and an iterative mass-update method to identify the mass of the system in the availability of scaled mode shapes is introduced. A theoretical implementation is also demonstrated based on the corresponding limitations and future scope of this method. Additionally, this chapter describes a simple experimental evaluation which was conducted by manufacturing steel frames with changing stiffness/damage states of its members. In these frames, since it is intended to study the possibility of modal analysis and material identification, the operational-modal analysis was performed to estimate natural frequencies and mode shapes, and then a modified identification procedure was applied to identify the stiffness of the members. The practical problems and issues of this method was discussed and corresponding alternatives and improvements are suggested

Chapter 4: Field Study and Identification of Buildings This chapter describes a field study which was conducted in Nepal to verify the applicability of the developed

method for obtaining the other parameters for numerical analysis, and also to understand the practical problems involved in obtaining the data and numerical modelling. This was achieved by measuring the dynamic properties of the buildings in addition to the qualitative assessment results obtained based on RVS. An Operational Modal Analysis (OMA) was also performed to estimate the natural frequencies and mode shapes of the system. Implementation of the two-step methodology developed in Chapter 3 is explained while emphasising certain modifications in application of the method as the field collected data had certain limitations for direct application of the method.

Chapter 5: Seismic Capacity Estimation of Buildings Continuing from the previous chapter, this chapter implements a damage index formulation from the estimates of AEM based simulations consisting of AEM-based numerical simulations based on the identification of storey stiffness of the real buildings in Nepal. Since, this is the first time to use such a formulation of AEM, it is validated with an experimental frame from literature. The seismic capacity of the structure is then discussed with an emphasis on using damage indices estimated from the numerical simulations by estimating the global damage indices.

Chapter 6: Discussions and Conclusions This chapter presents the conclusions of the study and how the proposed method could be useful in discussing the vulnerability of buildings for potential earthquakes. Furthermore, issues addressed in the study are examined, and the corresponding future scope of the work and its applicability are discussed. In addition, this chapter also consists of a way to estimate the scaled mode shapes by combining operational modal analysis and experimental modal analysis using a shaker.

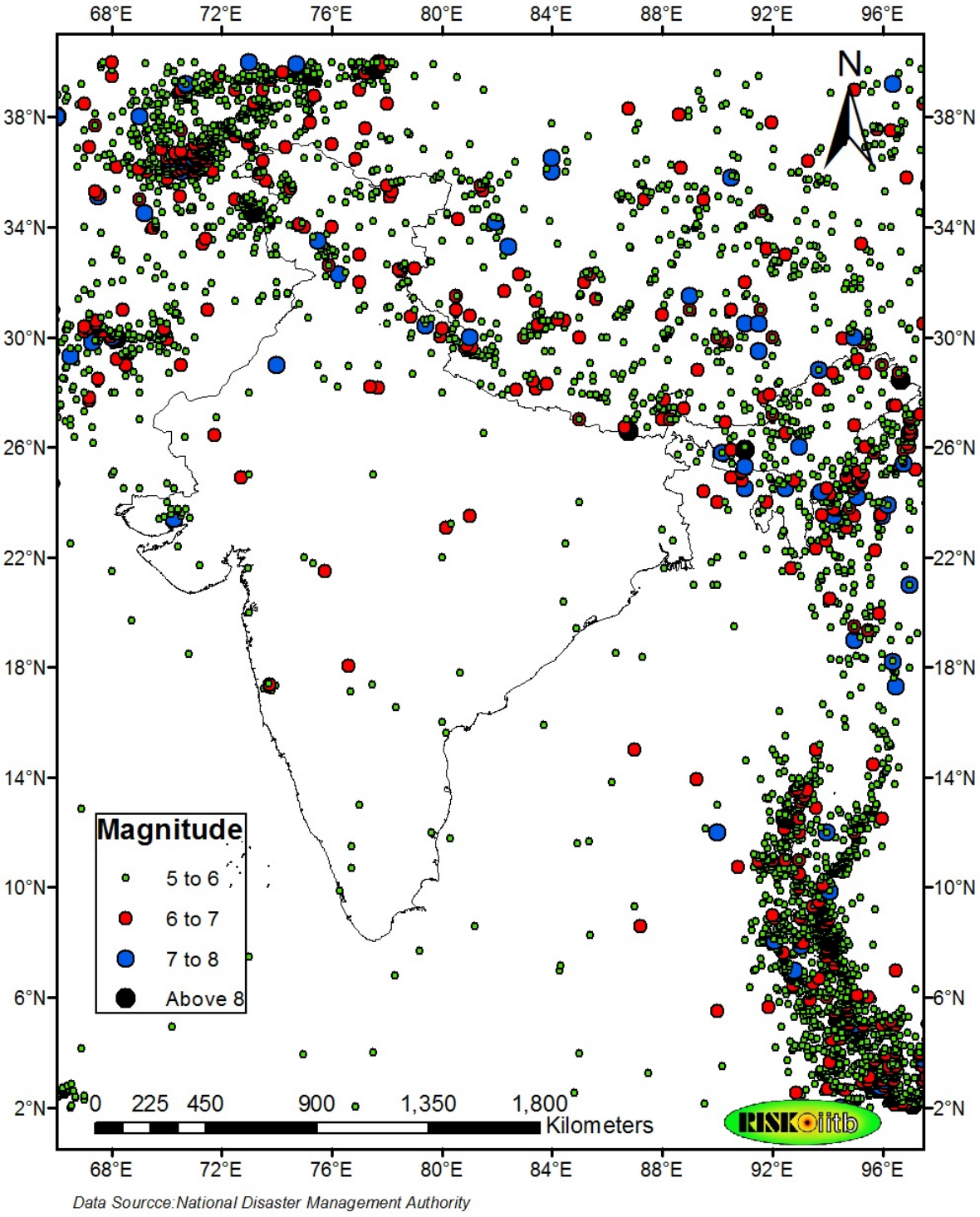

Figure 1.1: Past earthquakes in the Indian subcontinent, *data source:NDMA, India*

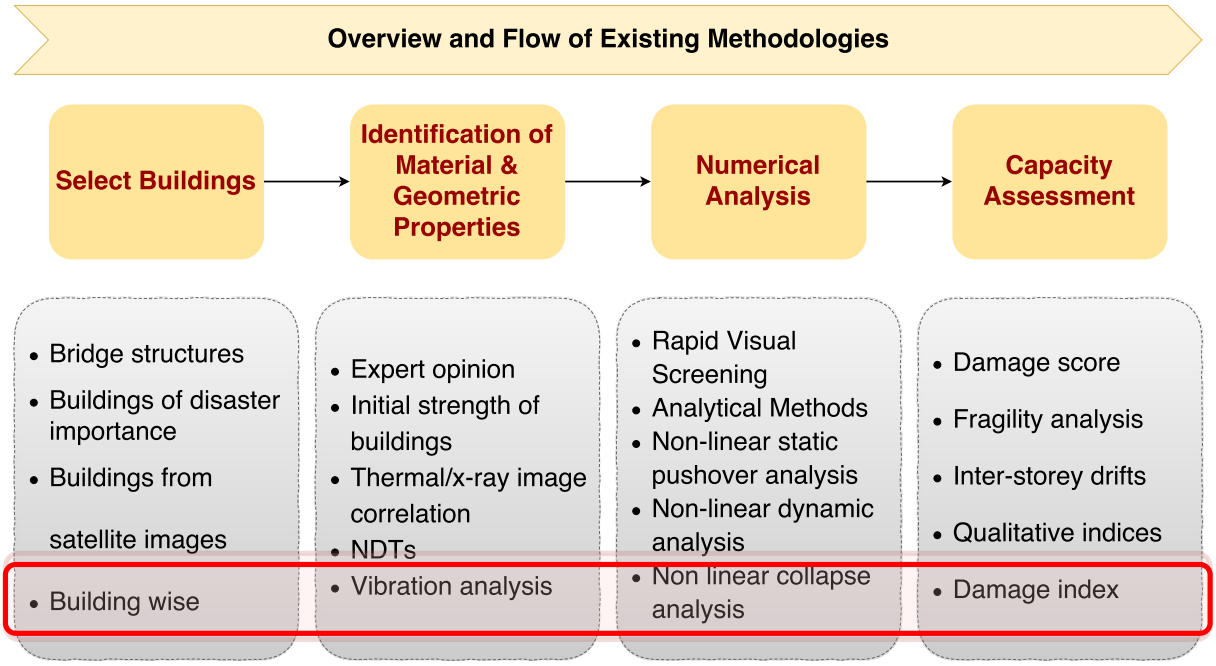

Figure 1.2: Classification and flow of different methodologies in the literature

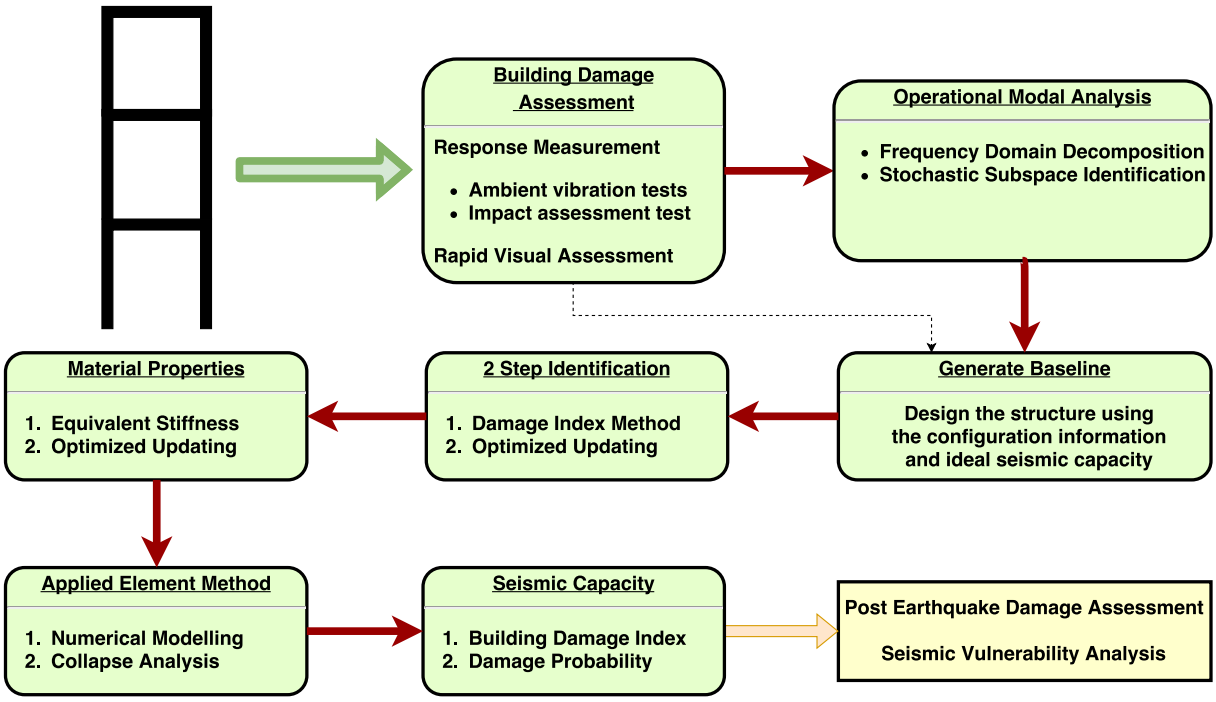

Figure 1.3: The overall flow of the proposed methodology for damage assessment

Chapter 2

Numerical Simulation Tool used in the Study: AEM

2.1 Introduction

In Chapter 1, it was mentioned that to carry out a damage/vulnerability assessment it is necessary to have a sound numerical tool, and therefore this chapter introduces a non-linear structural analysis tool called the Applied Element Method (AEM), which is based on a discrete arrangement of elements and displacements. The tool's ability to assess all ranges of damage states from continuum to discrete non-linear of an RC structure is discussed with a validation study to verify the capability of AEM to carry out inelastic analysis specific to this research and study the various damage states that could be estimated from the simulations involving earthquake loading, which causes severe deformations and stress recursions. In this process of validation, two components are considered, first, a structure subjected to static cyclic load and second, when a structure is subjected to dynamic earthquake loading. For the former case, an experimental database named Pacific Earthquake Engineering Research (PEER) for structural performance is used, which is a compilation of various experiments conducted on rectangular reinforced columns against monotonic cyclic loading. A column is selected for detailed analysis using AEM and two shortcomings, or in other words, necessary requirements in compression modelling, are identified and the corresponding solution by modification in the material models are implemented on AEM and consequently it is observed that the simulation results are improved and are closely validated by the experimental results. In the dynamic

earthquake ground motion case, a two bay two storey frame subjected to earthquake loading is selected from the literature and the corresponding partial validation is described here. The complete validation including its damage states is described in Chapter 5 with estimation of seismic capacities.

2.2 Applied Element Method

As already mentioned, the numerical analysis used in this study is the Applied Element Method (AEM), which acts as a powerful tool for practising engineers and researchers to model continuum, non-linearity and collapse. In this work, a structural member is modelled with a finite number of discrete square elements. Each element is connected to its neighbouring elements with several springs to a prescribed discretization. Each spring acts as an axial member having components in normal and tangential directions. Normal springs model the compression and tension properties of the material and tangential springs model the shear properties of the material. The presence of reinforcement bars is modelled with additional springs with the properties of steel. The compression springs are modelled with the Maekawa material model [34]. The tension and shear are modelled with a simple linear envelope. The failure is observed with cracks, which are dependent on stress block properties. If the principal stress on a representative block of a spring exceeds the rupture strength of the material, the corresponding spring is considered to have failed. In the stepwise numerical simulation, the unbalanced forces due to material and geometric non-linearity are redistributed at the consequent step. In addition to that, the failed spring forces and residual shear forces are redistributed to the load vector. A detailed development procedure and further information on AEM is provided in a thesis submitted to the University of Tokyo [54].

2.2.1 Advantages of Using AEM

- AEM uses simple material models catering for tension, compression and shear independently, but the outcomes at the macroscopic level are very good in both continuum and non-linearity in the separation phase.

- The modelling is done with an objective of providing deformations to rigid elements

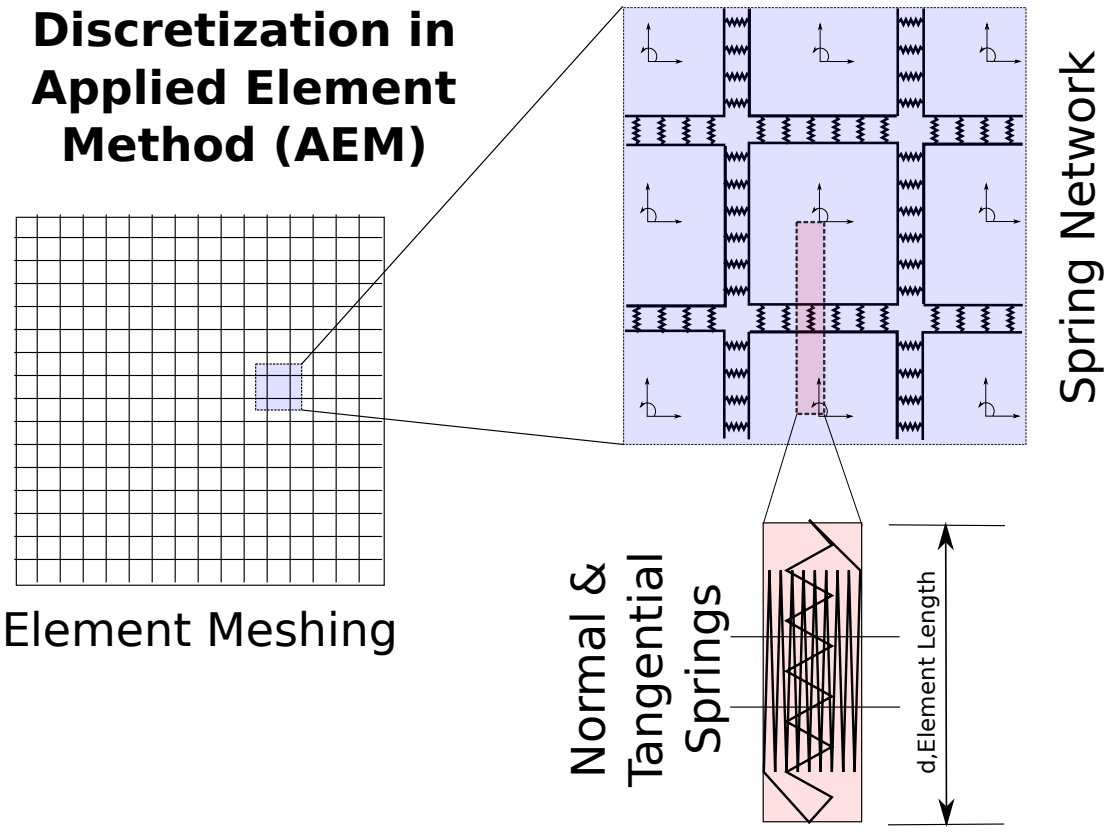

Figure 2.1: Discretization of a structure in AEM

after cracking, and therefore after a particular displacement the structure can go into collapse with explicit computation, thereby exhibiting complete failure with reasonable accuracy.

- Because cracks can be visualized as a separation between elements, qualitative damage assessment is made easier.
- AEM can be simulated in the phase of opened cracks unlike FEM, and therefore if there is any existing damage in the structure, it could be clearly modelled in it.
- In-fill masonry walls could be numerically modelled with certain modified material models in AEM to account for mortar and brick springs independently.

2.3 Issues and Modifications

Using AEM, several numerical simulations were performed on various types of columns subjected to a lateral cyclic load from the PEER experimental database, especially in

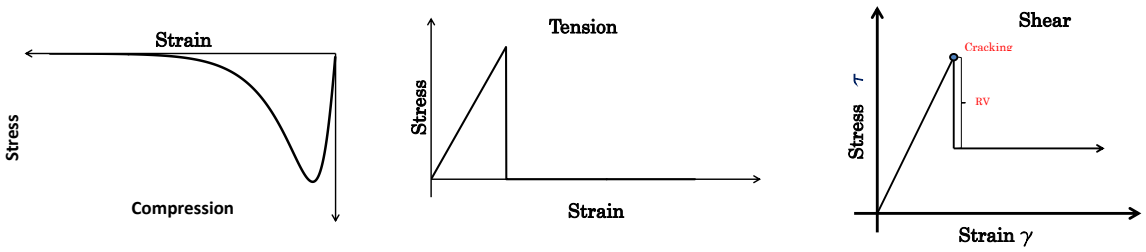

(a) Compression Model (b) Tension Model (c) Shear Model

Figure 2.2: Existing Material Models being used in Applied Element Method (AEM)

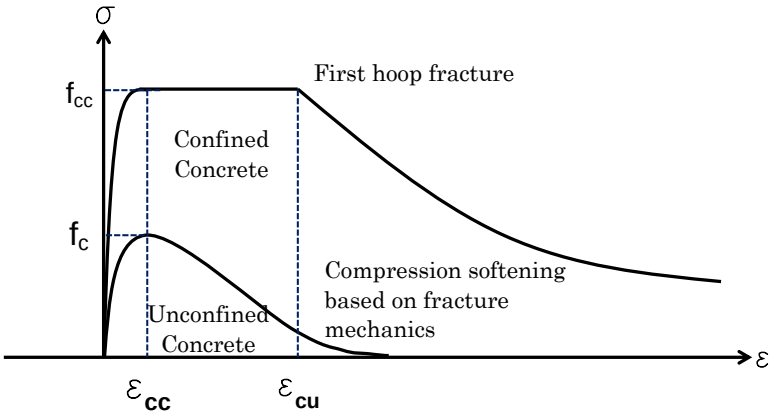

Figure 2.3: Mander'Confined Model with softening branch

the cases which had pre-applied axial loads, which were of special interest as this study is meant for RC buildings, where the lower storey columns usually receive higher axial loads. The necessity of a further investigation into the results for accuracy was desired as severe compressive failure behaviour was observed after the springs reached post-peak; this was also briefly mentioned in [54] during the initial stages of development of AEM. Therefore, this led to the examination of material models being used in the existing AEM while trying to validate the cyclic load cases. The uniaxial compression material model being used in AEM is based on Maekawa's Elasto-Plastic Fracture (EPF) model [34], which considers the single post-peak behaviour of concrete in compression. Observing this, it is considered that the possibility of size effects during post-peak softening of concrete under uniaxial compression and also in the presence of high axial loads, the compression

behaviour is observed to be very brittle, where an increase in strength is needed due to the lateral confinement in columns. Therefore, this problem is divided mainly into two parts, the compression size effects and confinement effects of concrete.

2.3.1 Compression Size Effects in Concrete

Modelling post-peak behaviour of concrete under uniaxial compression is a challenge in numerical tools intended for high accuracy. In a typical concrete stress–strain envelope, the ability of concrete in accepting a load after reaching the peak stress is called strain softening, which is a structure-dependent parameter and therefore material independent [62]. The AEM, which is chosen for the analysis, with existing material models for concrete causes a dependency on size of element, exhibiting brittle behaviour for smaller size of elements.

In this research, a combined material model is proposed by making use of material compressive fracture energy and the effect of localization due to the compressive failure of concrete. In other words, the new constitutive relationship is a combination of the existing material model up to peak stress and the post-peak envelope as a size-dependent material model based on constant fracture energy for varying sizes. Further, the newly proposed model has been validated with experimental results.

The post-peak or softening behaviour of the concrete stress–strain curve under compression has been discussed mainly using localization of strain and compressive fracture energy. The localized compression zone length or damage has been studied by researchers. Since then, estimating the appropriate length of localization has become a challenge in both experimental and analytical studies. Initially, a few researchers [61], [64] had investigated and confirmed the existence of localization using precise experimental techniques. In the initial phases of this identification, [36] had used the value of the length of localization as 2.5 times the smallest lateral dimension of the specimen. In addition to this, other researchers [33],[39] have obtained empirical relationships to estimate the length of the damage zone. As this study focuses mainly on the applicability of fracture mechanics in numerical modelling, different models have been studied for their implementation in AEM. Based on this, it could be seen that the model suggested by [36] was convincing with a simplified and lower number of parameters involved in modelling compression softening of concrete; however, it has a linear softening, which could be inconsistent with

the existing model. Further details pertaining to the application part are discussed in the later sections of this chapter.

On the other hand, compressive fracture energy has been defined by researchers [26], [62] that were similar to procedures in estimating fracture energy in tension. In all these procedures, the calculations proposed may be slightly different, however, the approach remains the same. In this study, definitions provided by [26] are used in estimating fracture energies, where the stress–deformation curves are divided into two parts A_{pre}, the energy required to load the specimen and A_{post}, the post-peak energy per unit of the specimen, which is the required compression fracture energy, defined as the area under the curve up to one-third the peak stress, as shown in the 2.5. In addition to this, the fracture energy, Gfc, is also estimated experimentally by estimating the energy absorbed per unit area in the damage zone [33], [39]. All studies yielded that the use of fracture energy of compression failure could be invaluable in understanding the post-peak softening behaviour of concrete.

As is well known, the constitutive relations play a vital role in governing the numerical modelling of concrete structures. There has been extensive research in the development of constitutive models based on the material properties of concrete. The numerical modelling in AEM under compression is based on the EPF compression model [34], which is also popularly called the 'Maekawa' concrete compression model at each spring, whose applicability and accuracy is already verified[54]. However, in the EPF model the size effect is not considered and therefore brittle failure was observed in the simulation results, which will be discussed in the later sections. Therefore, there is a need for a compression softening model based on the discussed concepts in fracture mechanics. The idea of multiple stress–strain envelopes existing for concrete in tension is well established, whereas such a condition in compression has come into consideration only in recent times. Similar to crack band theory in tension [8], an approach called crush band theory [14] was described for an appropriate finite element modelling of a few examples undergoing compressive crushing. In this approach, the author used a linear descending behaviour in the post-peak regime in the concrete stress–strain envelope as evaluated in one of their previous studies [15]. A more relevant compression softening model based on compression fracture energy named Compression Damage Zone (CDZ) was developed (Markeset), which considers the failure mode in the damage zone as distributed axial splitting and localized deformation. Both

the methods considered linear descent in the concrete stress–strain envelope because it is useful to have a smoother softening envelope to have wider applications and accuracy. A smooth post-peak behaviour was observed using a model based on effective moduli and finite element analysis over Van Mier's test results, which were carried out to validate the results. This model, however, does not consider the existence of fracture energy and is more complicated due to the effects of sub-localization assumptions. Further, a model based on fracture energy and localized damage zone was developed [57]. This model has shown more appropriate results in finite element modelling but failed to allocate stress for every strain automatically, which could cause inappropriate behaviour in the case of modelling in AEM.

The behaviour of post-peak drop with numerical insight is more convincing, as studied by [11] to understand stress–strain behaviour in a longitudinal bar for various discretizations. Suppose only a few elements have strength below the other elements and unload, in which case the overall strain would be less. Therefore, convergence to actual post-peak behaviour was absent in any of the cases. The post-peak behaviour was highly governed by the effective softening modulus and the brittle drop was increased with the increase in the number of elements. The practical condition of this situation is unacceptable, and hence reformulating the material model is essential to reduce the highly localized behaviour. Such highly localized nature was observed in AEM, which shall be discussed in the next section.

New post-peak compression modelling

AEM is capable of modelling the continuum and discrete nature of structures for various kinds of loading. The compression model being used in this tool is based on EPF developed by [34] as shown in 2.7. AEM is based on a discrete approach, where a structural component is composed of rigid square elements connected to one another with several springs. The material properties are governed by the constitutive relations mentioned earlier. To establish the problem further, the same concrete prisms tested by Van Mier have been modelled using AEM for different element sizes and simulated; the results are shown in 2.6. It clearly shows that the compression ductility is lost in the post-peak regime and as the size of the element is increased it can be noticed that the brittleness is reduced slightly. This confirms the need for considering size effects in concrete simulations.

In this numerical tool, the compression material non-linearity is modelled by redistribution of unbalanced forces in each step of loading. As the springs attain peak compressive strains, to avoid negative stiffness and an ill-conditioned stiffness matrix, a small stiffness is assumed and the difference in the unbalanced forces is redistributed into the force vector in the following step. This approach could also be a prime source in the localization of deformation in AEM with respect to the stiffness matrix, which shall be counteracted with the help of fracture energy parameters in this study.

Derivation of Combined Material Model

According to Jansen and Shah [26] the compression fracture energy is defined as the area under the compression envelope, as shown in the figure2.5 Nakamura and Higai [39], proposed an empirical relation for estimating compressive fracture energy based on many experimental observations:

$$G_F = 8.8\sqrt{f_c} \tag{2.1}$$

f_c is in MPa and, G_F in N/mm

The fracture energy from the definitions could be written as:

$$G_F = L_Z \left\{ f_c^2/(2E_c) + \int_{\epsilon_p}^{\epsilon_f} \sigma d\epsilon - (f_c/3)^2/(2E_c) \right\} \tag{2.2}$$

From this:

$$GFc = \left\{ G_F/L_Z - 4f_c^2/9E_c \right\} = \int_{\epsilon_p}^{\epsilon_f} \sigma d\epsilon \tag{2.3}$$

Lz is length of the fracture zone defined by Lertsrisakulrat and Watanabe [33], as:

$$L_z/D^* = \begin{cases} 1.36 & D^* < 100 \\ -3.53 \times 10^{-5} D^{*2} + 1.71 & 100 \leq D^* \leq 180 \\ 0.57 & D^* > 180 \end{cases} \tag{2.4}$$

$D^* = \sqrt{A_c}$;A_c =Equivalent cross section of concrete

Also, Nakamura and Higai (2000) proposed the following equation for the length of damage zone:

$$L_z = 1300/\sqrt{f_c} \tag{2.5}$$

However, both the equations are being subjected to further evaluation and three different values for the zone has been tested in this study which is described in the later sections.

The basic constitutive equation for softening is assumed to be exponential and it is of the form:

$$\sigma = Ae^{B\epsilon} \tag{2.6}$$

A and B are softening parameters and could be obtained from the fracture energy bounds: $(\epsilon_p, f_c) and (\epsilon_f, f_c/3)$ Therefore,

$$A = f_c/e^{B\epsilon_p} \tag{2.7}$$

$$B = -\ln 3\,(\epsilon_c - \epsilon_p) \tag{2.8}$$

The post peak constitutive relationship could be written as:

$$\sigma = f_c e^{-\ln 3(x-1)/(x_c-1))} \tag{2.9}$$

where,

$$x = \epsilon/\epsilon_p \tag{2.10}$$

and

$$x_c = \frac{\epsilon_c}{\epsilon_p} = 3/2 \ln 3 \frac{GFc}{\epsilon_p\ f_c} + 1 \tag{2.11}$$

Derivation of Combined Material Model

According to Jansen and Shah [26], the compression fracture energy is defined as the area under the compression envelope, as shown in figure2.5. Nakamura and Higai [39], proposed an empirical relation for estimating compressive fracture energy based on many experimental observations:

$$G_F = 8.8\sqrt{f_c} \tag{2.12}$$

f_c is in MPa and, G_F in N/mm

The fracture energy from the definitions could be written as:

$$G_F = L_Z \left\{ f_c^2/(2E_c) + \int_{\epsilon_p}^{\epsilon_f} \sigma d\epsilon - (f_c/3)^2/(2E_c) \right\} \tag{2.13}$$

From this:

$$GFc = \left\{ G_F/L_Z - 4f_c^2/9E_c \right\} = \int_{\epsilon_p}^{\epsilon_f} \sigma d\epsilon \tag{2.14}$$

Lz is the length of the fracture zone defined by Lertsrisakulrat and Watanabe [33], as:

$$L_z/D^* = \begin{cases} 1.36 & D^* < 100 \\ -3.53 \times 10^{-5} D^{*2} + 1.71 & 100 \le D^* \le 180 \\ 0.57 & D^* > 180 \end{cases} \tag{2.15}$$

$D^* = \sqrt{A_c}$;A_c =Equivalent cross section of concrete

In addition, Nakamura and Higai (2000) proposed the following equation for the length of the damage zone:

$$L_z = 1300/\sqrt{f_c} \tag{2.16}$$

However, both equations are subject to further evaluation and three different values for the zone have been tested in this study, which are described in the later sections.

The basic constitutive equation for softening is assumed to be exponential and is of the form:

$$\sigma = Ae^{B\epsilon} \tag{2.17}$$

A and B are softening parameters and could be obtained from the fracture energy bounds: $(\epsilon_p, f_c) and (\epsilon_f, f_c/3)$ Therefore,

$$A = f_c/e^{B\epsilon_p} \tag{2.18}$$

$$B = -\ln 3\,(\epsilon_c - \epsilon_p) \tag{2.19}$$

The post-peak constitutive relationship could be written as:

$$\sigma = f_c e^{-\ln 3(x-1)/(x_c-1))} \tag{2.20}$$

where,

$$x = \epsilon/\epsilon_p \tag{2.21}$$

and

$$x_c = \frac{\epsilon_c}{\epsilon_p} = 3/2 \ln 3 \frac{GFc}{\epsilon_p\ f_c} + 1 \tag{2.22}$$

All three test results modelled in AEM and the results based on fracture energy are in good agreement with experimental results. The size of the elements is varied as shown in the figure 2.8 and it can be seen that the dependence on size is eliminated. The concept of damage zone is under further examination and more experimental results are needed for acceptance. This model can be used with improved accuracy in different concrete structures subjected to compression.

2.3.2 Concrete compression confinement modelling

The basic material models used in this study are unchanged, as shown in 2.2b,2.2a and 2.2c. To increase the accuracy of estimation of the force–deformation values in AEM

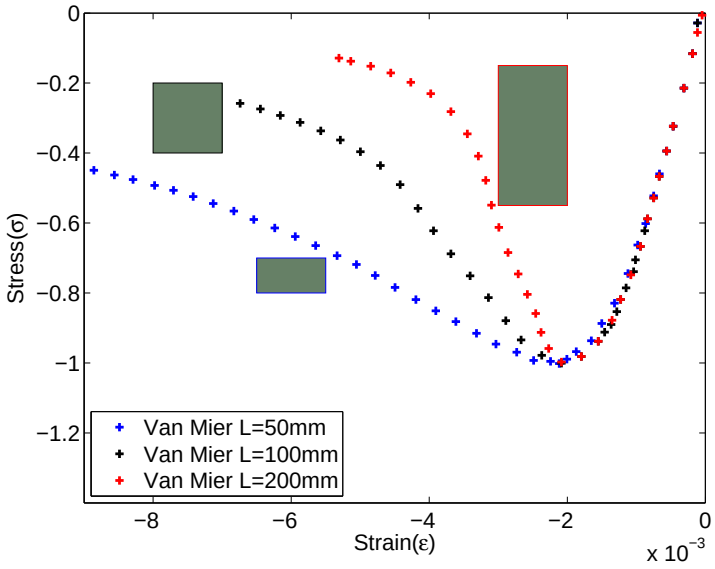

Figure 2.4: Van Mier's Experimental Results

Table 2.1: Material properties from the experiment

Property	**Value**
Compressive Strength of Concrete, f_c	32MPa
Modulus of Rupture, f_r	4.6MPa
Yield Strength of Longitudinal Steel, f_y	511MPa
Yield Strength of Transverse Steel, f_{yh}	325MPa
Axial Load, P	968kN

results, in this study, the compression material model is further modified to consider the effects of confinement due to steel reinforcement and compression fracture energy. The former is based on Mander's confined concrete models, which emphasize increase in peak strength f_{cc} and its corresponding strain ϵ_{cc}, as shown in the figure 2.3 based on the amount of confinement provided by the lateral steel reinforcement. The softening branch of the model is based on the previously developed compression fracture energy and localization of compression damage. The new f_{cc} and ϵ_{cc} based on Mander's equations are calculated in this study and the ultimate strain ϵ_{cu} is estimated by energy balance of the ultimate strain energy in the confining reinforcement and the excess energy due to confinement. However, for convenience and with a wider acceptance in the literature, in this study ϵ_{cu} from [44] is used to mark the first hoop fracture.

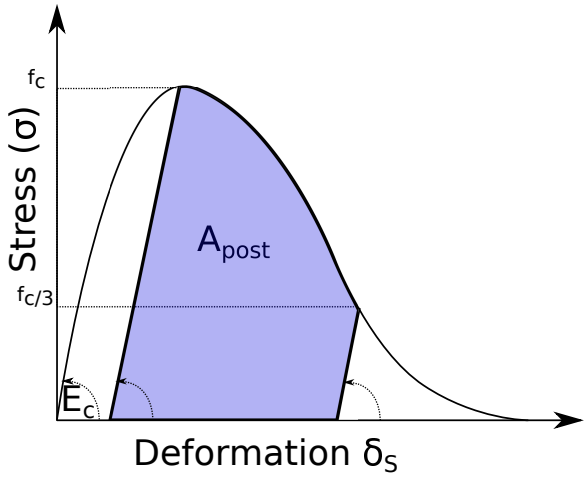

Figure 2.5: A way to determinate post peak energy in a compression material model [26]

2.4 Numerical Validation of AEM

2.4.1 Validation under static cyclic load

As mentioned earlier, the PEER experimental database consists of experimental results on rectangular reinforced concrete columns with its properties, force–displacement ($P--\delta$) relationship and maximum deflection reached before various damage states. The chosen column is a cantilever with a horizontal load applied to its free end with a horizontal reversible load cell and the axial load is applied with a vertical load cell, as shown in the 2.10. The bottom rectangular part of the experiment is heavily reinforced and fixed to the test setup to restrain it from any deformation or damage. The material properties provided for this test that are useful in this study are listed in table 2.1 and the geometric properties as extracted from the literature are shown in 2.11a and 2.11b. It also shows the confinement details of the lateral reinforcement, which is a square section with interlocking ties. The top displacement was measured at the elevation where the load was applied.

In AEM, a rectangular section with the actual dimensions of the specimen is modelled where only the cantilever part is considered in this study and the foundation concrete is assumed elastic with no or small deformations or failure. A total of 363 square elements of dimension 5 cm x 5 cm have been considered with the interface of two elements connected by 10 springs accounting for a total of 6820 springs. The bottom 11 elements are fixed with no deformations allowed and numerically implemented as a Dirichlet boundary

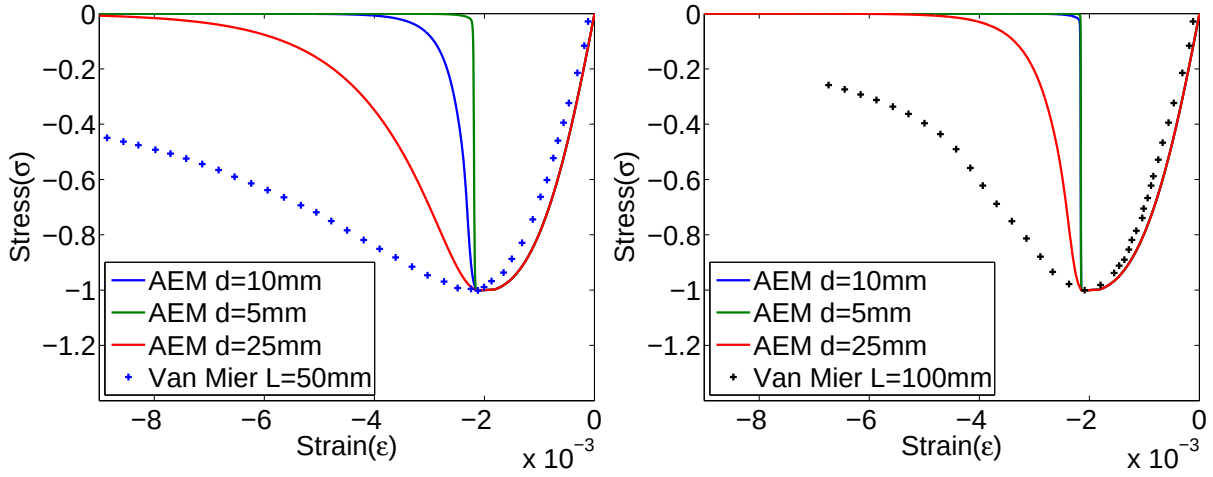

(a) 50mm specimen

(b) 100mm specimen

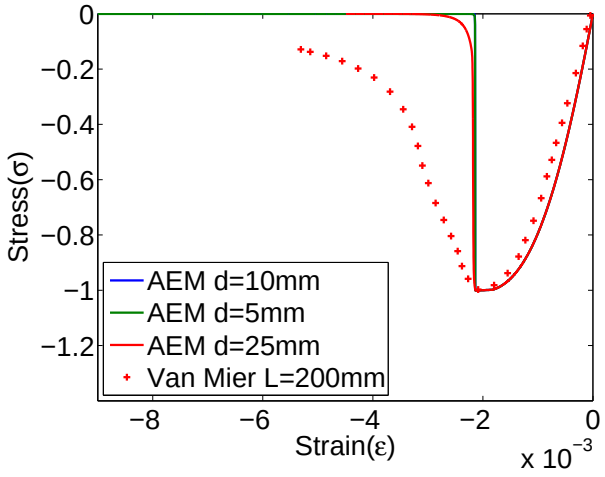

(c) 200mm specimen

Figure 2.6: AEM simulation results using existing material models

condition. The material properties have been considered based on the values estimated based on experimental tensile and compressive tests on plain concrete.

In the numerical model, the compressive material model parameters of Mander's model are estimated, $f_{cc} = 48MPa$, $\epsilon_{cc} = 0.006$ and the strain at the first hoop fracture according to [44] is $\epsilon_{cu} = 0.02$. The tensile strength is also increased by the same percentage as the compressive strength is increased due to confinement. The redistribution value of forces in shear is assumed to be very small due to the interlocking caused from axial loads. The load is applied as a displacement at the top 11 elements with very small increments of 1 mm in 1000 steps.

The numerical model described earlier is simulated for a cyclic load, as shown in 2.13a upon monitoring the force–deformation relationship at the free end of the cantilever col-

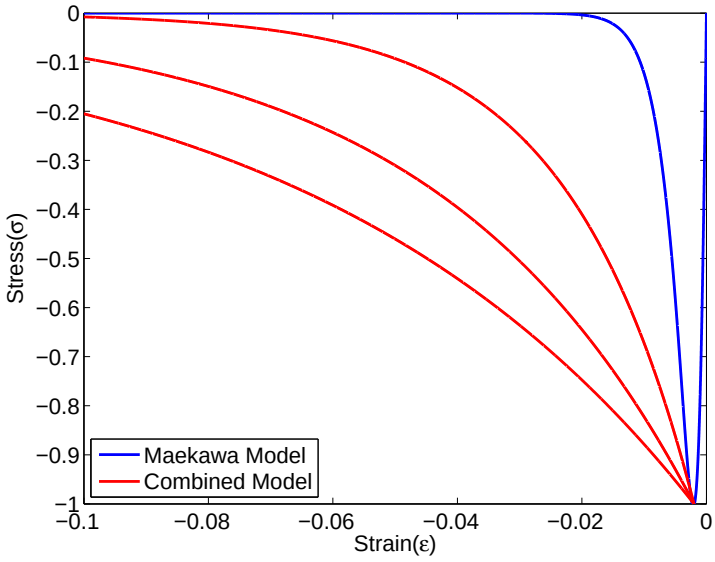

Figure 2.7: New constitutive model for different L_z values against existing EPF model

umn. Reasonably good accuracy was observed in the numerical results and also an acceptable match in the crack pattern was observed 2.13b. A very small difference in the numerical estimation and experimental values was observed and the reasons could be attributed to uncertainties and limitations in modelling concrete. About 45% of the total springs have failed, and the excessively failed springs could account for all the microcracks to visible cracks, as in AEM a spring is assumed to fail based on exceeding the principal stress with rupture strength over a representative stress block dependent on both shear and normal forces; therefore, the accuracy is subjected to practical limitations in estimating and distributing material properties and in addition to this the cracks are restricted to splines in the rectangles. In addition, due to the effect of confinement, the compressive strength and ductility are increased; however, to maintain the same initial stiffness the rupture strength is kept low. Hence, the attainment of these cracks need not ensure wide cracks only but would rather include internal forces also. In 2.13b, the deformed shape is plotted at the last loading cycle and before unloading, which shows the opened cracks over the left face of the elevation view, which closely resemble the experimental visible cracks. Flexural crushing is observed close to the support, as seen in the experiment.

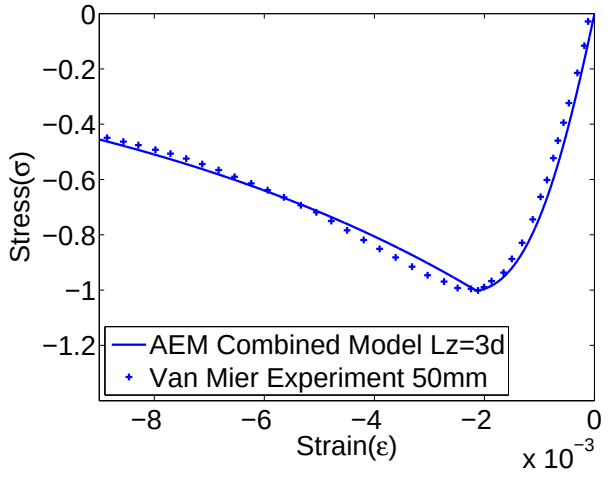

(a) 50mm specimen

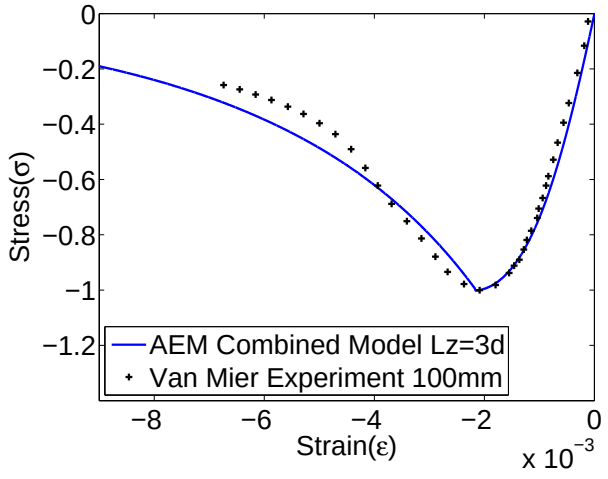

(b) 100mm specimen

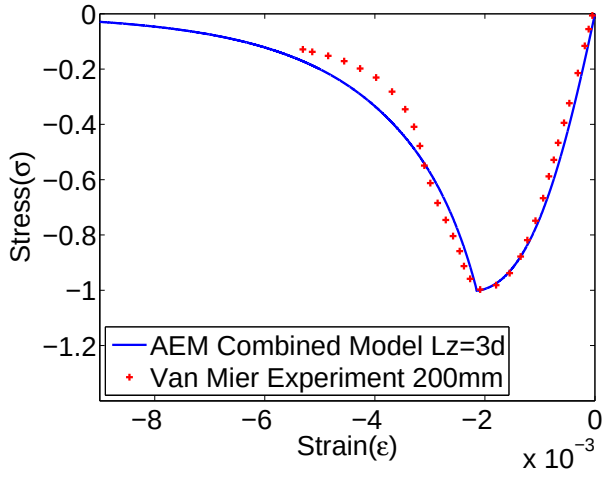

(c) 200mm specimen

Figure 2.8: AEM simulation results using derived model

2.4.2 Validation under Dynamic Loading

A test specimen from the literature [17] has been considered based on the simple requirements that it should be a 2-D frame with one direction of motion on it, with a clear explanation of input, response, observations and damage states in the structure. Among the tests, it is a two storey and two bay frame labelled R2 that is used in the analysis here. The building was a simple 1-scaled frame designed using NBCC 1995 code of Canada and among the multiple tests, this particular specimen was considered to be a non-ductile frame. To adjust the stresses due to scaling laws, additional weights of 95 kN were applied at the centre of four beams, which were loosely connected and supported with horizontal rollers to prevent any out-of-plane collapse. Two sets of ground motions,

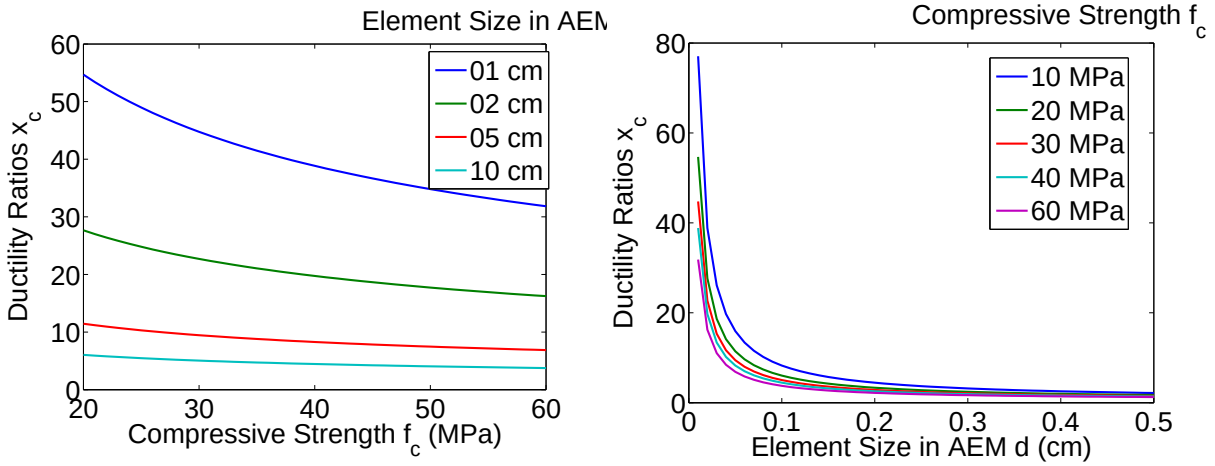

(a) Critical ductility changes over compressive strength

(b) Critical ductility changes over AEM element sizes

Figure 2.9: Changes in ductility with respect to compressive strength and element sizes

namely the N04W component of Western Washington earthquake scaled to 0.21g and 0.42g were applied using a shaking table.

This frame was modelled using AEM to confirm its modelling ability and further use the same frame to validate the damage index method to be used for estimating the capacities. The discretized model of the building is shown in figure 2.14. The frame was modelled as 3632 elements with an element size of 4 cm with 10 springs between two elements, accounting for a total of 66,990 springs; 13 boundary elements were fixed in all degrees of freedom and the prescribed ground motion is applied at a rate of 50 Hz.

In the dynamic response of the frame in this chapter, the validation is shown up to intensity I and the further validation and damage assessment with numerical quantification of damage states are carried out in chapter 5. The force–displacement histories seem to show a reasonable match with the experimental values in terms of both phase and amplitudes, however, the visible differences in amplitude can be treated as a numerical limitation at this moment.

The ground motions applied to the model are shown in 2.15 which have been scaled to 0.21g and 0.42g. The response characteristics of

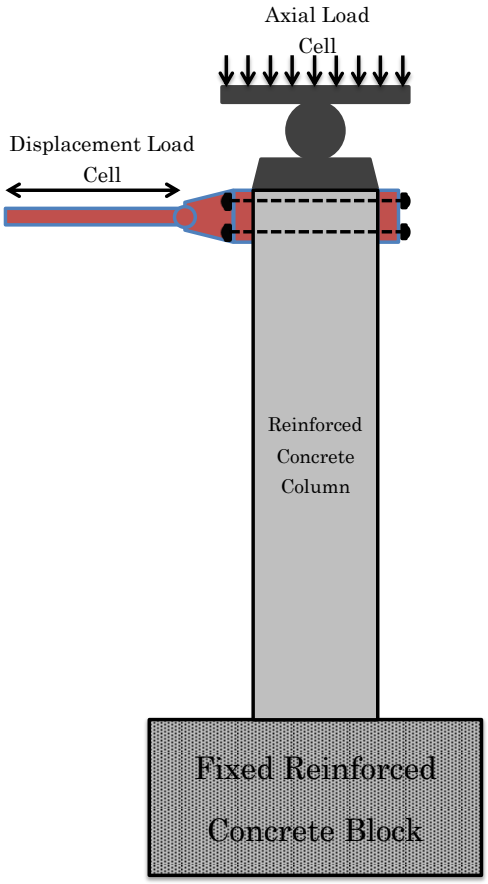

Figure 2.10: Experiment block diagram

2.5 Discussions and Conclusion

It was seen in the previous research and also in the previous sections of this chapter that AEM is indeed a very powerful tool in modelling continuum and non-linear behaviour of RC structures and it is also proven that this tool had sufficient capabilities to consider problems such as modelling existing damage, post-peak behaviour of elements, and even collapse. In this study, two major shortcomings have been identified in the areas of the regime in concrete compression behaviour. These problems lead to inaccuracies in the numerical simulation solutions, especially in the case of high compressive axial forces in combination with lateral seismic forces. This is actually the case in real RC buildings, where the axial loads are higher on the bottom stories due to walls, slabs, beams and other dead + live loads on the upper stories. The major reasons for these issues could

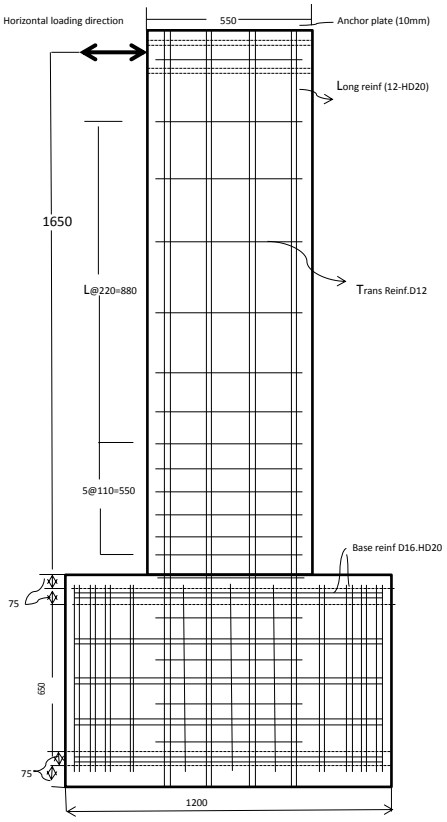

(a) Detailing in elevation

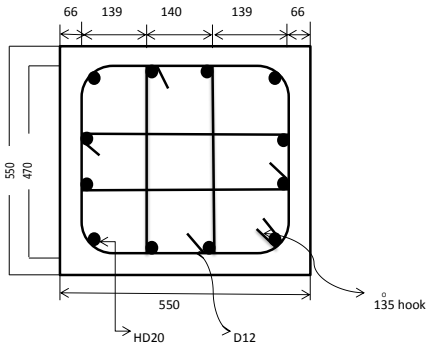

(b) Details of the cross section

Figure 2.11: Configuration of the Specimen

be mainly numerical problems due to the simplified modelling employed in AEM. These issues could be 1) due to the use of simple material models used, which operate independently at spring level distributed to axial and shear springs between interfaces of any two elements, 2) lack of Poisson effect in the non-linear phase at smaller deformations (this effect is, however, taken care of in the case of large deformations with geometric non-linearities), 3) use of simplified failure criteria, which are governed based on an equivalent stress block around a spring and the later failure of the spring in tension is defined based on estimating the ratio of principal stress and the rupture strength exceeding 1, when the corresponding stresses in the tension spring and shear spring are redistributed based on the material properties used; this failure criterion is acceptable due to its simple nature, however, it fails to address directly the compressive–shear interaction as used in other tools and its effect and the failure plane is fixed along the interface of elements and not providing angle of fracture, 4) finally, due to the use of tangent stiffness in the

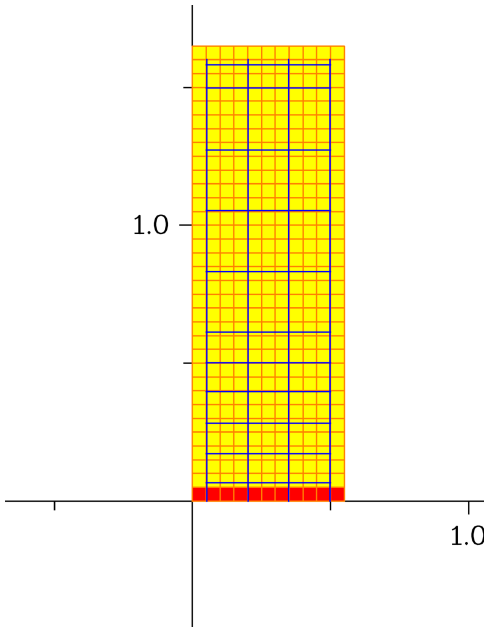

(a) AEM model with reinforcement details

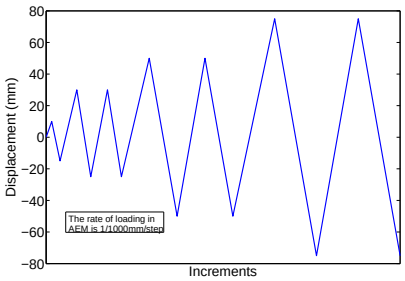

(b) Cycling load as in AEM and experiment

Figure 2.12: Numerical modelling in AEM

modelling, it is observed that when elements reach compressive failure, the strains soften with reduction in stress, which would cause negative stiffness, but in AEM to tackle this problem it was intended to have a small stiffness at the peak and the residual forces in the springs are redistributed; this becomes a source of ill-conditioning when many elements go into compression. Improvement of any tool is subjected to stepwise improvements, but it is observed that despite these issues the tool seems to be very useful in modelling RC members. As mentioned earlier, in this study the tool has been examined for two of the most important issues, first, uniaxial compression size effects and second, the confinement effects of concrete. These effects may seem to be more of a numerical problem as described by [11]; however, in the given limitations of the above-mentioned problems it seemed to be very important to understand with respect to the underlying physical phenomenon behind these issues and in this research it has been solved with adjustment in the compression material models used. In this study, AEM is validated for vertical members subjected to cyclic loading with good accuracy, which would ultimately lead to ways to estimate local seismic damage indices. In addition to this, a complete experimental building frame was selected and modelled with cases of different damages induced by applying ground motion. In this dynamic test, the specimen was validated for roof displacement histories

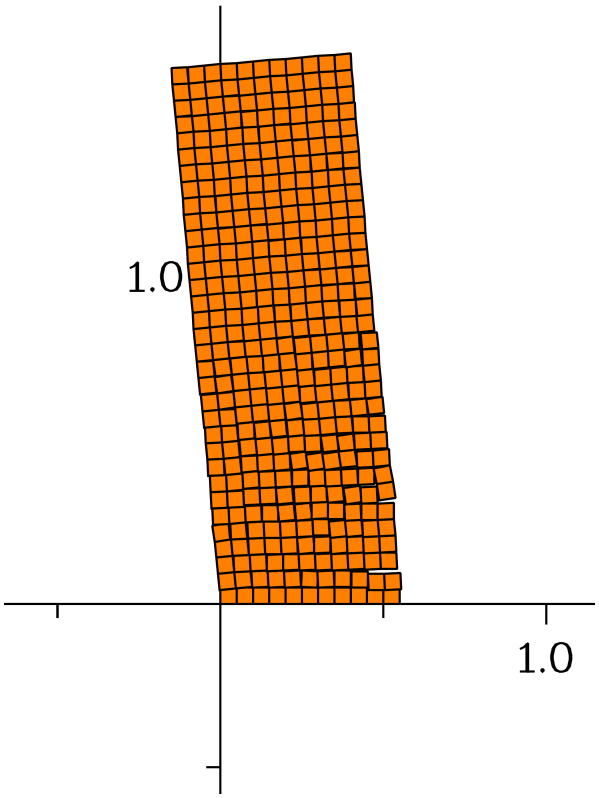

(a) Deformed shape with crack patterns

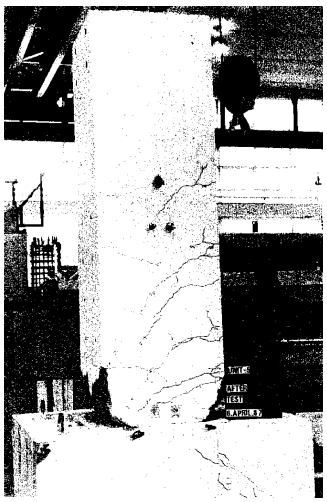

(b) Actual Crack Pattern[55]

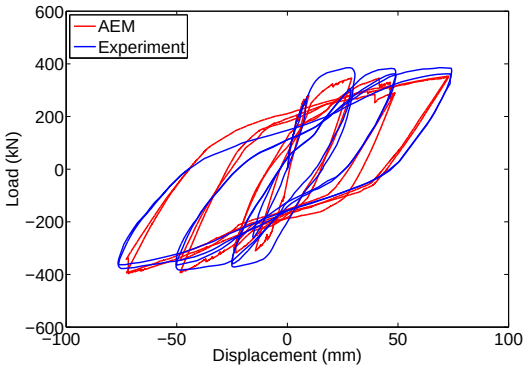

(c) Force deformation relationship

Figure 2.13: Numerical Results in AEM

at two different intensities of loading and the observations revealed good agreement with the experimental results.

Under these circumstances, it could be concluded that the tool is capable of analysing RC buildings in dynamic loading and can assess different damage states to columns, which is essential in estimating damage indices to its corresponding damage states to be used in the later chapters in evaluating and quantifying damage in a building.

The future scope of this method includes development of the tool to be able to incorporate various other numerical abilities to replicate real problems, especially those prevailing in the structures of developing countries. Some of the most common problems, particularly in the industries of these countries, could be categorized as non-engineered design and construction practices; examples are strong beam–weak column situation, provision

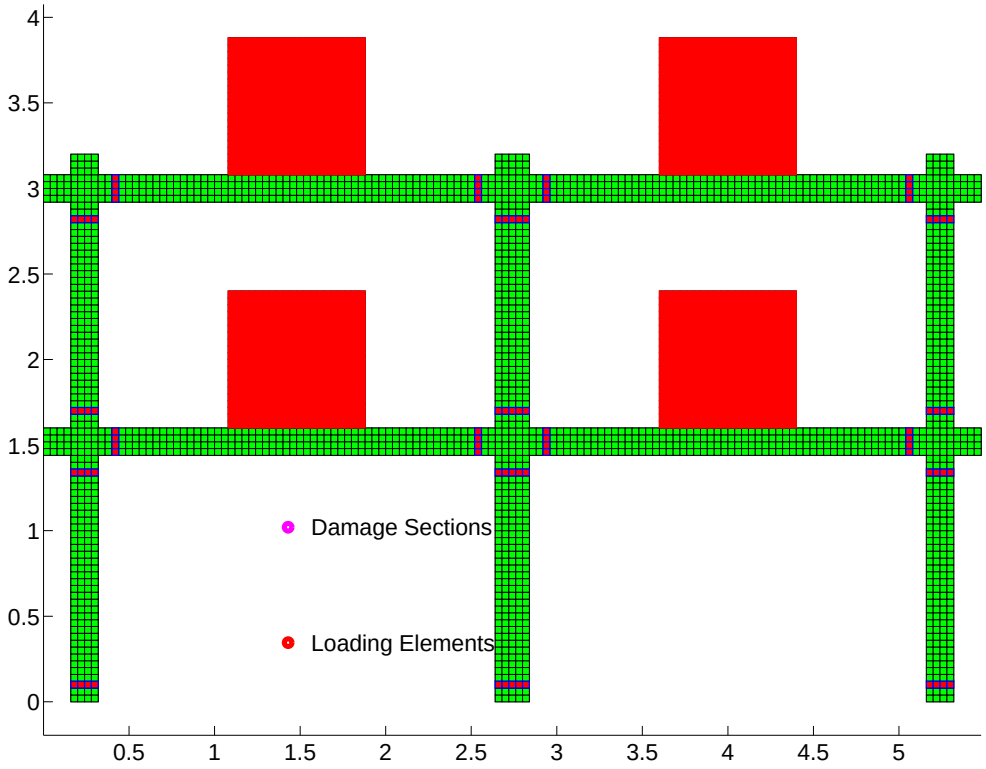

Figure 2.14: AEM mesh of the numerical model of an experiment frame: F01

of soft storey, weak reinforcement of column–beam joints, improper rebar splice, lack of confinement steel, low-strength concrete, provision of short column, inadequate concrete cover, improper alignment of formwork, improper curing, poor compaction, segregation and high content of water. The socio-technical reasons for these methods have already been mentioned in Chapter 1, but here it is essential to improve the modelling incorporating these problems and study these effects on the overall behaviour and capacity of the structure. This objective could be achieved in three stages; first is to improve the capability to detect the problem on site with location and detailing for modelling by using technology, visual judgement or other NDT, the second step involves categorizing all the problems already existing and prioritizing for an experimental investigation, and consequently the numerical tool could be improved at its material models or failure criteria. The third step is to be able to model the problem numerically and obtain the results with a probabilistic confidence.

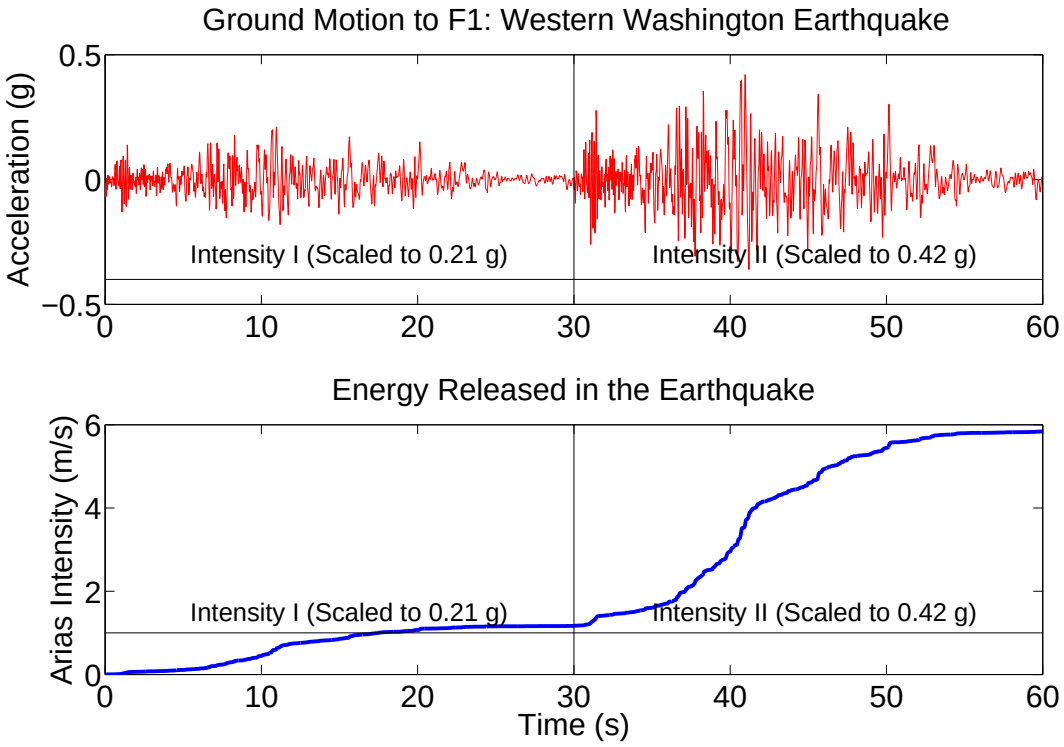

Figure 2.15: Ground motions applied to validation frame

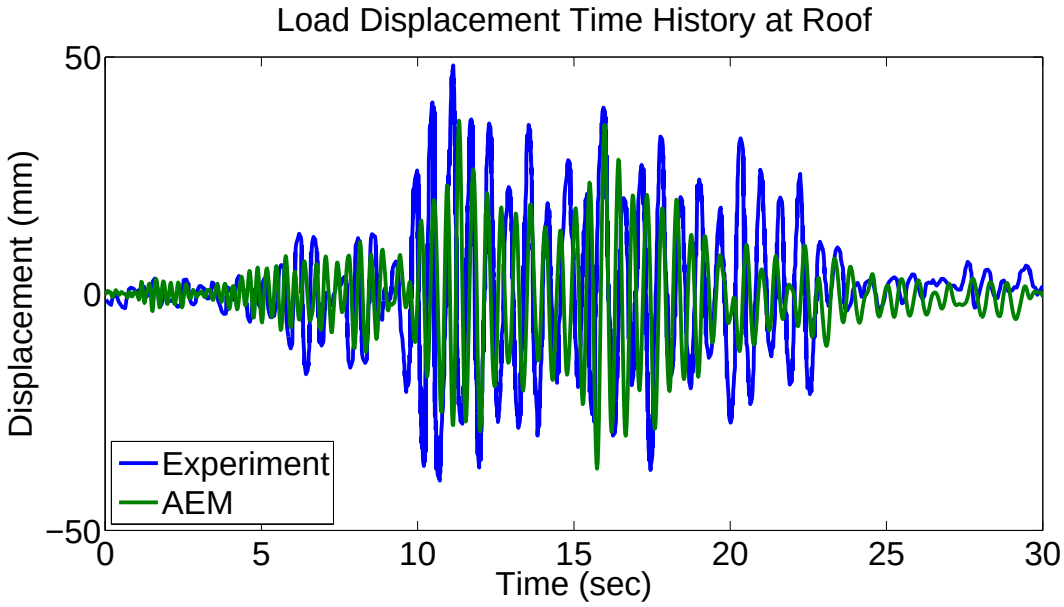

Figure 2.16: Response history of the frame F1 at the roof after Intensity I shaking to the frame

Chapter 3

Identification Methodology, Derivation and Evaluation

3.1 Introduction

As mentioned in chapter 1 extraction of material properties, localization and quantification of damages if any using modal analysis is the major objective of this thesis. In general, the complete assessment procedure for an existing RC building can be categorized into four levels based on the dynamic information, amount of effort and the computational cost and can be given as:

- Level 1: Determination that damage is present in the structure
- Level 2: Identifying the location of damage
- Level 3: Quantification of severity of damage
- Level 4: Prediction of remaining service life of the structure

This study focuses on level 2 and level 3 assessments which involve modal identification, damage localization and model updating.

For an existing building, the natural frequencies and mode shapes are extracted by conducting ambient vibration tests, however, since the baseline state of the structure is unknown, it is intended to estimate the initial state or designed state of the structure based on engineering judgment. Then, the deviation of material properties from the baseline state of the structure is estimated by using general dynamic evaluation and further a

sensitivity based update method is employed to meet the uncertainties in case of limited modes.

3.1.1 Overview

To demonstrate the complete procedure, a simple shear building has been considered with storey stiffness and mass. A known damage has been induced at a few locations by reducing the stiffness, and the modal parameters are estimated for both the states. From basic dynamic manipulations the current state is estimated. Due to ill conditioned-ness of the coefficient matrix, the error seemed to be spurious and random. It could be solved by increasing the number of modes of vibration, however it is practically difficult due to solid structures. The number of auxiliary equations could be increased by considering the orthogonality of mode shapes. This can however reduce the demand on the requirement of number of modes to estimate the damage from the baseline structure. It has been observed that this technique yields satisfactory results, but was inconsistent with aleatory uncertainties. For further accuracy, the updating of stiffness was intended here, with error between observed and estimated modal properties was minimized, with the stiffness vector slightly perturbed every iteration till a set criterion for convergence is achieved. This approach for with initial update vector equal to the outcome from the previous results showed good agreement even for limited modes.

3.2 Methodology

As mentioned earlier, the damage (stiffness reduction) identification and quantification is performed based on modal parameters of a structure. The general parameters lie in the zone of levels 2 and 3 that identify the damage, which could become invaluable in knowing the weakness of a structure. Based on the strengthening solutions, decisions could be made to perform additional reliability studies. The basic modal parameters, natural frequencies, mode shapes and damping are functions of physical properties of the structure mass, stiffness, damping and input forces of a system. Adhering to the objective of identifying stiffness of the system could be achieved by appropriate mathematical formulations in the modal domain; however, it is not direct because of input-parameter limitations regarding its quality and quantity. Quality refers to the amount of noise, un-

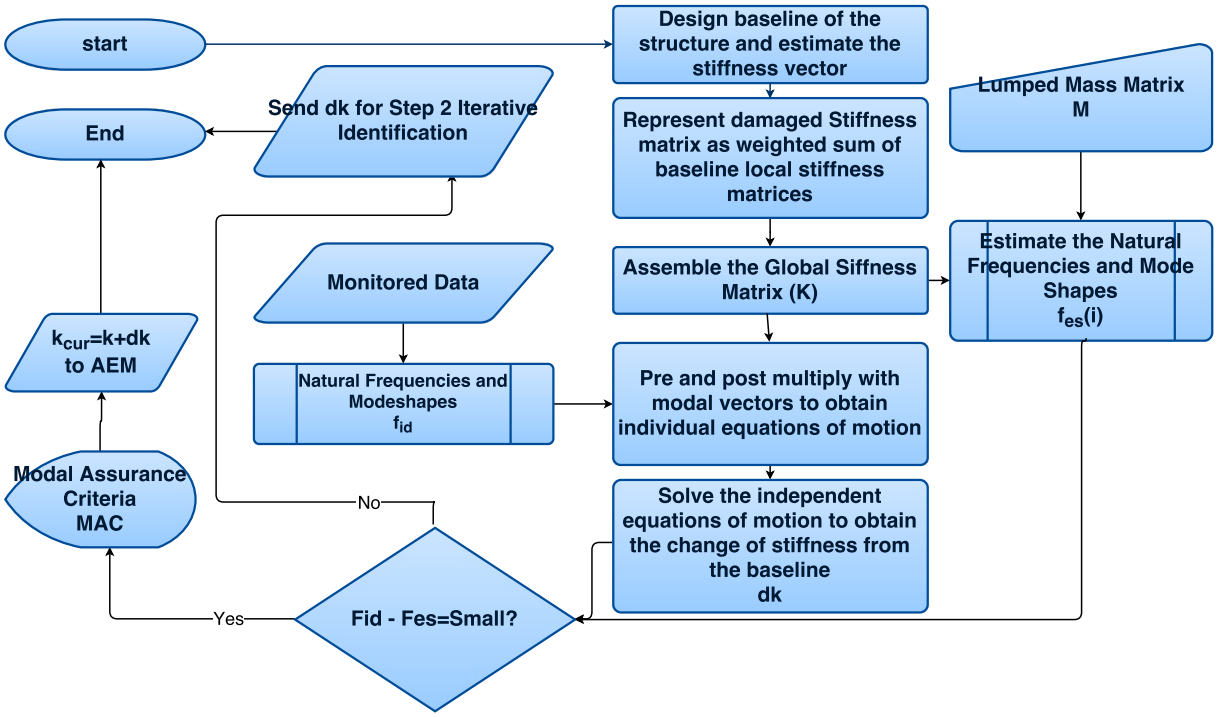

Figure 3.1: First step involving identification of damage coefficients

certainties, issues with assumed variables, quality of data, and lack of confidence in other interfering parameters in the identification domain (time or frequency); quantity usually refers to the number of identifiable modal quantities in structures that could be used to solve the problem, which causes a mathematical problem in the limited number of modal quantities. This chapter focuses on the quantity of modal parameters in the analysis; therefore, the parameter quality is assumed to be high in the derivations.

Thus, theoretically in the first step, the inputs are assumed to have good quality natural frequencies, and mode shapes are identified for the structure of interest with a limited number of mode shapes and natural frequencies. Practically, if the mode shapes are not accurate or not scaled to the unit modal mass (UMM) criterion, then it is imperative to know the mass with statistical confidence in terms of the variation coefficient or the identification formulations; however, this is not certain, as the number of unknowns increase and increase the number of equations or the previously mentioned quantity terms required to solve the identification problem. For the fixed quantity, this study is limited to assess stiffness, and the derivation is based on knowing the accurate mass or accurate mode shapes, as one of these unknowns could be solved by knowing another variable. To begin the identification, in this study, the damage in a building is defined as the reduced

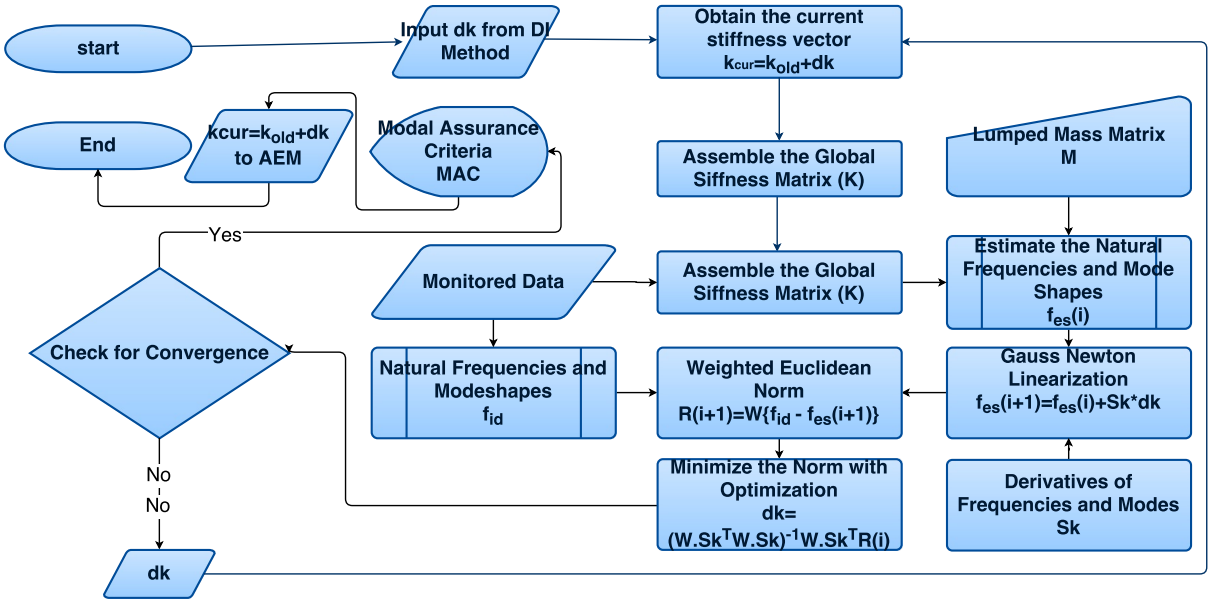

Figure 3.2: Second step of identification process involving optimization

stiffness of a member from the ideal baseline state of the building. The baseline state is the initial state of the structure from which the deviation of stiffness is measured or identified and is a reference for identification. The assumed baseline state is derived based on the subject of interest. If the study is limited for levels 2 and 3, the baseline refers to the initial state of the structure before the damage and when the overall capacity or reliability is not of interest. This is performed by designing the structure with the initial design values or by knowing a similar undamaged structure. On the other hand, if the final objective is level 4 and the identifications at levels 2 and 3 have a limited scope of understanding, then the restrictions on developing a baseline can be of reasonable accuracy only as the current stiffness is more important in the case of assessing the capacity of structures.

With this premise and understanding of inputs in the system, the damage or stiffness identification is performed in two stages. Stage 1 involves identifying the mass required for the dynamic equation of motion in stage 2, and it is performed by using the orthogonality property of modes, i.e. it uses the UMM property to estimate mass in an iterative minimisation of error between the required diagonalization and the diagonalization of the assumed mass with an innovative perturbation for convergence. Through this approach, the mass matrix could be identified even in the case of limited number of modes, and this approach is independent of any other parameters as it depends only on the mode

shapes in the system. Stage 2 involves two identification steps in which the first step is a noniterative stiffness deviation estimate which also uses the orthogonal property of mode shapes and simple dynamic equations of motion to estimate the deviation from the baseline of the system. However, the accuracy of the method can be related to the available number of mode shapes (assuming the quality parameters are reasonable), so lower availability of quantity is required to use step 2. In step 2, the output of step 1 is considered for the optimisation problem or minimizing the error between measured and estimated modal quantities. This is achieved by formulating a weighted residual of the mentioned difference and then iteratively perturbing the stiffness at each step by considering the sensitivity of residual parameters to the required stiffness. This approach is powerful, especially in the case of limited modes, but it is strongly dependent on the accuracy of mode shapes. In short, a two-step damage identification algorithm is introduced based on previously developed methods for damage identification and optimisation for estimating material properties from the modal properties. Detailed derivations and inspired sources are provided in the later sections of this chapter and theoretically validated with a sample problem with a simple experimental study. The details of the theoretical problem used throughout the chapter are given as follows:

$$k2 = [3\ 3\ 2\ 2\ 2\ 2] \times 10^9$$

$$m1 = [8\ 6\ 6\ 6\ 6\ 6] \times 10^5$$

The shear frame has been considered in this study that has the properties of stiffness $k2$ and mass vector $m1$. This is a simple frame that lets the undamped eigen frequencies and mode shapes be identified as shown in table 3.1. A known damage or reduction in stiffness is then applied to the stiffness vector as shown in figure 3.8, and the corresponding stiffness vector is $k2$. Under this situation, the undamped eigen frequencies and mode shapes are given in the 3rd column of table 3.1. In addition, let the mass vector or initial assumed mass be the following:

$$m2 = [6\ 4\ 3\ 2\ 6\ 4] \times 10^5$$

Therefore, the goal is to reach to $k1$ from $k2$ and $m1$ from m2 by using different quantities of the number of modes available to test its applicability and possibility to be used at various practical situations.

In the derivations, this theoretical frame is used as a reference for demonstrating its use and emphasising the importance of the methodology.

3.3 Procedure Derivation

As already mentioned, the development of the procedure includes two steps, namely step 1 for estimating the deviation of stiffness from its baseline and optimising the difference in error of estimated and measured modal properties, which assumes the baseline properties of the structure as follows.

The natural frequencies, f_m^* and mode shapes, ϕ_m^* of the existing structure are the known parameters, but the initial or baseline or reference state of the structure is primarily unknown, as shown in the figure 3.3.

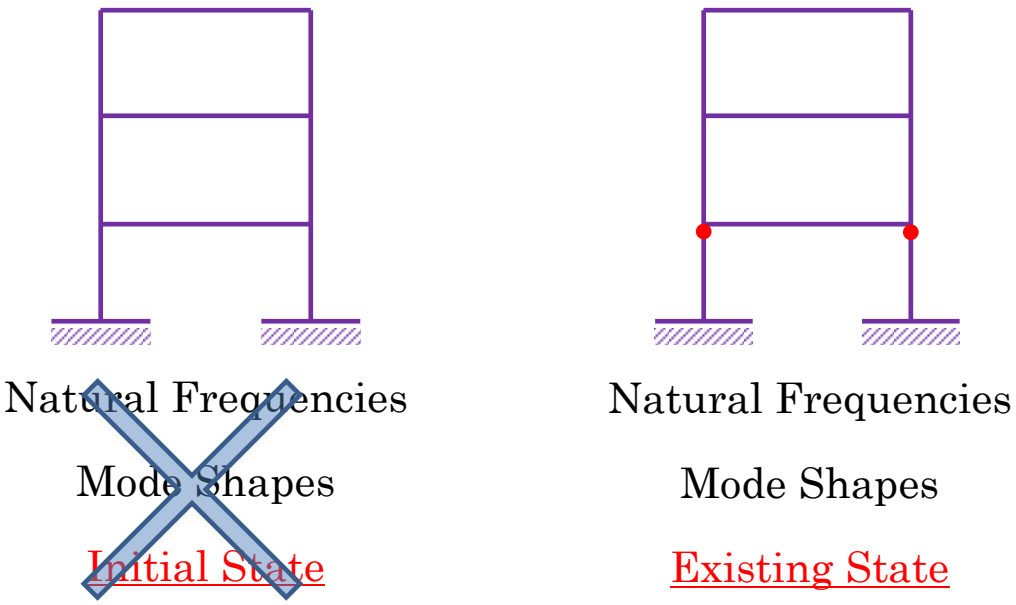

Figure 3.3: Information of a structure before and after damage

3.3.1 Stage 1: mass estimate

An optimum mass update procedure has been developed in this process which is based on Berman optimum mass matrix and the corresponding derivations are mainly cited in [9] and [10]. In these studies, the unit mass scaling property of the modes are utilized and the Lagrangian minimization is applied to estimate the ΔM required to the approximated mass. Here, the general mass matrix update form described in [60] is adopted in the beginning.

$$\phi^T \left[M_A + \Delta M\right] \phi = I \tag{3.1}$$

$$\Delta M = M_A \phi m_A^{-1} (I - m_A) m_A \phi^T M_A \tag{3.2}$$

$$M_{upd} = M_A + M_A^{1/2} [[Q^T]^+ - Q] Q^+ M_A^{1/2} \tag{3.3}$$

where

$$Q = M_A^1 / 2\phi \tag{3.4}$$

This updated mass procedure above is strongly dependent on the available number of modes as it is a non-iterative procedure. It can be seen in the figure 3.4 for the same case discussed in this chapter, this technique is suitable only when there is sufficient number of modes, the mass estimates have large errors. It can be seen that unless all modes viz. 6 the error looks looks higher, for instance with 5 modes the errors ranged upto 30%. Therefore, a simplified modification was intended in the update model to achieve the derived model which consisted of two stages of iterations. In the first iteration, it was intended to diagonalize the above general mass matrix by making use of the simple mass matrix in this study and also in the later upgrade of these methods, it would be intended to model in AEM, where the corresponding masses are lumped as well. Therefore, this property is utilized and in the case of limited modes, the mass matrix updated is forcefully diagonalized and used as an input in the same method. This is followed after every step and at a certain point it reaches convergence, however the errors, does not seem to converge to zero for the same example as shown in 3.6. The complete formulation for iteration 1 is as follows:

$$M_j = M_{upd}(i+1) = diag\left[M_{upd]}(i)\right] \tag{3.5}$$

$$M_{upd}(i+1)) = M_{upd}(i-1) + M_{upd}(i)^{1/2} \left[\left\{Q^T\right\}^+ - Q\right] Q^+ M_{upd}(i-1)^{1/2} \tag{3.6}$$

where $Q = M_{upd}(i)^1 / 2\phi$ and $i = 1, 2, 3...Convergence$

Since, the iterations dont converge to zero error, therefore to achieve a convergence the

mass estimates needed to be perturbed and in order to do this, it was decided to add random noise upto 10% was added to the mass matrix and the corresponding mass matrix was again reiterated in the loop with digonalization as given in iteration 1 and consequently, these values again converge when the perturbation is applied again to set the iterations in loop. This whole procedure is shown in the flow chart 3.5 and the formulation of iteration 2 is as follows:

$$M_{final} = \Sigma_{j=1}^{Convergence} M_{j+1} \tag{3.7}$$

$$M_{j+1} = M_j \left[1 + [X \sim [0,1]] \times PL(j)\right] \tag{3.8}$$

$[[X \sim [0,1]] \times PL(j)]$ is the random noise matrix and $PL(j)$ is the perturbation limit for achieving optimum convergence.

For the same example, the mass estimates were accurately made as shown in figure 3.7a and the corresponding random noise is shown in figure 3.7b. It could be seen in the figures that the errors converge to zero after about 1 million iterations and the random noise is gradually reduced towards the convergence. It could be seen that this method is powerful in estimating the diagonal mass matrix of the structure, in-spite of requiring large computational time. In a blind case where the actual masses are not known, the scaling property could be used as a criteria has to be used as a criteria for convergence.

3.3.2 Stage 2: step-1 derivation

First step in the derivation is to estimate the change of stiffness from an assumed stiffness matrix and this is done based on [56] as shown in the figure 3.1, the initial step is to generate the baseline stiffness vector k as an assumed parameter based on engineering judgment and further it is assembled into a global stiffness matrix, which is given as K, and the existing state of the structure be deviated by the unknown $\Delta\ K$, therefore its stiffness is given as:

$$K^* = K + \Delta\ K \tag{3.9}$$

The equation of motion of baseline state of the structure is given by

$$M\ddot{u} + Ku = 0 \tag{3.10}$$

Considering the existing or damaged state of the structure, the equation of motion is given as

$$M\ddot{u} + (K + \Delta\ K)\, u = 0 \tag{3.11}$$

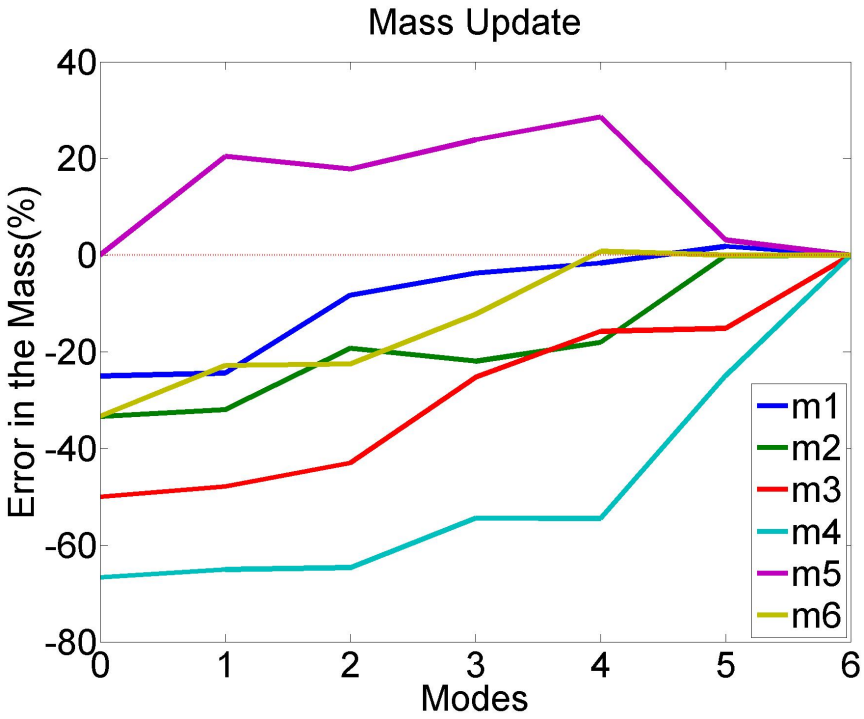

Figure 3.4: Optimum mass matrix update based on Berman (1976) method

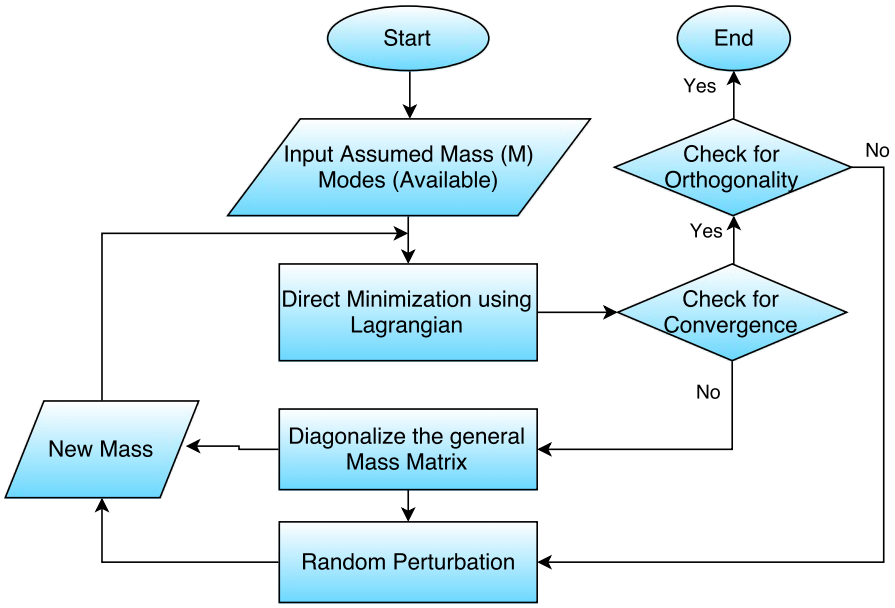

Figure 3.5: Modified mass update procedure in iterations

The modal forms of the system is given as

$$[(K + \Delta\ K) - \lambda_i^* M]\,\phi_i^* = 0 \tag{3.12}$$

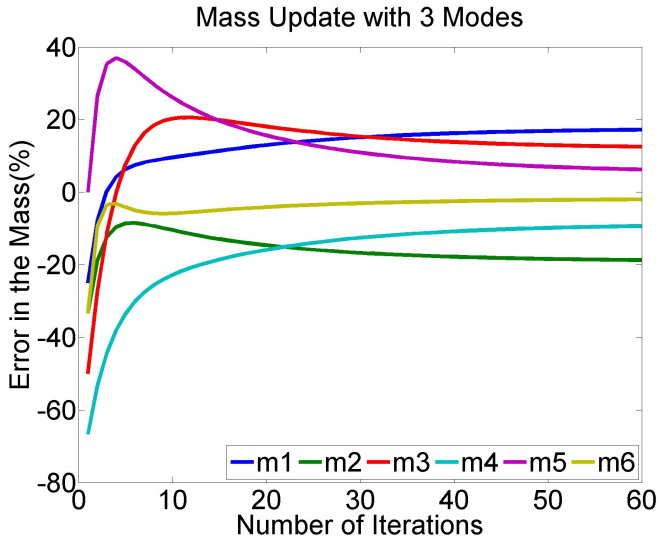

Figure 3.6: Iteration 1 by diagonalization of mass matrix

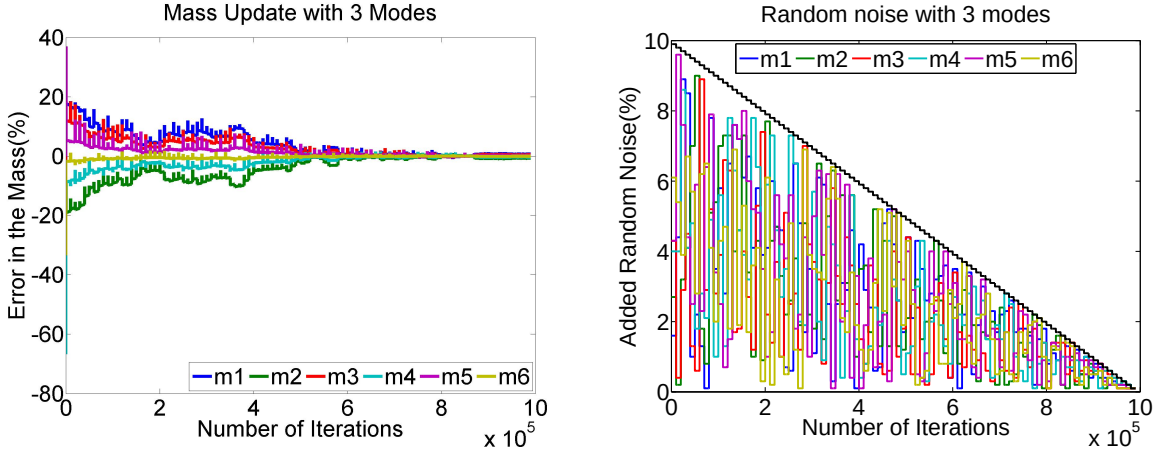

(a) Iteration 2 with random perturbation of mass matrix

(b) Corresponding random noise added to the 6 mode system

Figure 3.7: Random perturbation and diagonalization iterative update on mass matrix

here, i the number of mode shape identified from the measured responses and λ_i^* is the eigen value corresponding to ${f_m}^*$. Now pre-multiplying ϕ_i^{*T} to the modal equations

$$\left[\phi_i^{*T}\left(K+\Delta\ K\right)\phi_i^* - \lambda_i^*\phi_i^{*T}\ M\phi_i^*\right] = 0 \tag{3.13}$$

The damaged stiffness matrix, $\Delta\ K$ can be written as the weighted sum of independent components of stiffness contributed by each element to the global stiffness matrix K_j,

where the weights α_j represents the contributing damage to each member

$$\Delta\ K = \sum_{j=1}^{NE} \alpha_j\ K \tag{3.14}$$

NE is the number of elements

$$\frac{\phi_i^{*T} \left(\sum_{j=1}^{NE} \alpha_j\ K \right) \phi_i^*}{\phi_i^{*T} (K) \phi_i^*} = \frac{\lambda_i^*}{\phi_i^{*T} (K) \phi_i^*} - 1 \tag{3.15}$$

Therefore these set of equations can be formed into a matrix by considering these equations for all modes and thence the left hand side can be written into a matrix and be given as

$$F_{ij}\alpha_j = Z_j \tag{3.16}$$

Solving for α would yield a solution, but however the demand on the number of equations or number of modes NM is higher. Therefore, considering the orthogonality of mode shapes as suggested in the literature, the number of auxiliary equations are increased. The orthogonality of mode shapes are given as:

$$\phi_k^{*T} (K^*) \phi_l^* = 0 \tag{3.17}$$

With simple algebraic modifications, the additional sets of equations can be obtained as

$$\frac{\phi_k^{*T} \left(\sum_{j=1}^{NE} \alpha_j\ K \right) \phi_l^*}{\phi_k^{*T} (K) \phi_l^*} = -1 \tag{3.18}$$

This simple modification has proven to be very useful as additional auxiliary equations and this has to be added to the same sets of equations 3.16 have been added. The demand on the number of modes needed have been significantly reduced, and its effect is discussed in the later sections of this chapter with theoretical evaluation of an example.

3.3.3 Stage 2: step-2 derivation

A lot of optimization schemes have been developed based on finite element updating, among which sensitivity based updating has proven to be the most reliable one. This updating scheme is simply based on minimizing the error between measured (from field) and estimated (from numerical) parameters by changing or updating iteratively, the sensitivity of certain physical parameters such as mass, stiffness, geometric properties, or

even reinforcement in the case of buildings selected in this study. In the present context the reinforced concrete buildings have many limitations in the assessment and hence it reduces the number of parameters or equations for solution significantly and therefore, it was intended to simplify the complexity by assuming stiffness as a perturbing parameter for the problem. Fundamentally, this derivation is based on [38, 66] and the derivative of modal parameters are based on [18]. But the inputs of this algorithm is obtained from the output of the previous step. The significant advantages of this connection between step 1 and step 2 is dicussed later.

Independently, step 2 is an optimization algorithm, developed with an objective of minimizing the error, ϵ, which are ${\lambda_m}^*$, ${f_m}^*$ and ${\phi_m^*}^T$ and the estimated modal parameters, which are λ_{es}, f_{es} and ϕ_{es}^* at each step:

$$\epsilon = \begin{pmatrix} \lambda_m^* \\ {\phi_m^*}^T \end{pmatrix} - \begin{pmatrix} \lambda_{es} \\ \phi_e s^T \end{pmatrix} \tag{3.19}$$

It is intended to consider the normal form of these errors and the equations are reformulated as

$$\epsilon = \begin{bmatrix} \lambda_m^* & \lambda_{es} \\ {\phi_m^*}^T & \phi_e s^T \end{bmatrix} \times \begin{bmatrix} \frac{1}{\lambda_m^*} & \frac{-1}{\{M\phi_m^*\}^T \phi_m^*} \\ \frac{1}{\lambda_m^*} & \frac{-1}{\{M\phi_m^*\}^T \phi_{es}} \end{bmatrix} \tag{3.20}$$

Here, M is the global mass matrix of the structure. For convenience, this could be written as,

$$\epsilon = Q_m - Q_{es} \tag{3.21}$$

In this, step 1 acts as a constraint and is directional in obtaining convergence in the procedure. Therefor the initial value required for the iterative algorithm is considered from the α values obtained from step 1, therefore k_{cur}, the current stiffness of current step is given as

$$k_{cur} = k\,(1 + \alpha) \tag{3.22}$$

Using Taylor's series expansion on $Q_{es}\,(k_{cor})$, with corrected stiffness k_{cor} and neglecting the higher order terms:

$$Q_{es}\,(k_{cor}) = Q_{es}\,(k_{cur}) + \frac{\partial Q_{es}\,(k_{cur})}{\partial k} \Delta\ k \tag{3.23}$$

Here, the derivatives of the modal parameters with respect to element stiffness is termed as modal derivative or sensitivity matrix and is given as

$$S = \frac{\partial Q_{es}\,(k_{cur})}{\partial k} \tag{3.24}$$

Now, the objective function of this optimization problem is established as the weighted difference between measured and current estimated modal parameters;

$$\epsilon = W\left[Q_m - Q_{es}\right] \tag{3.25}$$

In this study, the weights for frequencies and mode shapes are separately considered and are taken as,

$$\begin{pmatrix} W_\lambda \\ W_\phi \end{pmatrix} = \begin{pmatrix} {f_m}^* \\ \frac{1}{\phi_m^*} I \end{pmatrix} \tag{3.26}$$

Substituting it in the corresponding equations, it can be seen that

$$\epsilon = W\left[Q_m - Q_{es}\left(k_{cur}\right) + S\ \Delta k\right] \tag{3.27}$$

The concise form of this is given as,

$$\epsilon = \left[R_W\left(k_{cur}\right) + S_W\ \Delta k\right] \tag{3.28}$$

where,

$$R_W\left(k_{cur}\right) = W\left[Q_m - Q_{es}\left(k_{cur}\right)\right]$$

and

$$S_W = W\left[S\right]$$

Upon applying this in the minimization of the error, i.e. $\|\epsilon\|_2^2$, the linearized minimization problem could be written as

$$min\left\|\epsilon\right\|_2^2 = min\left\|\left[R_W\left(k_{cur}\right) + S_W\ \Delta k\right]\right\|_2^2 \tag{3.29}$$

Taking derivative of this equation with respect to Δk and equating it to zero gives a least square solution to this problem and is given as

$$\Delta k = \left[\left\{S_W S_W^T\right\}^{-1}\right] S_W^T R_W \tag{3.30}$$

The most important step here involves in estimating the derivatives of modal parameters or the modal derivative matrix S_W, which is obtained as,

$$S = \begin{bmatrix} K - \lambda_{es} M & -M\phi_{es} \\ \left\{M\phi_m^*\right\}^T & 0 \end{bmatrix} \times \begin{bmatrix} -K'\phi_{es} \\ 0 \end{bmatrix} \tag{3.31}$$

3.4 Results and Investigation

To understand and evaluate various aspects of the two steps in the procedure, this section discusses each step independently. Firstly, upon applying Step 1 and without considering orthogonality, the results shown in figure 3.10 show that dependency on the available modes is very high and that the outcome is random and spurious. The number of modes required for the identification is found to be at least 5 among 6 modes. Here, the demand on the number of modes is high; therefore, a reduction was expected by considering orthogonality. When orthogonality is implemented, as shown in figure 3.10a the estimated stiffness had already converged to the actual stiffness. However, when the number of modes reduced in figure 3.10b, irrespective of orthogonality, the errors were spurious and random in nature.

To tackle this problem, it was further decided to complement with optimisation schemes to estimate the stiffness; when step 2 was implemented on the system, the estimated values agreed with the actual ones, as shown in figure 3.11.

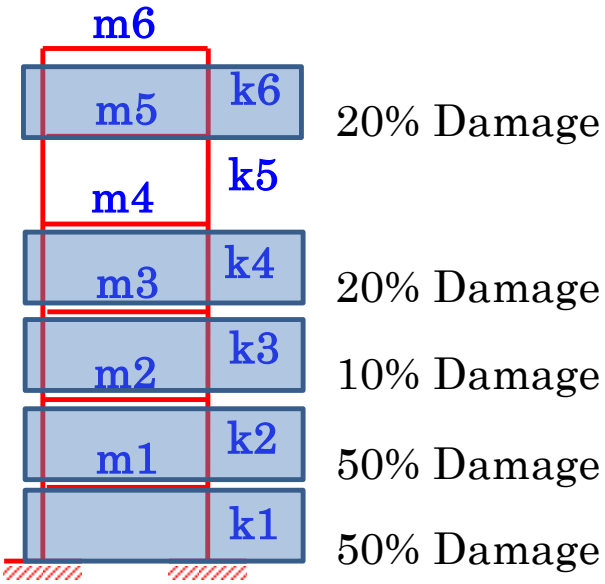

Figure 3.8: Undamaged and damaged parameters of the frame

Table 3.1: Natural frequencies of the example frame

Mode No.	Undamaged Frequency	Damaged Frequency
1	2.45	1.97
2	6.87	5.8
3	10.52	9.1
4	14.02	11.64
5	16.89	14.75
6	18.61	16.61

3.4.1 Convergence and Importance of Step 1

The optimisation problem is consistent when the parameters for updating is close to the actual values or are converging to certain values; however, this cannot be true in many cases, especially in buildings where the deviation from the actual values could be large. For example, in the same building for the same six parameters, convergence has been achieved in mere 6 iterations when step 1 is included as an input for step 2, as shown in figure 3.12a, and the corresponding convergence of error is shown in figure 3.12b.
On the other hand, in the absence of step 1, convergence is not achieved; and the results are beyond limits, especially due to wider assumption of input bounds (figure 3.13a and 3.13b). In contrast, if the bounds of assumption are closer to the point of convergence or the initial inputs are closer to reasonable values, there is a possible stable solution, as shown in figure 3.14a, with corresponding error shown in figure 3.14b. Even in this case, a stable convergence is achieved but error does not converge to zero. This places an important emphasis on using the mass independent step 1 as an input for the optimisation problem in step 2.

3.4.2 Solutions to the inverse problems

As discussed in the earlier sections, the equations solved in equation 3.30 is an under-determined problem, and the solution to this is usually achieved by the least squares solution as suggested earlier. An alternative solution to this problem could be achieved by using the spectral value decomposition (SVD) to decompose the coefficient matrix to obtain a conservative solution by utilising all or lesser singular values in the system. Using

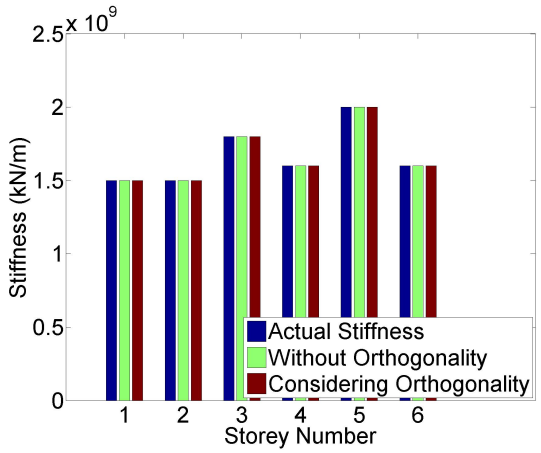

(a) Five Modes

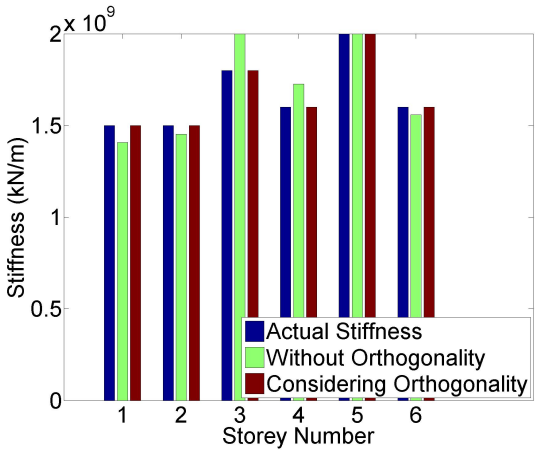

(b) Four Modes

Figure 3.9: Step 1 Results

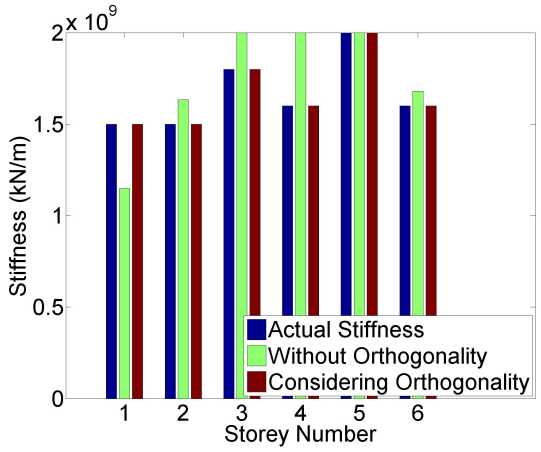

(a) Three Modes

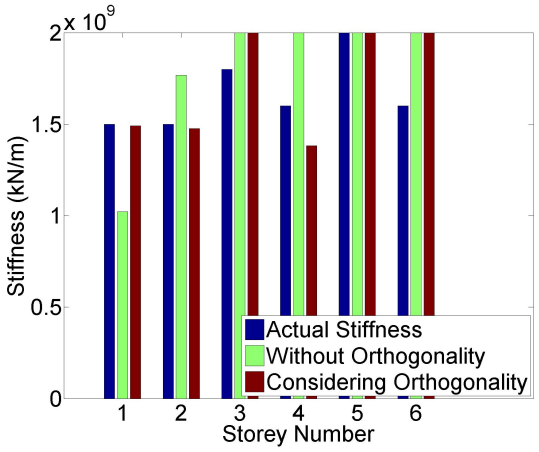

(b) Two Modes

Figure 3.10: Step 1 Results

SVD and considering all singular values yielded solutions coincident with the least squares solution. In addition, algorithm modules can be used for regularisation of the solutions in heavily ill-conditioned cases and noise in the system, where regularisation schemes have proven to be invaluable in improving the quality of the solutions.

3.4.3 Implementation on AEM

The most important process of this methodology is to utilise this technique in the numerical tool and these two approaches are being followed A critical discussion on various applications of the method. The following are the strategies for implementing the 2-step identification method in AEM

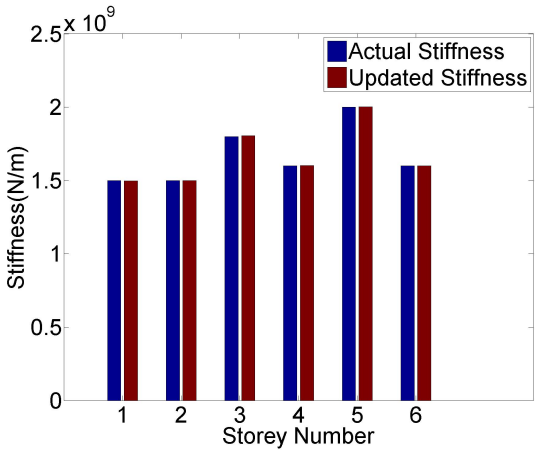

Figure 3.11: Results with step 2 optimization and with only 2 modes

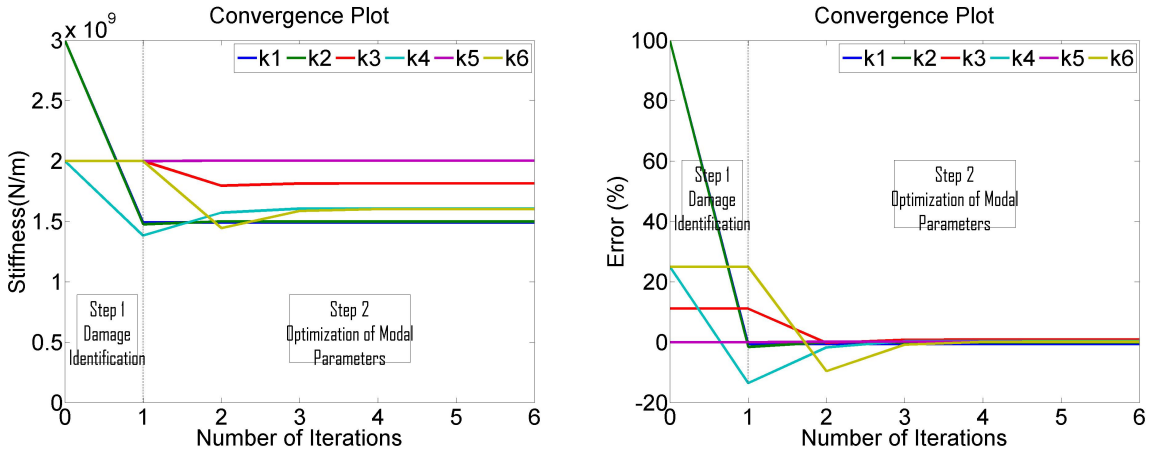

(a) Convergence with Step 1 as input for step 2 (b) Error with Step 1 as input for step 2

Figure 3.12: Stiffness convergence against number of iterations with step 1 as an input

- Strategy 1:

  1. Map the stiffness of members on the members by using relative stiffness and qualitative engineering judgment of other material properties.

- Strategy 2:

  1. Consider average hinge length of each member and discretization into several elements
  2. Use 2-step identification in each zone within the AEM environment

However, in this study, the first strategy has been implemented based on storey stiffness correlated to the appropriate member stiffness.

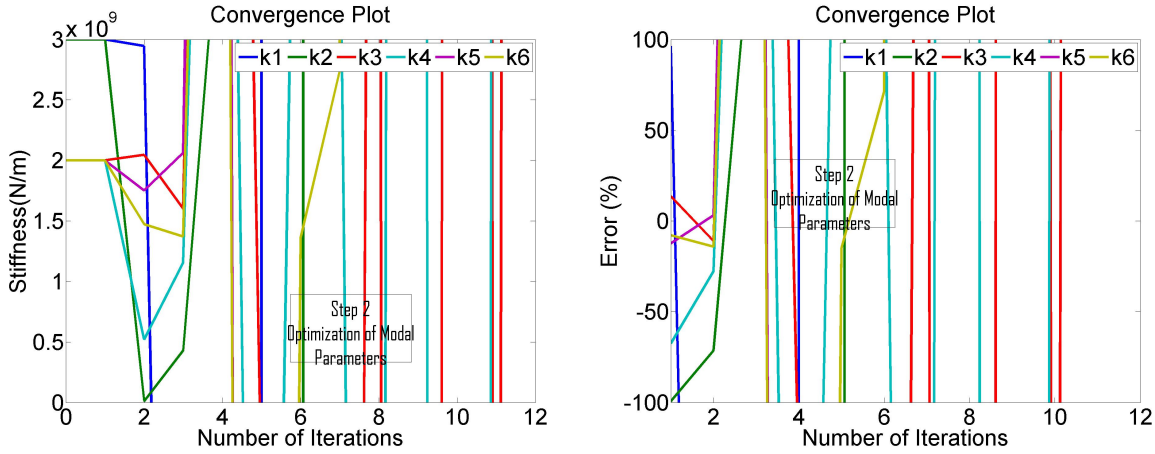

(a) Convergence without Step 1

(b) Error without Step 1

Figure 3.13: Stiffness convergence against number of iterations without step 1 but with same input

3.5 Experimental Evaluation

The previous sections present the developed methodology to identify the mass, damage location and stiffness of the structure, and theoretically, the methodology is proven to be very useful with limited modal parameters. This section focuses on the experimental evaluation of this method to determine its applicability, accuracy, limitations and understand the problems on practical implementation. In this context, an experimental evaluation is conducted by using steel frames made of circular columns, which are subjected to dynamic tests to extract modal parameters. The fundamental intention is to apply the identification procedure on the extracted modal parameters, but it is not as direct, because the dynamic tests are performed based on operational modal analysis and the requirement for the derived methodology for scaled mode shapes or accurate masses. Nonetheless, it is still essential and intriguing to use the technique whose second step is based on masses and not on accurate mode shapes; however, to make the tests more reasonable in terms of applicability and since the masses are estimated with a reasonable accuracy because the mode shapes obtained are proportional, the mode shapes are scaled using measured mass. The details of the scaling used are discussed in the forthcoming sub-sections.

The overall objective of the experimental verification of the method could be enumerated as follows:

1. Manufacture an apparatus and specimen for dynamic testing to measure modal

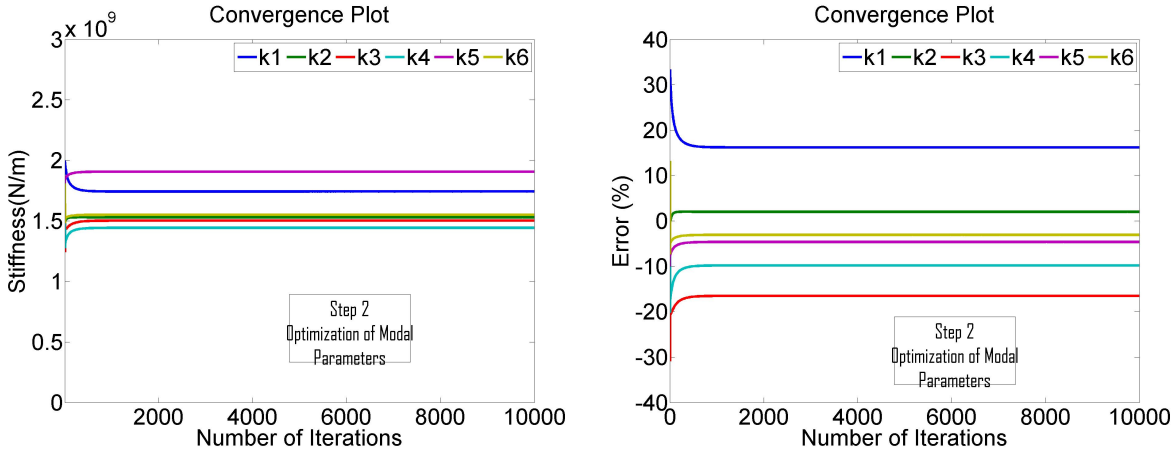

(a) Convergence without Step 1

(b) Error without Step 1

Figure 3.14: Stiffness convergence against number of iterations without step 1 but with close bounds

parameters

2. Estimate the response of a scaled 3-Storey frame with different cases of damage in its columns using unknown input of white noise.

3. Apply Frequency Domain Decomposition (FDD) to estimate natural frequencies and mode shapes.

4. Scale the estimated operational shapes with measured mass of one contributing node.

5. Conduct a cross verification monitoring by using a non-contact type of vibration measuring system called U-Doppler to estimate the same modal parameters.

3.5.1 Test Setup

A simple frame is required in this study; therefore, a 3-storey building frame is made of steel nuts and wooden slabs as shown in the figure 3.18. It is made of circular cross section columns connected using bolts to beam sections, made of 5-mm-thick aluminium C section, and the flanges of the C plates are connected to wooden slabs. All connections are fastened to be rigid, and the total height of the structure is meant to be 90 cm. Simple clamps are attached to provide surface for the laser of U-Doppler, and accelerometers are attached to the rigid wooden slabs of the frame. Four different types of column sections

are made, columns with simple circular steel cross sectionsand three other columns with reduced stiffness. These are represented as damage states required for the study and are represented as D0, D1, D2 and D3, which represent a particular damage state of the column, and the material is used as explained in table 3.3, and the table shows that the material and diameter of damage are selected so the stiffness reduces gradually as the damage increases.

Five cases of frames have been considered, in which different conditions of damages to the frame have been studied. From one case to the other, the damage is increased gradually with an objective to see a change in stiffness. The case condition is prefixed as shown in the table **??**, in which case 1 is considered to have no damage and would serve as a reference to be compared with other cases. In the two sets of measurements, the input forces are not measured and operational modal analysis is required to be certain that white noise is the input to the frame. In the case measuring with the accelerometer, the sensors were not sensitive enough to measure ambient shaking for a stiff frame (7hz); therefore, small shaking is applied to the frame by tapping all points of it using a pencil to confirm the assumption; however, in the U-Doppler case, the natural vibration was measured as the instrument is accurate and sensitive enough to measure the response of the structure under natural conditions.

The duration of the test was approximately 120 seconds in all cases with a sampling rate of 500 Hz with acceleration and velocity for slab mounted sensors and a non-contact type vibration measuring device.

3.5.2 Modal Analysis

The fundamental objective of modal analysis is to find the shapes and frequencies at which the structure amplifies the effects of vibration, and these shapes and frequencies are termed modal parameters. Due to limits on measurement devices and an objective to consider practical situations to measure these properties of real buildings, the operational modal analysis is used for identifying natural frequencies and mode shapes of the structure. Analytically, the natural frequencies and mode shapes are estimated by solving the Eigen Value Problem of fundamental equation of motion

$$M\ddot{x} + Kx = 0$$

$$\ddot{x} + \omega^2 x = 0$$

where, ω is the natural frequency of the system

$$\omega = \sqrt{\frac{K}{M}}$$

Typically, in a structure, a known input force and the corresponding output displacement response is measured, and further transforming them to the frequency domain and taking its ratio gives the Frequency Response Function (FRF), as shown in figure C.4. This method of analysis is more powerful, as the input is usually a sweep wave or an impact load, which is easy to apply to a structure, and the resulting mode shapes are scaled due to known input. In a practical situation, it is not possible to excite buildings which have variable material properties because destructive tests, as mentioned earlier, can damage the structure. Therefore, this study intends to perform Operational Modal Analysis (OMA), which is another representation of output-only modal analysis.

In this type of analysis, unlike the previous type of analysis, this type of analysis only requires the output of the system and the input of the system to be 'broadband random' (White Noise), i.e. the structures are assumed to be in the state of vibration due to micro-tremors due to various sources such as traffic on the road, human activities in buildings, wind or microtremors in the ground due to insignificant earthquakes. In this research, while conducting experiments, to match the natural vibrations with sensitivities of the measurement sensors while maintaining the white noise assumption, a constant supply of tapping with a light impact amplitude is provided, which could replicate similar behaviour exciting all frequencies. There are many advantages in conducting modal analysis using OMA, such as the analysis is convenient, non-destructive in nature and can be used on large structures which are hard to excite.

- Frequency Domain Methods
  - Peak picking method (classical method)
  - Frequency Domain Decomposition (FDD)
  - Extended Frequency Domain Decomposition (EFDD)
- Time Domain Methods
  - Ibrahim Time Domain Technique (ITDT)

- Random Decrement Technique (RDT)
- Eigen Realisation Algorithm (ERA)
- Stochastic Subspace Identification (SSI)

In this study, the Frequency Domain Decomposition or FDD has been incorporated due to its simplicity and had been extensively used for estimating the modal parameters in experiments and real buildings in the field.

3.5.3 Frequency Domain Decomposition

FDD is an output only modal identification technique that uses Singular Value Decomposition (SVD) and was first developed by Brinker in 2001 [12]. It has the advantage of not measuring the input for the system, which is similar to a FRF having peaks, and SVD can be performed by picking the peaks individually, is user friendly to apply even in the case of limited knowledge on the collected data, is widely accepted specially in the case of civil engineering structures, can identify closely spaced mode shapes, can eliminate harmonics which could be identified from all mode shapes and this method uses decomposition of the power spectral density matrix which consists of the cross power spectrum, therefore, cancelling a large amount of noise from the system. This technique assumes that that the input loading is white noise, i.e. the power spectrum of the input is always constant. Therefore,

$$G_{yy}(i\omega) = H^*(i\omega) \times G_{xx}(i\omega) \times H^T(i\omega)$$

$$where, G_{xx} = Const.$$

The identification can be further simplified into a limited number of steps such as the following: 1. Calculate the power spectral density (PSD) matrix G_{yy}
2. Decompose PSD using Spectral Value Decomposition (SVD)

$$SVD(G_{yy}) = U \times S \times D$$

3. Pick the natural frequencies using classical peak picking methods from first and second singular values obtained as S, and the corresponding U is the operational mode shape of the structure.

3.5.4 Data analysis

The measured data is unfiltered discrete time data, but using FDD requires no additional filtering and modelling; therefore, the analysis is directly performed using standard transformation and movement. The discrete time data of each storey is collected into a vector, and the corresponding power spectral density matrix is obtained using Hamming window with 50% overlap over two cross signals and discrete Fourier transform using the nearest power of 2 for both signals of each element of the power spectrum density matrix. The obtained 2×2 matrix at each frequency is further separated into USD, as described in step 2, and the values and two singular values are then plotted in the measurements using accelerometers and Udoppler; in addition, the peaks were mostly noted at the first singular values. The corresponding U vector at each of the corresponding peak gave the operational mode shape of the frame.

As mentioned earlier, in this study, the obtained mode shapes were not UMM-scaled; therefore, scale the mode shapes are appropriately scaled so the developed methodology for identification could be applied to the data of the frame to determine if damage identification and updates could be performed. In this situation, if the basic UMM law is used where the mode shapes are scaled, then

$$\phi^T [M] \phi = I$$

However, in the case of operational mode shapes, the condition of scaling becomes equal to a constant, i.e.

$$\phi^T [M] \phi = c^2 I$$

By keeping the mode shape constant at c^2, it is imperative to assume that all mode shapes are scaled uniformly in this case. Merging this with the mass vector, The equations with three degrees of freedom become

$$\phi' \times CM \times \phi = I$$

On expansion of the values,

$$\begin{bmatrix} p11 & p21 & p31 \\ p12 & p22 & p32 \\ p13 & p23 & p33 \end{bmatrix} \begin{bmatrix} \frac{m1}{c^2} & 0 & 0 \\ 0 & \frac{m2}{c^2} & 0 \\ 0 & 0 & \frac{m3}{c^2} \end{bmatrix} \begin{bmatrix} p11 & p12 & p13 \\ p21 & p22 & p23 \\ p31 & p32 & p33 \end{bmatrix} = \begin{bmatrix} 1 & 0 & 0 \\ 0 & 1 & 0 \\ 0 & 0 & 1 \end{bmatrix}$$

On simplification and taking terms of unknowns into one side, the equations have three unknowns and represent nine equations of motion.

$$\begin{bmatrix} p11^2 & p21^2 & p31^2 \\ p11*p12 & p21*p22 & p31*p32 \\ p11*p13 & p21*p23 & p31*p33 \\ p11*p12 & p21*p22 & p31*p32 \\ p12^2 & p22^2 & p32^2 \\ p12*p13 & p22*p23 & p32*p33 \\ p11*p13 & p21*p23 & p31*p33 \\ p12*p13 & p22*p23 & p32*p33 \\ p13^2 & p23^2 & p33^2 \end{bmatrix} \begin{Bmatrix} \frac{m1}{c^2} \\ \frac{m2}{c^2} \\ \frac{m3}{c^2} \end{Bmatrix} = \begin{Bmatrix} 1 \\ 0 \\ 0 \\ 0 \\ 1 \\ 0 \\ 0 \\ 0 \\ 1 \end{Bmatrix}$$

The above overdetermined system of equations is then solved using the Penrose inverse technique to obtain the most optimised solution for the CM matrix, and then c value is solved by knowing the value of $m1$, and the corresponding equivalent $m2$ and $m3$ could be estimated. The modes could be approximately scaled by diving the ϕ matrix with c, which is further used in the analysis of identification.

A total of five cases of this 3-storey miniature frame was tested in the study, and the damaged condition of each building is as shown in figure 3.18. The miniature frame in an initial state, i.e. in a state of no damage, has a fundamental natural frequency 9.2Hz, as measured using piezoelectric accelerometers attached to each floor earlier against artificial white noise excitation, which was then analysed using FDD. This same set of experiment was performed using U-Doppler by measuring the response at each floor of the 3-storey frame using ambient vibration for all the cases, and the results were then verified with the results obtained earlier. The identified frequencies using accelerometers are shown in figure 3.19, and the frequencies using UDoppler are shown in 3.20. The extracted mode shapes (unscaled) are plotted as shown in figure 3.21. Then, the mode shapes are scaled using the methodology derived earlier based on the measured masses of one storey in each case. This way of scaling is approximate and is meant to help understand the technique for further analysis. The error in scaling each mode is shown in table 3.5, and the errors are in the range of 0 to 8%, which suggests that the methodology can be used for material identification.

3.5.5 Identification

The identified frequencies and mode shapes are used in the 2-step identification procedure and a faster convergence is shown in figure 3.22, and the corresponding modes were also in good agreement with its experimental counterpart, which the evidence for the same is shown in table 3.6. The results of the experiment to detect damage is shown in table 3.7. It could be seen that a significant difference in the errors could be seen and the reasons for this difference is mainly due to various issues. Firstly, the frames tested were hand manufactured and tightened; therefore the consistency in maintaining the material properties could be doubtable. Secondly, the calculated masses were based on slab weight and members but however, the exact contributing mass is not judged exactly. Thirdly, the scaling was done based on mass normalization of the operational modes but an artificial input to the system was applied in the form of tapping which has sources of human error. Also, the damage is spread to the nearest member giving an evidence that the member with lower stiffness dominates and this also calls for the need of more measurement points for analysis. Finally, there could be extreme noise in the system which causes highly inconsistent outcomes from the identification algorithms.

Nevertheless, the outcomes of this experiment could give some information on the reduction of stiffness though it is not reliable but the method has a theoretical significance. Hence, following this condition, in this research operational modal analyis is carried out for identification but the weights for modes have been reduced for real buildings instead of approximate scaling as performed in this section.

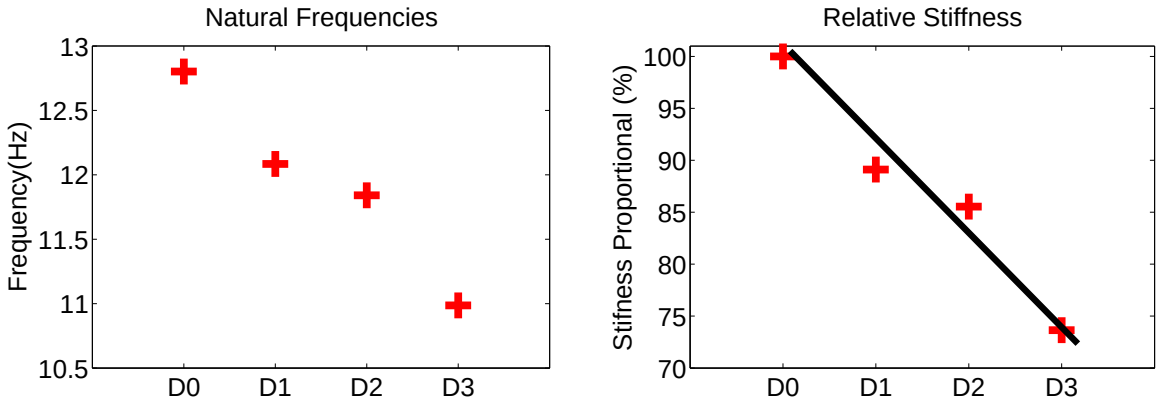

(a) Natural frequencies of damaged columns (b) Relative Stiffness of the Damaged Columns

Figure 3.15: Modal Analysis of Columns

Table 3.2: Experiment cases in the study

Experiment Cases	Storey 1	Storey 2	Storey 3
Case 1	D0	D0	D0
Case 2	D1	D0	D0
Case 3	D2	D1	D0
Case 4	D2	D2	D0
Case 5	D3	D2	D0

Table 3.3: Different Damage States used in the Experiment

Damage	**Damage State**	**Material**
D0	No Damage	9mm Nut
D1	Slight Damage	Rubber + Steel 8mm Nut
D2	Moderate Damage	Rubber + Thin Steel 6mm Nut
D3	Severe Damage	Rubber

Table 3.4: Natural frequencies of all cases of experiments

Frequencies (Hz)					
	Case 1	**Case 2**	**Case 3**	**Case 4**	**Case 5**
Mode1	9.25	7.87	7.08	6.71	6.04
Mode2	26.64	24.51	21.97	20.90	20.05
Mode3	44.16	40.62	36.07	34.33	34.48

3.6 Discussions and Conclusions

In this study, a two-step methodology has been developed and analysed with the engineered baseline assumption, which promises to be a reliable technique to assess the material properties to estimate the seismic capacity of a structure using numerical simulation.

The aim of this methodology works is to develop practical and feasible solutions to identify the material properties of a real building, and for such a building, one of the most important aspects is to provide the fundamental dynamic properties of the building i.e. the natural frequencies and mode shapes.

Table 3.5: Error in unit mass scaling of each mode

	Case 1	**Case 2**	**Case 3**	**Case 4**	**Case 5**
Mass 1 (Kg)	*2.3*	*2.7*	*2.7*	*2.7*	*2.7*
Mode 1 Error (%)	6.98	5.24	6.22	6.65	5.27
Mode 2 Error (%)	5.62	5.91	7.17	8.48	7.95
Mode 3 Error (%)	0.44	1.78	2.78	4.91	4.92

Table 3.6: Modal assurance criteria (MAC) in %

	Case 1	**Case 2**	**Case 3**	**Case 4**	**Case 5**
Mode 1	97.69	98.88	98.33	98.11	97.27
Mode 2	95.54	98.99	98.62	99.35	89.97
Mode 3	98.53	99.67	99.54	99.96	91.20

Operational Modal Analysis (OMA) is a useful technique in estimating modal parameters. The basic assumption of OMA is that the input of the system is white noise and is broadband; therefore, the power spectrum of the white noise is assumed to be constant, and a corresponding methodology, such as FDD and SSI, is used in the identification. As mentioned earlier, the input forces are unknown and the mode shapes are not scaled. Nonetheless, the mode shape needs to be scaled to have accurate applicability of the methodology and to scale various methods proposed recently based on modifications in the dynamic behaviour of the structure by changing stiffness or mass.

In this methodology, Step 1 does not depend on the mass matrix directly, but the accuracy of it mainly depends on the scaled mode shapes. Previously, research has been performed in obtaining scaled mode shapes, but the methods are subjected to concep-

Table 3.7: Relative change in stiffness over the actual expected change in stiffness (%)

	Case 1	**Case 2**		**Case 3**		**Case 4**		**Case 5**	
Storey	**Ref**	**Expt**	**Actual**	**Expt**	**Actual**	**Expt**	**Actual**	**Expt**	**Actual**
1	0.0	17.1	10.0	28.7	15.0	34.1	15.0	49.8	30.0
2	0.0	1.9	0.0	35.5	10.0	38.1	15.0	12.0	10.0
3	0.0	-7.3	0.0	-4.4	0.0	4.6	0.0	27.7	0.0

tual understanding. One of the most direct methods is to use a known excitation i.e. an impact hammer and pull out test; however, these methods are inappropriate because the magnitude of force required to cause an dependable response for the structure raises concerns on the safety of the buildings and the social issues. Technically, this could also violate the linear-time invariant assumption. Secondly, scaling has most popularly done by the addition of masses at a few locations to measure the changes in the modal properties. This method can be applicable on smaller structures positively, but in case of large structures, it is difficult to add additional mass. Thirdly, optimisation methods such as the finite element model are used to optimise the scaling parameters for the mode shapes. To check the applicability and limitations of the methodology, a simple set of experiments were manufactured. By changing the stiffness of columns, the characteristics of modal analysis and the results were studied.

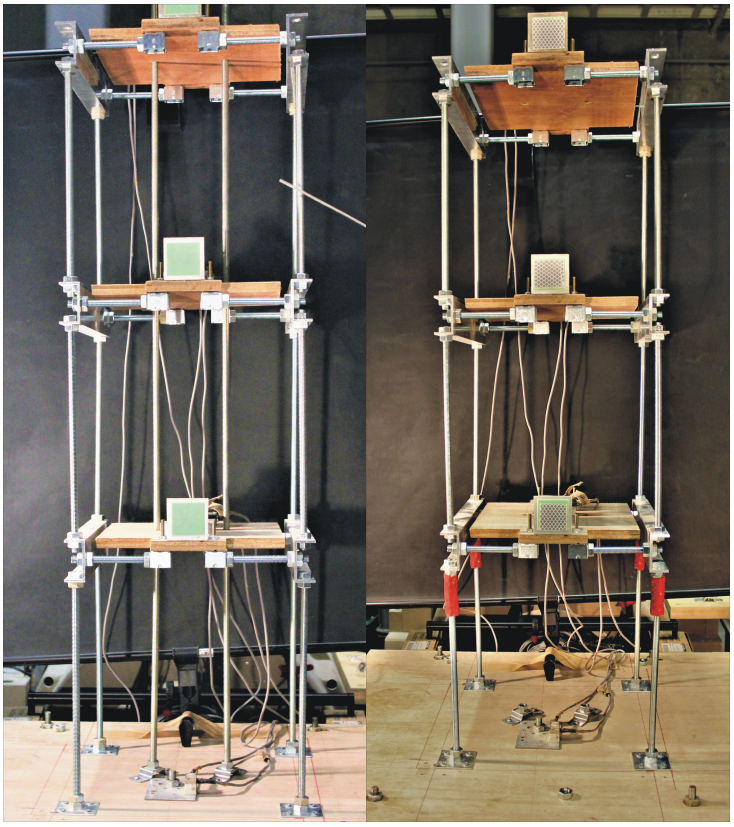

(a) Experiment Case 1 (b) Experiment Case 2

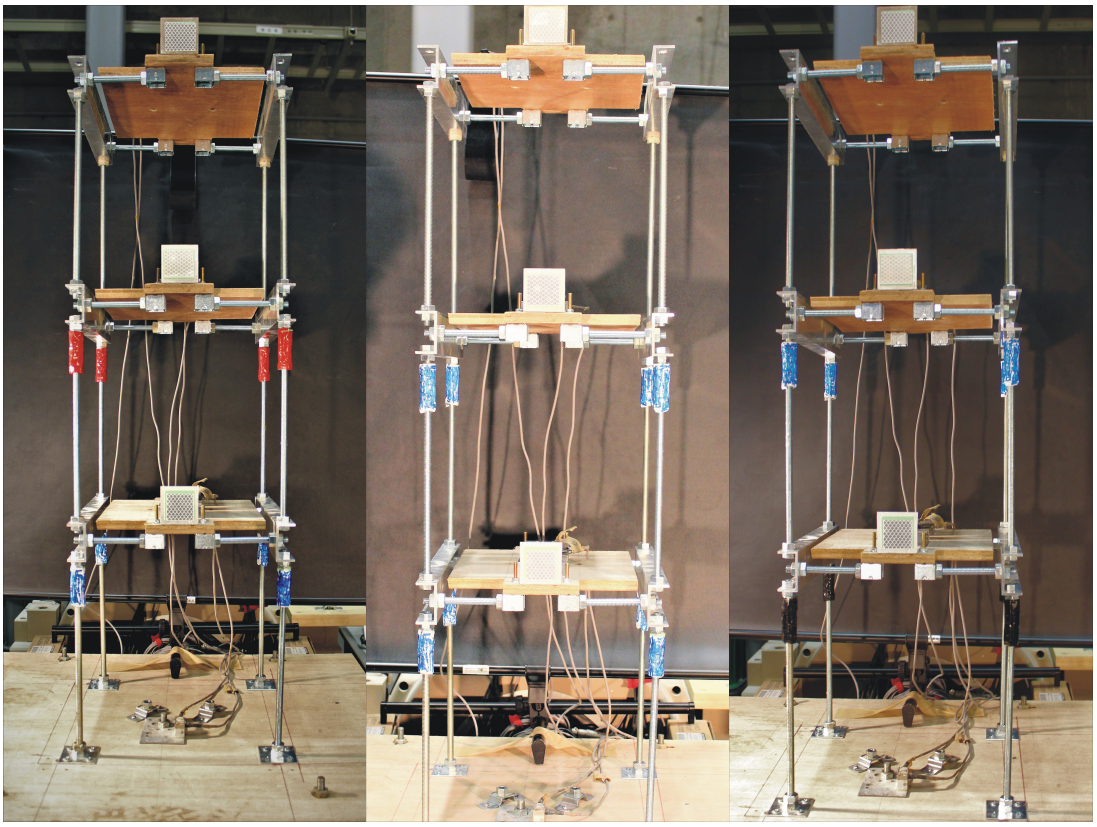

(c) Experiment Case 3 (d) Experiment Case 4 (e) Experiment Case 5

Figure 3.16: Experiment cases with different damage states

Figure 3.17: Experiment setup using UDoppler

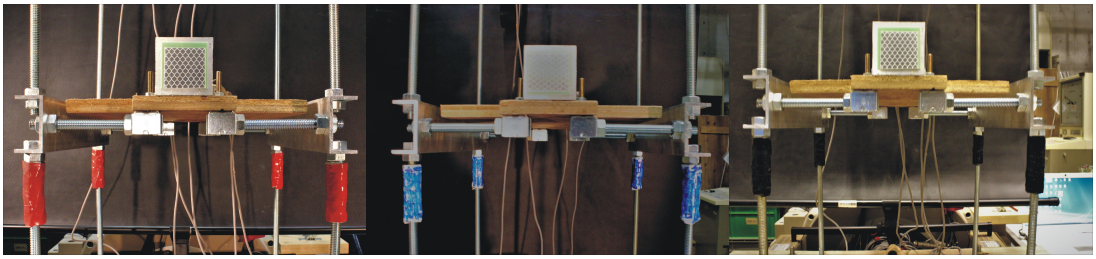

(a) Damage State D1 (b) Damage State D2 (c) Damage State D3

Figure 3.18: Experiment cases with different damage states

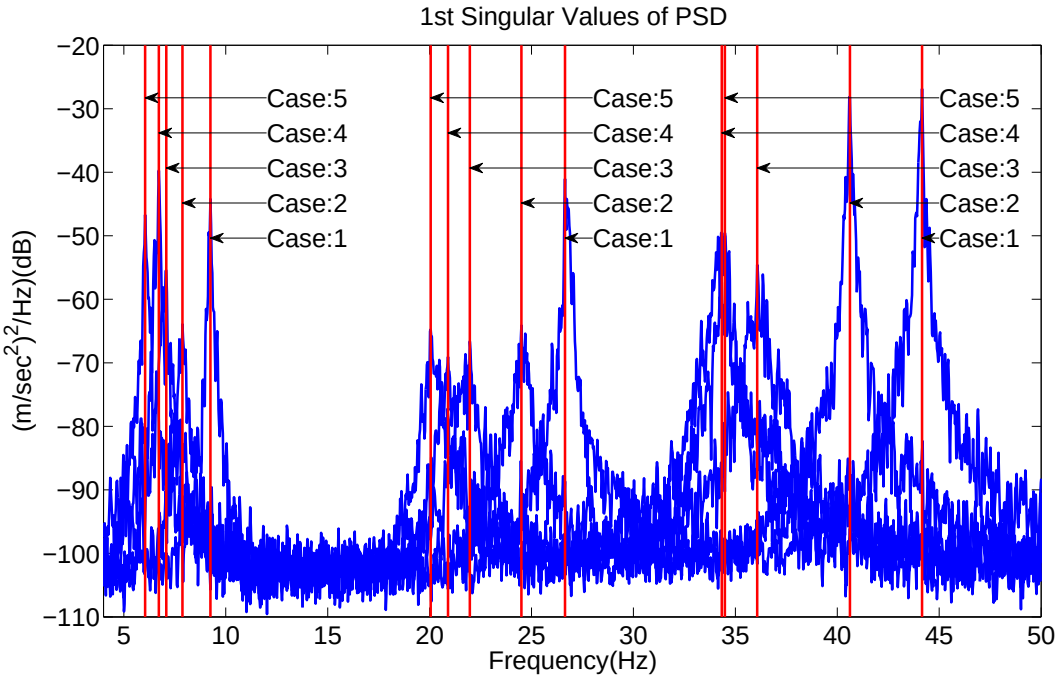

Figure 3.19: Modal analysis of all cases of the experiment using accelerometers

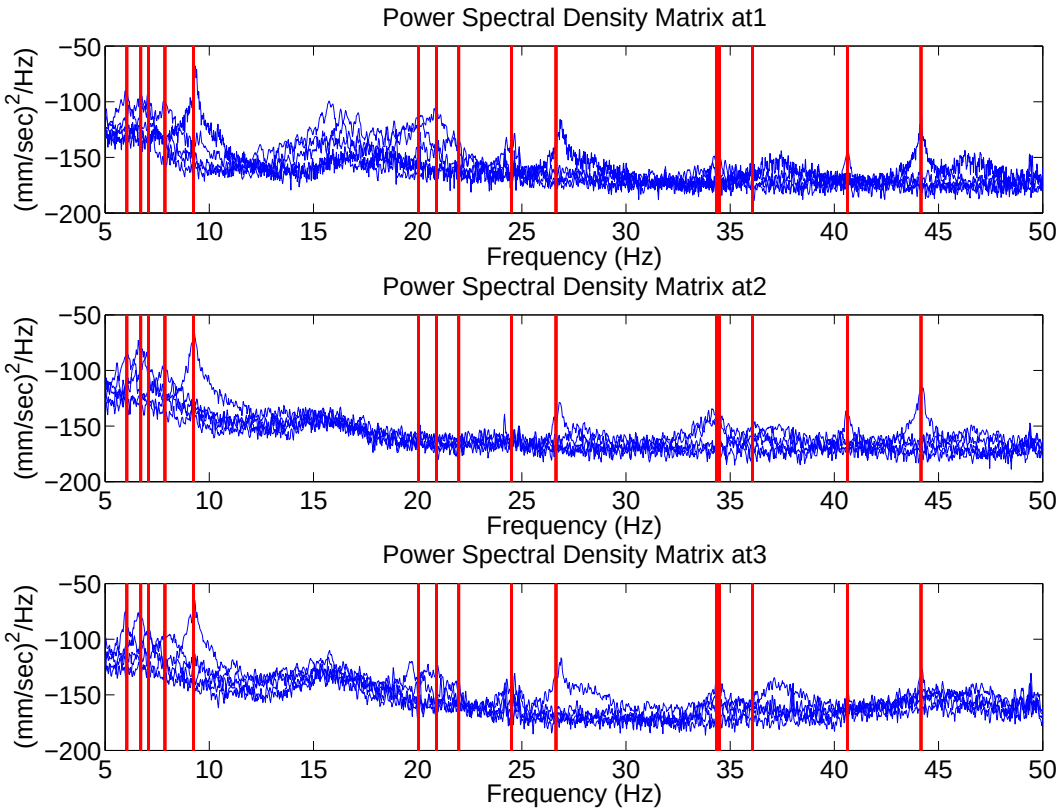

Figure 3.20: Modal analysis of all cases of the experiment using UDoppler

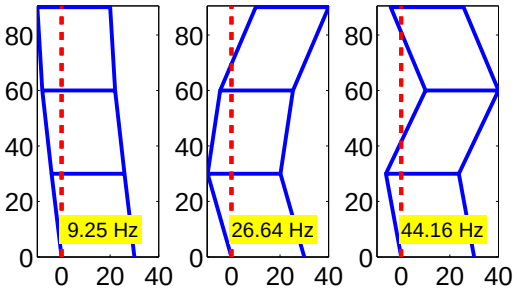

(a) Mode shapes of case 1

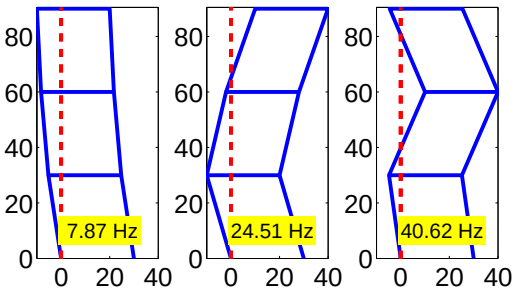

(b) Mode shapes of case 2

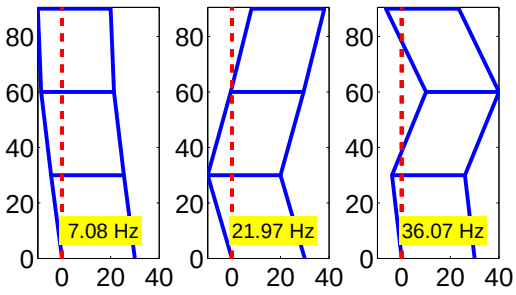

(c) Mode shapes of case 3

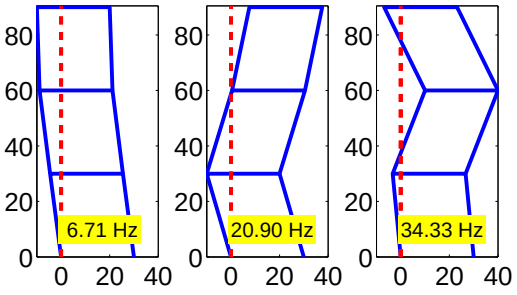

(d) Mode shapes of case 4

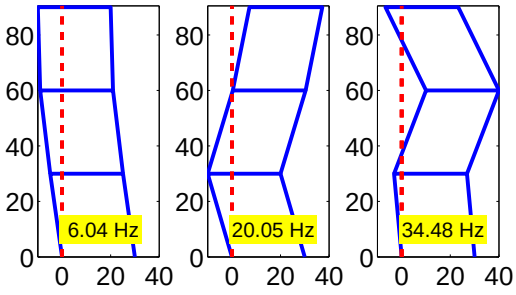

(e) Mode shapes of case 5

Figure 3.21: Mode shapes extracted using FDD from experiments conducted using accelerometers (All shapes are scaled by a factor of 10)

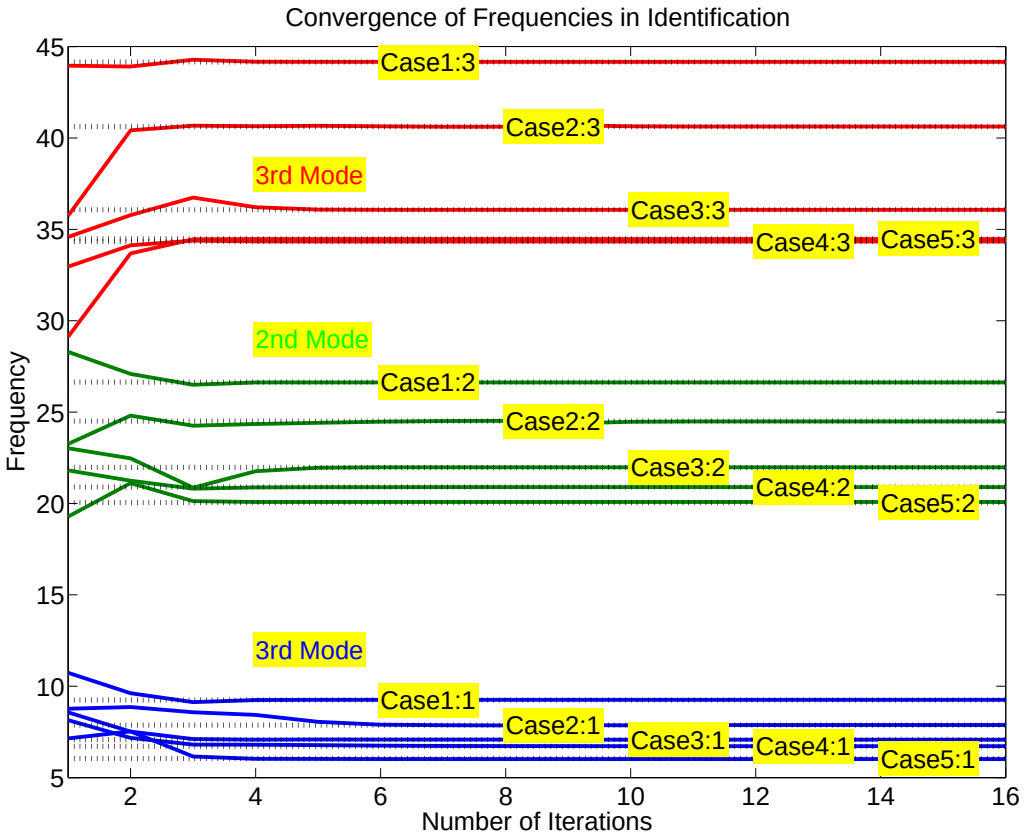

Figure 3.22: Convergence of frequencies in experiment using identification

Chapter 4

Field Study and Identification of Buildings

4.1 Introduction

In the last chapter it was demonstrated that the identification methodology has a potential to estimate the material properties or storey stiffness of a reinforced concrete building at macro scale subjected to a few limitations related to estimating the masses and accurate mode shapes. This chapter investigates into the application of this methodology to real buildings or in other words, it is intended to demonstrate its feasibility and also understand its practical limitations.

Therefore, a field study was conducted to analyze the RC buildings, whose principal objective was to measure the dynamic properties of a building using micro-tremor measurement, and analyse it is using the 2-step identification methodology, which would further be integrated with the numerical tool Applied Element Method. In this simulation it is required to apply multiple ground motions of increasing intensities and then further to estimate the global and local damage states of the building and its vulnerability. With this objective in this survey, Nepal was chosen as the study area, which is a seismically active country lying in the Himalayan range and it was also affected by a moderate earthquake with significant damage in the year 2015. This earthquake is locally named the Nepal Gorkha earthquake, which occurred on April 25, 2015, which released energy equivalent to a magnitude of Mw= 7.8 causing a MMI scaled intensity of IX attributed to violent shaking.

In this study, a group of buildings were chosen in Nepal (at different locations) which were affected in the earthquake of 2015 but are still either in operation or abandoned or retrofitted. A non destructivenon-destructive test (NDT) equipment called GEO-DAS/ANET micro-tremor measuring instruments was used to monitor the vibration response on the main frames of RC buildings under its operational condition.
This chapter has compiled the whole field study, however only one building had been considered for detailed analysis; however the information could be useful in the understanding the environment, parameters for numerical modelling, issues in the site, selection of ground motion in the perspective of more buildings subjected to severe motion and other considerations such as re-bar detailing in the numerical model. The overall purpose could be enumerated as:

- To observe the real state of a RC building in the site.
- Preliminarily to check the feasibility of these studies by understand various other problems involved in the field to carry out an engineering survey.
- To evaluate the number of modes which could actually be extracted for real buildings, as they are stiff entities which sometimes causes limitations on extracting even one mode of vibration, when the response to ambient noise is very less.
- To confirm the implementation of Frequency Domain Decomposition (FDD) for carrying out operational modal analysis as its applicability for real buildings.
- To study the general condition of the building stock in the region over major earthquakes in the past by estimating the pseudo spectral acceleration of the buildings
- To select a building for detailed analysis and carrying out the identification of stiffness.

Three types of RC buildings were selected in thise study, for further analysis and the corresponding typological classes are RC moment resisting frame with un-reinforced masonry infill walls, RC moment resisting frame designed with seismic features and RC moment resisting frame with no infill walls (eg. bare frame building under construction). In order to have sufficient information from the buildings, relevant to this study; the following criterions were set in the selection of a building:

- The fundamental criteria was to do this study for seriously affected RC buildings in the past and therefore low rise buildings were selected with 2-6 storeys complying with the previously mentioned typologies.
- The target sample included occupancy classes pertaining to residential buildings, under construction, schools, hospitals, shopping malls, etc.
- Also, location of the buildings werewas preferred to be in the affected areas of Gorkha earthquake in 2015.
- The buildings which were damaged, such as cracks, visible deformation were in priority
- In addition to this the selection of building also focused on the existence of inadequacies, soft storeys, bad maintenance,etc.

4.2 Monitoring and Field Survey

The survey was conducted from 24th June 2016 to 28th June 2016. In this survey a total of 18 RC buildings and 1 mud masonry building was investigated. The study mainly included two components,components; one is the monitoring ambient vibration of building and a rapid visual screening (RVS) of buildings to extract typological and seismic features for better numerical modelling. In order to obtain the dynamic behavior of framed buildings, the structures have been monitored using sensitive veloci-meters manufactured by Anet-GEODAS to measure the ambient vibration/response in its operational condition. Further to this, in order to know vulnerability of the buildings and to typologically classify the buildings, detailed information of buildings was collected. The building stock in this study mainly consisted of schools, residential buildings and partly commercial buildings. The damage classes ranged from no damage, moderately damaged, to a few buildings which were damaged but retrofitted. Mainly 3 locations were chosen in Nepal where there were still a few RC buildings were damaged either structurally or non structurallynon-structurally (most of the buildings are either demolished or retrofitted in the period of 15 months of the earthquake). The locations were Kathmandu valley, which had a damaged school building and a few reasonably well constructed/retrofitted buildings at a location called Dolkha situated in Charikot district of Nepal, which had significant non

Figure 4.1: Building 1 and its corresponding damaged state in the field study conducted in Nepal

structuralnonstructural damages and buildings with bad construction practices.
Firstly, a building selected for study was inspected briefly to extract some basic knowledge of the construction materials, methods, time, considerationsand considerations in the study. Later, detailed reconnaissance was carried out with measurements including height, dimensions and location of beams, columns and walls was done. Then, the location of Portable Intelligent Collector (PIC) sensors were decided including the number of sets of readings to be taken.
With a reasonable judgement and understanding of numerical simulation, the vibration data of some critical frames of the building is measured. Later in due course of this chapter, it is demonstrated how this data is processed by using operational modal analysis to estimate the natural frequencies and mode shapes of the building.

As already mentioned a PIC was used for measuring the response, which is connected to the recording station and the recording station is self poweredself-powered with an LiC battery. A total of 4 PICs could be installed at a time with two power connections for them.

1. Preliminary reconnaissance of the building, talk to the landlord for extracting some information like maintenance, usage, age, availability of drawings, etc.

2. Identify the building to be monitored and index the building with a unique label. Note down the GPS coordinates of the building and photographs of the buildings.

3. Collect the building details such as ownership (government, private, etc.), its predominant use, visual condition of the building, construction drawings, etc.

4. If the visual damage of the building is bad then the condition of the building is evaluated using the damage classification guideline.

5. Note the basic geometric information of the building by making a rough plot including column and beam configurations/dimensions.

6. Identify the important frames which are less stiff, have damages, in critical position.

4.2.1 Monitoring of building B01

As mentioned earlier for monitoring building B01 the same instrument GEODAS is used with PIC sensors to estimate the response of the building for ambient noise in the building. These sensors are veloci-meters which can measure in 3 directions, and since the ultimate use of data is mainly for obtaining modal parameters and therefore these quantities were accepted for the use. These sensors are called CR4.5-2S which has a sensitivity of 1V/cm/sec, made of hard aluminium body weighing approximately 1.5kg and a power input of 6V for each sensor. The GEODAS measuring station has a capacity of 6 channels with 2 power inputs, and an attached computer with LiC batteries of 12V.
The frame shown in figure 4.2 is the outermost frame of the building B01 and as shown 4 sensors aligned to the same position on each floor (close to the corner column) were connected to the instrument station by running cables over the structure. The top storey was not accessible in the building which is a practical limitation in real building in countries like Nepal, India, etc. and hence 4 sensors were placed starting from the ground to measure response in the frame and all four values were measured at the same time, hence a roving sensor was not required in this case. This building was locked after the Gorkha earthquake and hence there was no human activity in the building and the unwanted noises were low, and could be considered a silent building. The measurement parameters

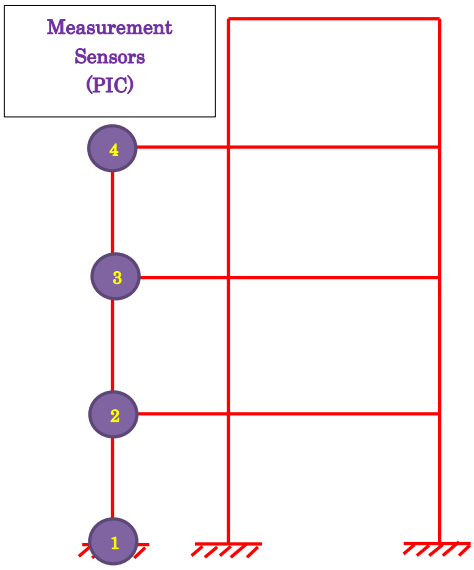

Figure 4.2: Monitored frame of building B01

were common to most of the buildings in Nepal, however, in this case a sampling rate of 100 Hz was used as the range of frequencies were less than 50hz for the building, the total duration of measurement was considered to be 20 minutes in total and no instrument filtering was used as it was intended to be applied if required during the post processing phase. The velocity response history of the building for 4 points is shown in figure 4.3.

4.3 Modal Analysis and Visual Analysis

As mentioned earlier, the RVS of buildings were conducted and the corresponding available information for a certain number buildings is are already tabulated to study the general characteristics of buildings to have confidence in the assumptions to be considered in the numerical modelling. However, in this study building B01 is considered for further detailed analysis and it is intended to discuss major observations at the site especially for the frame of reference for numerical modelling. This building (B01) was damaged during the 2015 Gorkha earthquake and the research expected various structural parameters in the study. Mainly, it was observed that the columns were of dimensionof dimension $300mm \times 250mm$ and overall geometry seemed to be symmetric, which gives an implication that it was built with general practice of construction in the country (though not with

seismic prescription of design) which could have a possible mix design proportions as 1:1.5:3 leading to M15 M20 concrete in practice. The failure showed some predictions on the poor reinforcement, cover of concrete, and lesser aggregate used exhibiting failures such as crushed concrete, spalled cover, and beam column joint failure. This could be substantiated from the general observation that when a ready mix concrete (RMC) is not used in practice due to the social and economic conditions, the concrete is hand or machine mixed and the target mix design strength, consistency and proportions is not accomplished leading to insufficient compressive strength, bad quality and detailing of reinforcement steel and sometimes even bad execution at the foundation as Nepal is considered to have hilly terrain at many locations. There mentioned information is useful in assumptions needed in the numerical modeling and discussing issues/challenges in the evaluation of response to the structure.

Table 4.1: Fundamental frequencies of select buildings

Building ID	**Number of Modes**	**Frequency (Hz)**	**Time Period (s)**
B01	3	1.41	0.71
B02	2	3.46	0.29
B07	2	3.67	0.27
B09	1	4.69	0.21
B11	1	5.93	0.17
B12	2	3.78	0.26
B13	2	3.16	0.32
B17	1	2.92	0.34

The data collected from this study is output-only data caused due to ambient excitation such as traffic on roads, human activities on buildings, wind, micro-tremors in the ground due to insignificant earthquakes, etc. In this condition, the structure is said to be in its operational condition and with an assumption that the input on the structure as white noise, in this study the technique called Frequency Domain Decomposition (FDD)[**?**] is being used for the modal analysis. FDD is an output only modal identification technique,technique makes use of Singular Value Decomposition (SVD) but is similar to the Classical Peak Picking method.

In the first step the power spectrum of all the four velocity time histories are as estimated as shown in figure 4.4 and in this it can be seen that the power of the first sensor is reasonably flat as it is on the ground and peaks could be seen at three locations in the remaining sensors. Confirming the quality of data collected in the experiment, the FDD is applied by extracting the PSD matrix of the response and corresponding SVD. The singular values of power spectral density plot of building B01 is as shown in figure 4.5. Similarly, the estimated frequencies (Hz) and and number of mode estimated of the other select buildings in Nepal is shown in 4.1.

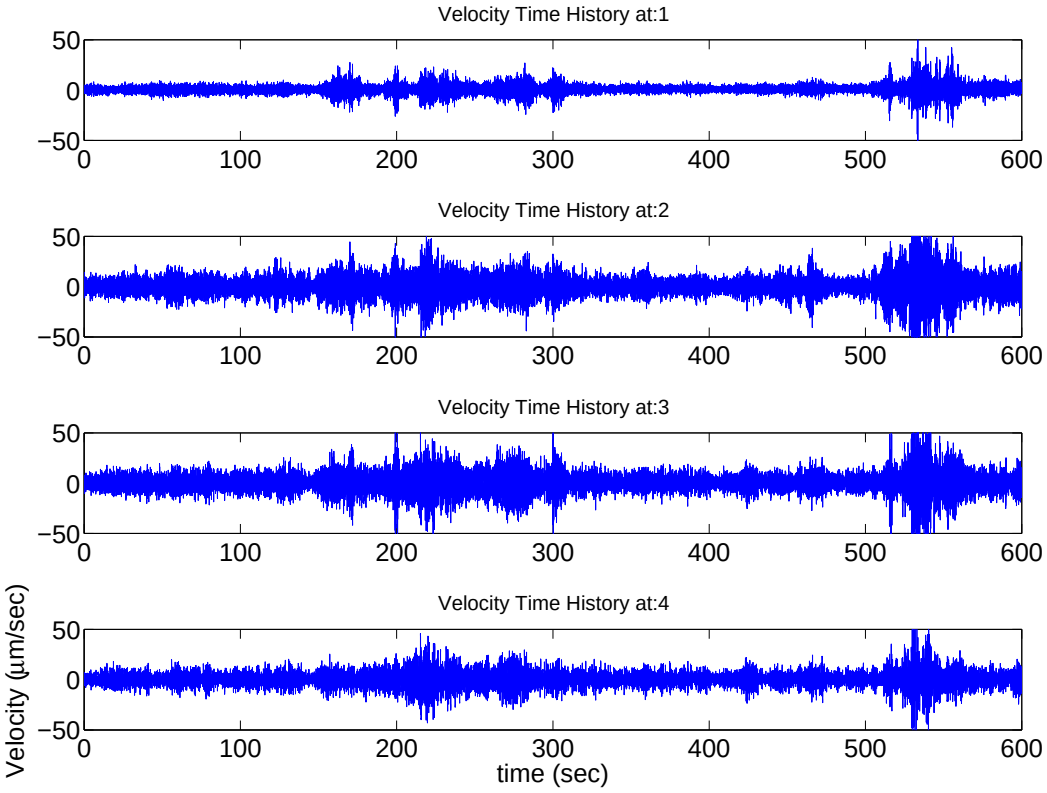

Figure 4.3: Velocity time histories recorded in B01

4.4 Material Identification

In this study, one building B01 has been selected for further analysis using identification and capacity assessment. In any case, there are two parameters which have been considered uncertain parameters and they are mass and scaled mode shapes. Firstly, mass is

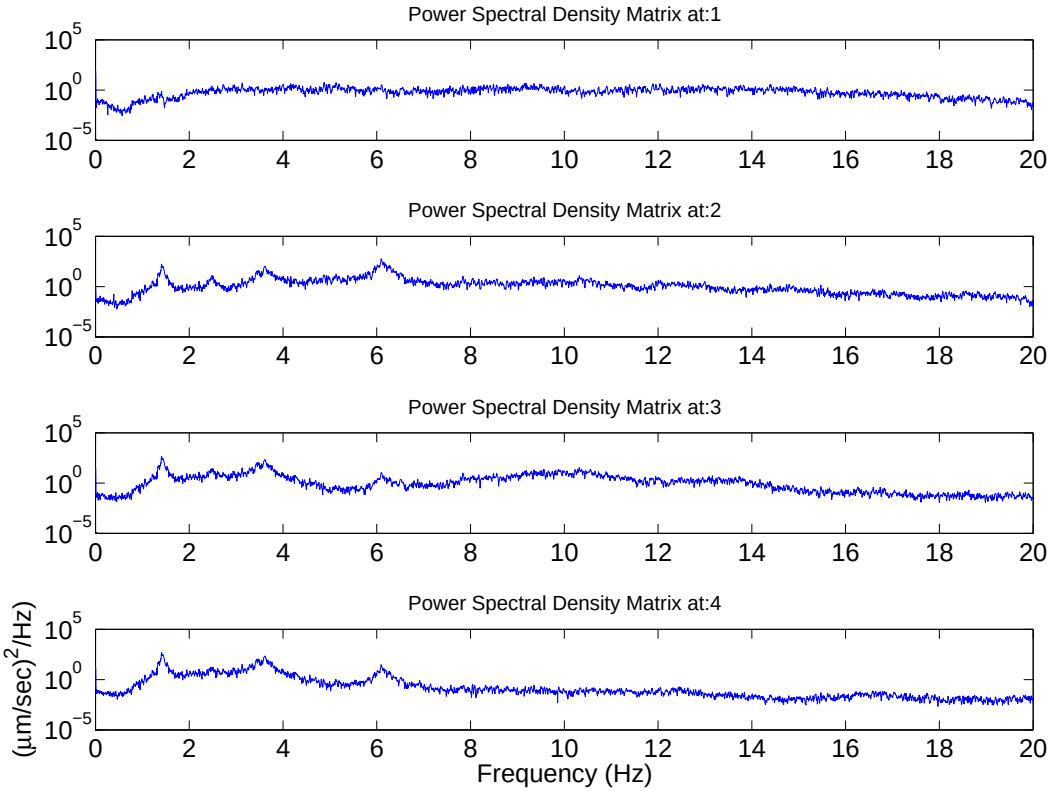

Figure 4.4: Power spectrum densities measurements of building B01

an uncertain parameter, initially it has been estimated based on the member dimensions and its standard densities and then two different cases of masses have been discussed in which it has been first reduced and then increased by 30%. These two values seem to be very uncertain however, the uncertainties could be this big as the whole structure is simplified into a small frame and the contributing masses could sometimes be huge and therefore it was reasonable to consider these cases as shown in table 4.2. Secondly, the scaled mode shapes is another uncertainty which is not dealt with in the current study but however, the ratios of the shapes remains to be reasonable through the vibration analysis, so the weightage in the step-2 of the optimization problem the weight-age of the residual has been reduced to 10% by retaining only the proportion of mode shapes and giving importance to the frequency residuals in further to have more confidence on assumed masses instead of scaling in the way explained in chapter 3. The results of the identification procedure are shown in table 4.3. In this case, the top point measurement of the building was not done due to lack of access to it and therefore in the simulation

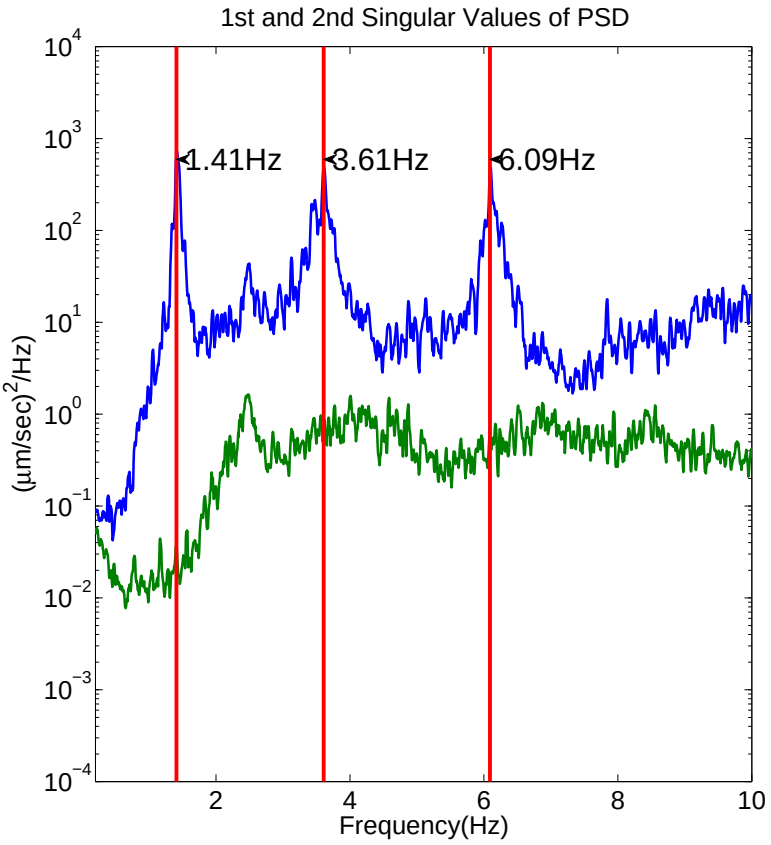

Figure 4.5: Natural Frequencies of B01

the modes were not correlated for the top, instead of which the whole mass was lumped to the 3rd degree of freedom and therefore it could be seen in the table 4.3, the effective stiffness of the top floor is very less as compared to the first two storeys.

From the simple identification procedure, each storey stiffness is identified but initial stiffness of sections areis needed for the modelling in AEM. Therefore, to obtain the equivalent initial stiffness, reverse of the procedure recommended by Hosseini in [24] is used. In this, the same equations are used in back calcualtionscalculations estimate E, or initial stiffness of a member for the current condition of the member. The equivalent frame obtained for building B01 is as shown in 4.10 and firstly, the assumed masses and estimated stiffness are based on 3 locations. The column and beam stiffness to moment of inertia are calculated first for simplified equivalent frame based on,

$$k_c{}' = \frac{k_c}{E_i} = 1/2\sum_{1}^{m} I_{ci}; k_d{}' = \frac{k_d}{E_i} = 1/2\sum_{1}^{m} \frac{I_{gi}}{l_i}; k_u{}' = \frac{k_u}{E_i} = 1/2\sum_{1}^{m} \frac{I_{gi}}{l_i} \qquad (4.1)$$

and then the equivalent initial stiffness is estimated from

$$E_i = \frac{k_{i-identified}}{k'_{fc}} \tag{4.2}$$

where,

$$k'_{fc} = 12\frac{k'_c}{h^2}\frac{k'_c(k'_d + k'_u) + 6k'_d k'_u}{{k'_c}^2 + k'_c(k'_d + k'_u) + 3k'_d k'_u} \tag{4.3}$$

In the calculations, the values are mostly based on measured and observed frame components, also the initial stiffness of beam is considered 5 times higher to cater for the masonry walls which are added as masses in the analysis The estimated initial stiffness of the structure for varying masses is as shown in the table 4.4

Table 4.2: 3 cases of simulations based on masses

Variations of Mass (tons) (3 Cases)		
Case 1: Calculated	**Case 2: -30%**	**Case 3: +30%**
16.4	11.5	21.4
16.4	11.5	21.4
25.9	18.2	33.7

Table 4.3: Identified stiffnesses in the cases

Identified Storey Stiffness (MN/m)	**Case 1**	**Case 2**	**Case 3**
DOF 1	8.37	5.86	10.89
DOF 2	9.17	6.42	11.92
DOF 3	4.35	3.05	5.66

4.5 Discussions and Conclusions

Majorly, the observations and inferences were obtained from the conducted visual survey [1-9] and response monitoring [10-14] of the buildings is enumerated as follows:

1. Most of the buildings in the survey had simple architectural feature providing mostly regular geometryregular geometry for numerical analysis

Table 4.4: Initial column stiffness of each storey

Initial Column Stiffness (GPa)			
Level	**Case 1**	**Case 2**	**Case 3**
Storey 1	12.97	7.91	14.69
Storey 2	14.20	10.30	19.13
Storey 3	17.99	12.59	23.39
Storey 4	17.99	12.59	23.39

2. The ground profile in most of the surveyed regions had slope terrains providing insights to use soil-structure interationinteraction in the numerical analysis

3. Buildings had no code compliance and had poor workmanship with significant non engineering defects such as improper stirrups arrangement, poor connections between storeys, etc.

4. Some of the buildings had achitecturalarchitectural demand such as short columns due to sloped terrains, basement storeys are shorter than the top storeys, and due to balconies caused vertical irregularities in the columns.

5. Balconies, non structuralnon-structural masonry parapets, and over hangs are observed to be very common practice.

6. The damages is seen in the buildings, though it is only non structuralnon-structural such as masonry unit cracks or mild cracks on the frame. These buildings were only a few years old, i.e. were constructed after year 2000.

7. A common problem observed in a few buildings is the existanceexistence of a shop on the ground storey, makes it a soft-storey, which is a seismically dominating phenomenon governing collapse in buildings.

8. A few buildings had re-entrant corners, non engineerednon-engineered designs these buildings could attract torsion in the moment resisting frames.

9. Some other peculiar issues noticed in the built environment included the exposing of reinforcement for the purpose of construction work in future, also construction of pent-houses in future. Some buildings in the town called Dolkha had buildings with

staircases, pathways, etc under masonry components or supported with masonry post which could fail in brittle way.

10. Generally, the buildings of interest were residential ones and therefore due to privacy concerns, running of cables into spaces, inaccessible roofs, some locations were inaccessible for placing the sensors and the methods of material identification becomes more precise with location of stiffness reduction, when the number of measurement points increases. Therefore, this calls for a need for instruments which can remotely measure the response of the buildings.

11. In this study the dynamic testing was done using microtremor measuring instruments, which are very sensitive devices for estimating the response of building for ambient vibrations, but since buildings are stiff and sometimes the modes are not excited by the ambient response of the building and therefore sometimes, this test would yield only one mode of vibration, which is vitrified from the results of a few buildings as shown in the table 4.1

12. The identified first fundamental frequencies of the buildings were in the range of 1.4 hz to 5.9 hz with a mean of 3.6 hz and standard deviation of 1.3 hz. This significant deviation is because of the variation in heights of different buildings and one building had very low stiffness as compared to others due to its damage in the 2015 Gorkha earthquake.

13. To better understand these fundamental frequencies, a set of earthquakes have been selected from seismically active regions in the world. The corresponding earthquake time histories and arias intensities are plotted in the figures 4.6 and 4.8. These spectral accelerations of these earthquakes are calculated for different time periods, and the specific building fundamental frequencies are overlayed on the on the plot of SPA in figure as shown in 4.7. It could be seen that the fundamental frequencies are mostly in the zone of peak spectral acceleration of the buildings.

14. In addition to damage, reasonable symmetry, building B01 had 3 clear peaks of frequencies from the analysis and was of interest in further analysis using Applied Element Method.

The analysis of the instrument collected data is categorized into three parts; firstly, the estimation of the vibration parameters of the structure, natural frequencies and mode shapes, secondly, the identification of location of damage and its severity of damage, thirdly, integrating the former two into the numerical tool, AEM to carry out further analysis to quantify the damage due to potential earthquakes to each of the buildings. This will be used in the development of fragility functions for this category of buildings.

Table 4.5: Assessment information from the Nepal field study 1

Bldg Id.	**Predominant Use and Ownership**	**Built year**	**Workmanship and Code Compliance**	**Site Morphology and Building Level**
1	Govt. school building	2000	Poor and no code compliance	Flat site
2	Govt. school building	Under construction	Poor and no code compliance	Adjacent to hill slope and entrance is on higher slope
7	Private Residential cum Shop Building	Not known	Poor and no code compliance	Downward slope with entrance on higher slope
9	Private residential	2009	Poor and no code compliance	Downward slope with entrance on lower slope
11	Private, office and residential	2014	Good workmanship	Downward slope but flattened for construction
12	Private residential	1999	Poor and no code compliance	Adjacent to hill slope but flattened for construction
13	Private, residential and commercial	2004	Poor and no code compliance	Downward slope and built on split levels
17	Private Residential Building	2010	Good workmanship and designed with seismic features	Flat site

Table 4.6: Assessment information from the Nepal field study 2

Bldg Id.	**No. of storeys**	**Average floor Area (m^2)**	**Architectural Features**	**Geometric Features**
1	4	140	Relatively more symmetric	Parapets at the roof
2	2	117		
7	4		Presence of short columns	Balconies and cantilever slabs in each floor
9	3	59.5	Short columns at the staircase	Balconie
11	4	64.8		Parapet, balconies and walls in cantelever projections
12	3	94.24		Parapet, balconie and sunshade
13	4	40	Presence of short columns, Basement storeys are shorter	Parapet, balconie and over hangs of 1.5m
17	3		Outer dimensions at the plinth level smaller than at roof	Parapet, Balconie, Sunshade

Table 4.7: Assessment information from the Nepal field study 3

BldgId.	**Visual Condition**	**Irregularities**	**Damage History**	**Other Comments**
1	Damaged	Top floor staggered	Cracks at coulumn joints, rupture in columns, cracks in staircase, out of plane failure of in-plane walls	
2	Not good			Poor construction practice with exposed reinforcement and inaccurate form work
7	Damaged		Out of plane failure of infill walls, 2-5mm in-plane diagonal cracks in some walls	Open storey on ground due to a shop
9	Poor		Damage at plinth	
11	Good	Penthouse on the top	Minor cracks in infill locations of the walls	
12	Damaged	Penthouse on the top causing re-entrant corners, partial open storey and masonry posts on 1st storey	Out of plane failure in inplanein plane walls, diagonal cracks on basement storey walls, cover spalled off from columns	Penthouse was constructed after 10 years of original construction
13	Damaged	Mass irregularities (top floor), rentrantreentrant corners, slabs and beams resting on URM	Storeysories noticeably leaning, minor cracks in columns, out of plane failure of masonry wall and cantelevercantilever wall heavily damaged	Stair case and escape way was in the cantilvercantilever bay with masonry posts
17	Good	Re-entrant corners		

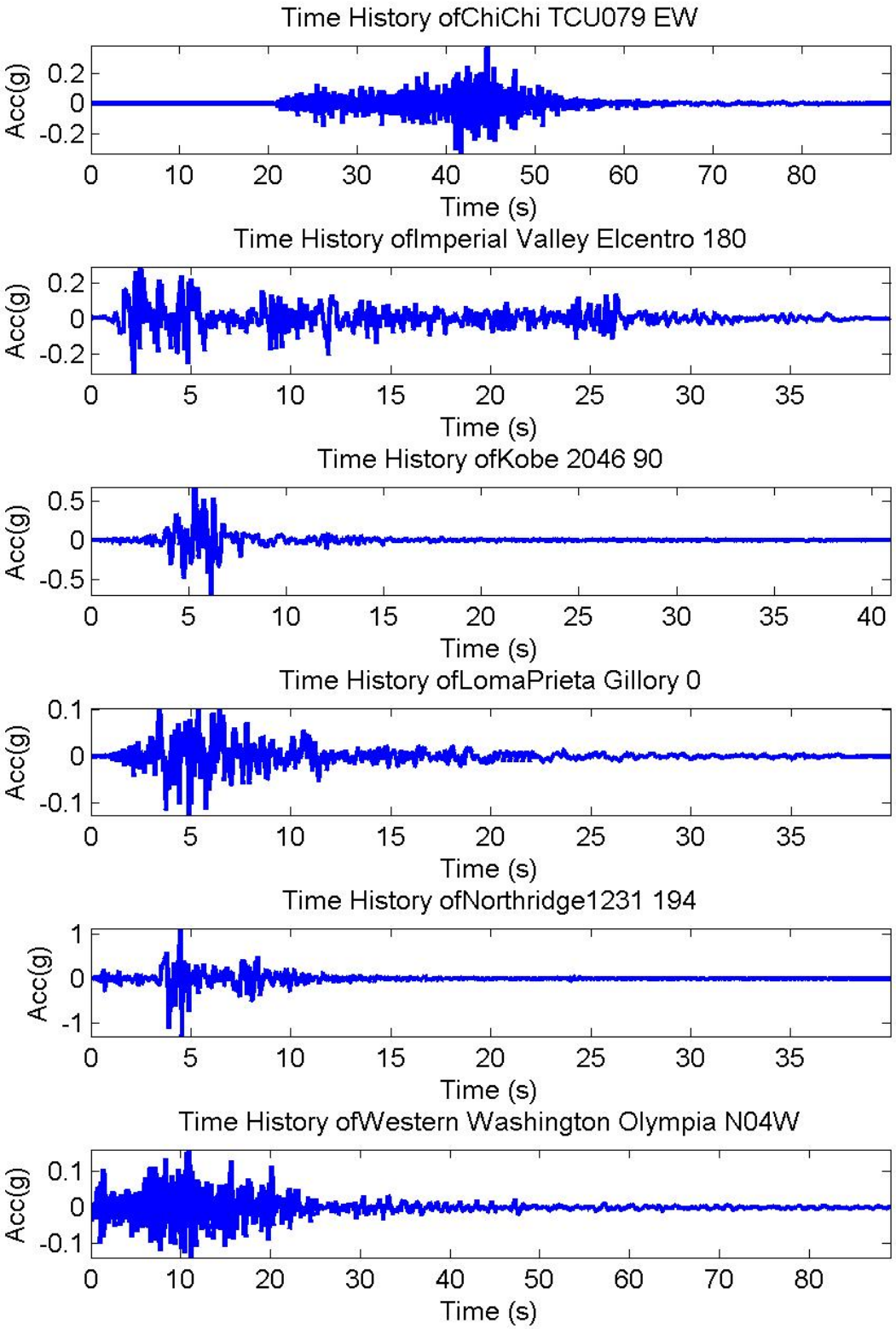

Figure 4.6: Acceleration time histories of past earthquakes

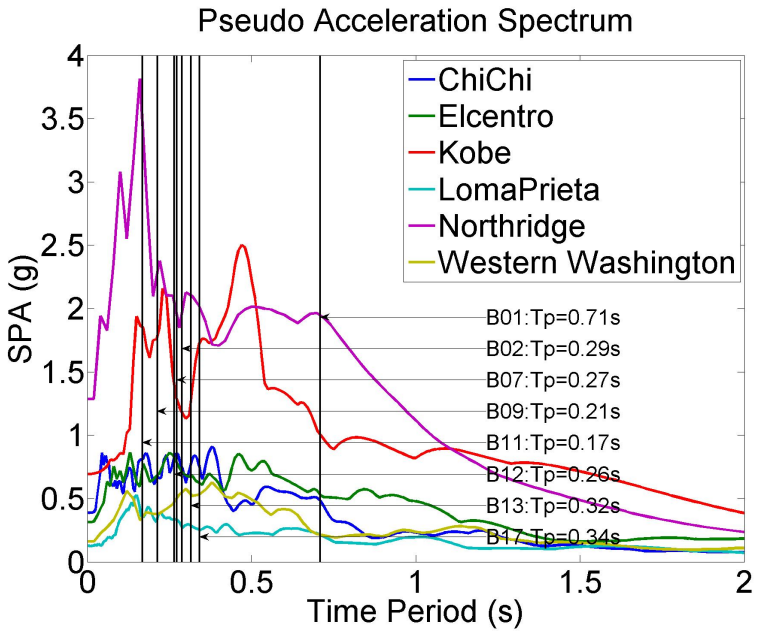

Figure 4.7: Pseudo spectral acceleration of different earthquakes

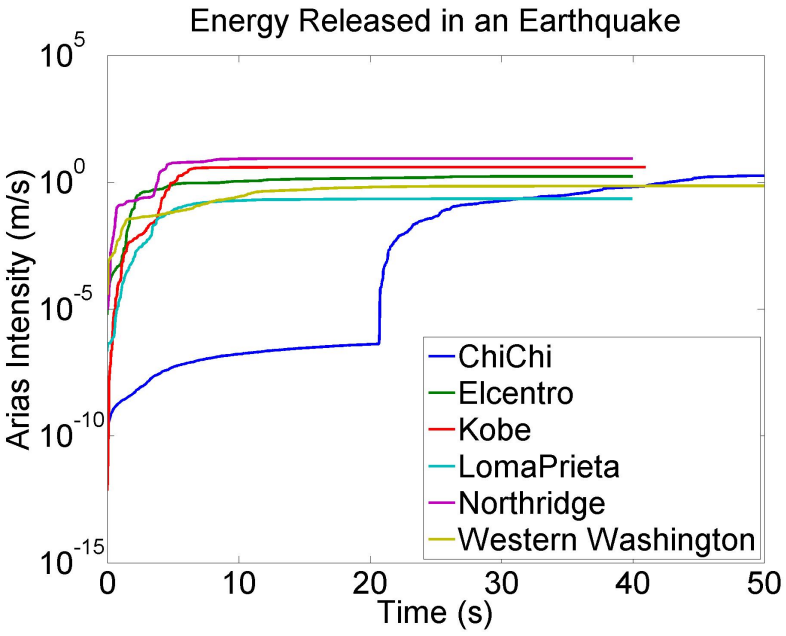

Figure 4.8: Arias Intensities of different earthquakes

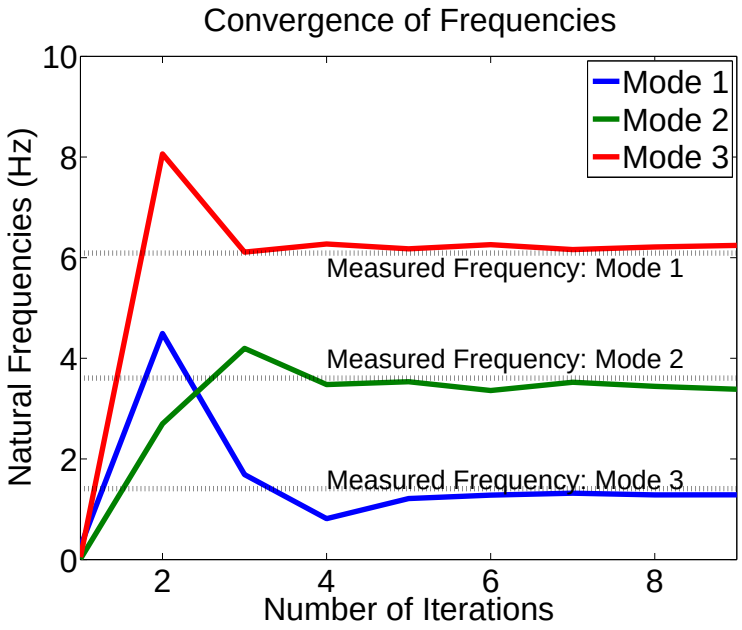

Figure 4.9: Frequency convergence after identification in B01

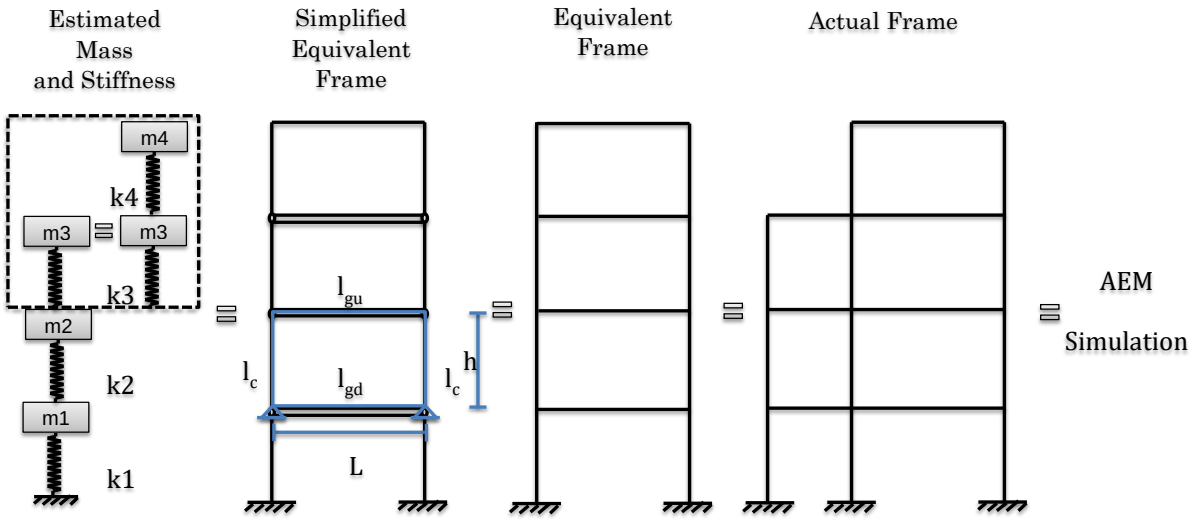

Figure 4.10: Estimation of initial stiffness of members from equivalent frame

Chapter 5

Seismic Capacity Estimation of Buildings

5.1 General Remarks

In chapter 3 it was introduced that the damage assessment procedure is divided into 4 levels and the ultimate goal of the methodology is to estimate the seismic capacity of buildings. In the previous chapter the modal analysis was carried out for real buildings in Nepal and identification was done with certain modifications in the optimization routines. However, by using the identified stiffness of the buildings, it is intended to estimate the seismic capacity of the buildings. In this chapter, the seismic capacity of RC buildings is estimated based on damage index formulations of member deformations. Initially, this capacity estimation has been validated based on simulations results of AEM for a previously validated frame and then the 3 cases of building B01 which was discussed in the previous chapter have been simulated for seismic capacity estimation.

5.2 Background and Methodology

Seismic capacity is assessed by applying incremental dynamic or earthquake loads to the numerical model of a structure. It is carefully understood by knowing the details of deformation, stiffness, strength and energy dissipation characteristics of a structure levels of seismic demand on the structure. These response characteristics are estimated at different levels of a structure such as members, storeys and even the complete structure.

Ideally, it is intended to estimate these parameters at member levels in more detail and extend it to capture the behavior at the complete structure level to be able to discuss the overall capacity of it. In this study, the capacity is estimated based on damage indices, which is defined as a measure of damage as functions of estimate-able response parameters from numerical simulations. A damage index is correlated to a structural damage state, which is usually an observable condition or state of a building which is developed based on observed, experimental or simulated state of damage for building after seismic effect on a number of structures. A damage index is usually normalized to lie between 0 and 1, where the former one represents no damage and the later represent complete or collapse state of damage. Initially, damage states were formulated for post-earthquake assessment of damaged structure visual condition, however its generalized form has been of extensive use in the field on seismic vulnerability and reliability studies of against potential earthquakes in future. Therefore, local damage indices (LDI) are estimated based on damage variables and then corresponding global damage indices (GDI) are intended to be estimated, which is further compiled with different damaged states to obtain the damage probability matrix. Here, it is intended to estimate the local damage index (LDI) of each member using Park and Ang Indices, modified to consider chord rotation of members. Then the global damage index of the building are estimated using Weighted sum of LDIs obtained. Though there are many capacity assessment methods in the literature and among them Park and Ang [43] is one of the most widely accepted parameter due to it's extensive validation over a large number of experimental cases. In this study the same damage functional has been studied, however, certain modifications were incorporated for ease of calculations in the case of distinct element methods which has opened crack and rigid element modelling. Though the fundamental intention of this study is to use these techniques for studying the capacity and vulnerability of all typologies existing in RC buildings but however, as a preliminary step; this study focuses on a particular non-ductile type of building in Nepal which was previously subjected to an earthquake in the past, therefore considering this lack of ductility, the damage index developed by Park and Ang was modified to include only the deformation component of the function, which is published by [31]. The local damage index is given as

$$LDI = \frac{\theta_m}{\theta_u} + \beta \frac{\int E}{M_y \theta_u} \tag{5.1}$$

Where, θ_m is the chord rotation of member end sections obtained from AEM, θ_u is the ultimate chord rotation of the member obtained in monotonic loading, $\int E$ is the energy dissipated at the cross section of member end sections, M_y is the yield moment capacity of the member obtained in monotonic loading and β is the parameter for deciding the contribution of energy dissipation of the members. The mentioned formulation represents local damage states of members based on the same damage states provided by Park and Ang as shown in table 5.1. In this study, the frame B01 chosen for further analysis was a non ductile frame and therefore the damage caused by the dissipation of energy could be ignored and therefore the LDI of beams of columns got reduced to

$$LDI = \frac{\theta_m}{\theta_u} \tag{5.2}$$

And the storey damage index (SDI) is considered equally weighed with LDIs and the GDI is estimated as weighted sum of LDIs, where the weights were obtained as the inter-storey drifts ($drift$) of the SDIs.

$$SDI_{i_{storey}} = \sum_{1}^{i_{storey}} LDI \tag{5.3}$$

$$GDI = \frac{\sum_{j=1}^{n_{storeys}} drift_j \times SDI_j}{\sum_{j=1}^{n_{storeys}} drift_j} \tag{5.4}$$

However, this simplified modification for convenience and ease of calculations in the quantification of damage needs further evaluation and comparison with other damage index formulations developed for similar purposes. Nevertheless, a validation has been performed in this research which is discussed in the consequent sections.

5.3 Validation of Deformation Based Damage Indices

In the previous section, a method to estimate the damage index of members and global damage state is described with a few necessary modifications, and for the purpose of better understanding of this evaluation, it was understood that this method had the potential to represent real quantification of non-ductile buildings, a comprehensive validation is needed. Therefore, the same frame (F01) validated in chapter 2 has been selected and as mentioned there 2 sets of ground motions scaled to 0.21g (Intensity I) and 0.42g (Intensity II) have been applied there, in which the first set was already discussed where the intention was to see the effectiveness of the tool, now the complete validation where the intention

Table 5.1: Damage states to damage index obtained from [43]

Damage State	**Visual State**	**Damage Index**
D1	Local occurrence of cracking	<0.1
D2	Minor cracks; partial crushing of concrete in columns	0.1-0.25
D3	Extensive large cracks; spalling in weaker elements	0.25-0.4
D4	Extensive crushing of concrete; disclosure of buckled reinforcement	0.4-1.0
D5	Partial or total collapse of building	>1.0

is to validate damage indices and the damage states, which is being discussed with an emphasis on how the correlation between experimental observations and estimated values are. The complete displacement history with both the intensities are shown in figure 5.2 and it has good match with phase and amplitudes. The visual damage state could be verified with the deformed shape and crack pattern as shown in figures 5.1 after intensity I and after intensity II ground motions.

In the experiment the experiment was conducted upto the two intensities and the experiment was stopped as the authors observed that the frame had already lost all the moment resistance and joints were fully damaged, consequentially it would collapse with little amount of energy of loading. This appropriation is considered and an additional loading is applied to the frame in the form of ground motion until high deformations were verified. In addition to completing the basic forms of validation in the form of response histories and cracking pattern, rotations of end sections of each vertical and horizontal members accounting to a total of 10 members with corresponding 20 cross sections, have been calculated, which is the chord rotations θ_m of elements in one line of a member. In the defined local damage index function these values have to be compared with the ultimate chord rotations θ_u in principal. An ultimate chord rotation of a member is the maximum capacity of that cross section of the member which could be obtained from monotonic loading applied on it, alternatively it could also be obtained from member dimensions, strength parameters, reinforcement and dead loads acting such as axial forces

on the structure. In this study, θ_u was calculated using the empirical relationships based on [42]. Further, the ratio of damage index was estimated for each cross section of each member and the damage state definitions provided by Park and Ang have been used to define damage states based on the damage indices estimated. Now, these indices have to be validated with the experimentally observed damage states, therefore, based on the published literature the visual damage states were estimated based on engineering judgment which could give a close match to the real damage states. These damage states were collected at the end of both intensities of loading and the estimates are correlated to the observed values in the experiment as published in the literature of the experimental study, the correlation plots are shown in figure 5.6. The first 10 values in the scatter ratios correspond to the columns and the later ones to the beams, and it could be seen that the column damage states are well correlated and the remaining ones are reasonably correlated and it could be attributed to simplified formulations and limited calibrations. However, more importantly the local damage states are more important in columns in the requirement of severe and collapse damage states especially when contributing to the global damage states. It can be seen in the figure that the all member cross sections have reached complete damage states immediately after some loading on to the frame. The estimated damage index for each member is shown in figure 5.4 and the storey damage index is estimated as the mean of the member damage indices since the effect of energy dissipation in low in the case of non ductile frames, the overall global damage index of the structure is obtained as the weighted sum of the storey damage indices. Since non-ductile buildings are drift controlled, the weights were decided based on the inter-storey drifts of each building. The corresponding storey damage indices and global damage index is shown in figures 5.5a and 5.5b. The global damage state of the structure after the two intensities reached collapse phase as mentioned by the authors in the literature.

The results of four different time steps shows change in different damage states at different joints. At 15s, the frame has minor damage at all intermediate joints which tend to become severe as the time step increases. After 60s the joints at first floor shows severe damage state while the base joints also shows minor damages. From figure 5.4, the different damage states can be predicted from the estimated damage index values for 20 different members of F01 frame. Almost half of the members of F01 frame shows minor damage after 20s which turns into moderate damage after 40s. The simulation results

shows that almost all members have severe damage after 60s time. The corresponding story damage indices and global damage indices from figure 5.5 have been shown. There is a little difference in storey damage indices after 40s but the trend of damage in both storeys is similar with respect to time so the global damage index result also has same pattern. From the figure 5.6, the numerical results can be validated at intensity I and intensity II. The scatter ratio values of columns could be correlated very well as compare to beams for which these values are not much correlated but as the local damage states are more important in columns so it can fulfill the requirement of severe and collapse damage states to give global damage states.

5.4 Numerical Simulations

In this study, one of the monitored buildings have been selected for detailed capacity and vulnerability assessment. In this purpose, building identified as 'B01' is chosen for detailed analysis. The identified properties of this building was already discussed in the previous chapter. The numerical modelling of this building is discussed in this section. As already discussed there are various parameters which are involved in a numerical model to represent a real building, however concerned with the preliminary modelling of this building, it is intended to simplify a few characteristics and the identified stiffness is studied with primary focus. Three cases of building B01 has been chosen in this study, and in each case the applied masses and estimated stiffness from the identification is incorporated in AEM. In addition to this, a verification of the field study is also conducted for verifying the damage occurred to the building B01 after Gorkha earthquake. The various simulation parameters used are discussed in this section for all the 3 cases and a verification case.

5.4.1 Input parameters in the simulation

Geometry

The geometry of the building is observed to be reasonably symmetric with only rectangular columns and beams. The outer dimensions of the building was measured during the field observation in which the frame of interest is measured to be of 7 m in length with two

bays of 1.6 m and 5.4 m and a total height of 11.2 m, is divided into 4 storeys. The columns were of two types, one with 250 mm x 300 mm and 300 mm x 300 mm cross sections; the beams were monolithically casted with the slabs with a dimension of 250 mm x 250 mm. The slab depth and wall width are measured to be 0.3 m and 0.12 m, which were used in calculating the approximate contributing storey mass of the building. The exact configuration of reinforcement in the building is not extracted accurately but inquiring with the common practice and some information from the spalled cover, an approximate information on the steel bars and lateral reinforcement was extracted. The main reinforcement used was 16 mm dia re-bars and 12 mm dia rebars and 8 mm stirrups with 200 mm spacing. This model was numerically modelled in AEM as 10 sections comprising of 2351 elements,9 boundary elements, 10 springs on each side with 40340 springs in total and 243 rebars including stirrups.

Material properties

The major material property of interest in this study is based on the field study (from both response monitoring and visual survey). In this research, the preliminary modelling has been discussed and the initial stiffness of each material property is considered, which is obtained from the analysis using ambient response monitoring. The results of initial stiffness from lateral storey stiffness identified from the identification procedure is carried out using the equivalent frame technique and is of each member is discussed in the previous chapter. The same values are used in this chapter for numerical simulations for all three cases (1, 2 and 3). In the case 0, the initial stiffness of all storey is taken to be top storey stiffness with a premise that that the lateral stiffness of top storey is unaltered during the earthquake. This study is shown in the figure 5.8 and the corresponding natural frequency estimates to be 1.6 hz (whereas, the current fundamental frequency is 1.4 hz) which is assumed as the initial state of the structure. In addition to this, the other properties of strength of the structure is estimated based on visual survey and inquiries as discussed in the previous chapter. The compressive strength from the mix design followed in the area is approximately to be 15MPa to 20 MPa, but considering the non engineered construction practices and limitation, a conservative value of 15 MPa is considered for all 3 cases (one to three) but a compressive strain of 0.002 is considered for case 0 or the verification case of the building. The rupture strength is kept 5MPa to account for the heavy inertial

forces occuring from the non structural masses in the preliminary model. The modal damping of $\zeta = 5\%$ has been assumed in the study. The rebar stiffness is retained with a minimum reduction to 180 GPa but however, the condition of the bars were bad ask seen in the sight, so to be on the conservative side the $fy = 250MPa$. The same material models of AEM were used but the concrete post peak residue was kept a constant of f_c. The residual factor in shear material model is kept equal to $rv = 0.5$ as suggested by [54] for the frames. In addition, in this preliminary model the masonry infill in the structure had been modelled as additional elements with corresponding masses and therefore, the elements are considered rigid to avoid inertial effects.

Ground motion selection

In case 0 for verification, the real ground shaking from the 2015 Gorkha earthquake is chosen as input. The ground motion is recorded at a station called Lamjung, in Nepal and the earthquake had a PGA of 0.15g causing it to be a small earthquake, however no reliable information is available to ascertain the claim. The ground motion and its pseudo spectral acceleration is shown in the figure 5.9. It could be seen that the maximum spectral acceleration is seen on the East-West (EW) component of the earthquake and therefore, it is selected as input in the analysis, however the duration of the earthquake is longer and therefore, considering the simulation time the ground motion is further trimmed to 60 secs to have the maximum energy from the motion.

Three cases, 1,2 and 3 of B01, the vulnerability assessment had to be conducted using real earthquake quake time histories as input data. In order to do this, a catalog of earthquakes are prepared selected from active seismic areas. All the time histories were studied based on previous observational data against PGA values to be able to cater for extensive damage states. The corresponding time histories and their pseudo acceleration spectrum are shown in figure 4.6 and 4.7. The corresponding Arias Intensities of this earthquake is shown in figure 4.8. Based on these inputs 3 sets of ground motion time histories have been chosen incrementing from Chi-Chi earthquake, then Elcentro motion and then Northridge Earthquake are applied to the three cases of the building. A series of incremental dynamic loads in the form of ground motions is to be applied to this structure. Figure 4.7 suggests that the building B01 has the lowest fundamental frequency with respect to any other buildings in the field and attracts higher pseudo spectral accel-

erations from all earthquakes; therefore, the 3 critical ground motions mentioned earlier is prioritized with increasing energies is selected for application as shown in figure 5.10. The reason for using lower earthquakes from the collection of earthquakes lies in the fact that the building seems to be reasonably weak and has very low ductility and a brittle failure was possible.

5.4.2 Assumptions and considerations

The discretized numerical model in for all three cases are as shown in the figure 5.7a. Further, due to limitations and scope of this study the numerical model has been simplified and for this purpose it is called a preliminary model. The major considerations in the simplified model are

- The properties are identified at only a limited number of locations causing insufficient measurements.
- Material stiffness is averaged to a storey
- Damage is considered as reduction in stiffness of the material
- The masonry infill walls are modelled as non structural rigid masses attached to the beams
- Since the rebound hammer test was not conducted, the material strengths are assumed based on experience
- To assess the capacity of the structure, only a single type of Damage Index (Park and Ang) is considered
- The reinforcement information was based on judgment and from the RVS done in the field survey and was approximated based on the general practice
- A 5% damping has been assumed for RC buildings
- The strength of the building (f_c and f_t) is equally distributed to all elements in while modelling

5.5 Simulation results

A verification analysis case 0 and three cases 1, 2 and 3 of B01 have been simulated with the ground motions. The results are discussed as follows:

5.5.1 Verification of B01: Case 0

The verification of damage to building B01 due to 2015 Gorkha earthquake is being done using the simualtion on AEM as mentioned earlier. However, adequate information is not available in terms of the initial condition of the building as well as the exact ground motion which occurred at the site of the building. This is due to the reason that the Gorkha earthquake occurred in a quiescent state and the preparedness levels were lower, therefore there was only one strong motion recording center was present at the time of the earthquake, which is significantly away from the location of the building B01. Hence, the simulation results would only be a representative of the earthquake and this could also be a major source of uncertainties. The roof displacement response time history of the same is plotted in the figure 5.11 and it could be seen that the maximum displacement was seen at the PGA of the ground motion with almost the same period of motion which essentially informs that this long period building was affected during the Nepal earthquake. The corresponding damage could be seen in the form of deformed shape and cracked springs in figure 5.12 and it could be seen that compressive failure in the columns are in a way similar to what was observed in the field. In addition to this, the damage state seen in this is also similar to the identification estimated from the simulations, where the stiffness had actually reduced towards the top storeys. The excessive cracking seen in higher storeys are due to micro cracks in the top storey columns could be due to internal cracks of springs and also due to dominating interial forces of excessive masses, these limitations could be eliminated by making a detailed model in the analysis.

5.6 Damage analysis of B01: case 1,2 and 3

The roof displacement response time histories of the three cases are shown in figures 5.13, 5.14 and 5.15. It could be seen that all the three cases had attracted similar response of

which Case 1 and Case 3 fail faster than Case 2 which has lighter structural mass and stiffness for the same capacities. The building suffered severe damages towards ChiChi earthquake ground motion and had gone into collapse at about $t > 50s$ in all cases. The corresponding member damage states of these buildings are shown in figure **??**, **??** and **??** which shows that initially all members have suffered moderate damage but as the energy of earthquake increased, had caused a sudden brittle collapse in the buildings. The visual damage states at time steps of 30s, 40s and 50s for the buildings which is shown in the figures **??**,**??** and **??** and it could be seen that since the deformations are larger on the top storeys, they have attained collapse state faster. The larger damages are seen in the top storeys in the damage index figures because of higher deformations and stiff horizontal elements due to wall weights from rigid elements and also the capacities of the frame is lower due to damage, which would make it fail faster than softer members.

The extracted global damage states are required to be converted into probabilistic damages for a group or class of buildings and therefore, the input ground motion to the analysis is needed to be converted to corresponding ground motion parameter, here one of most widely accepted intensity parameter MMI is selected because of its comprehensive significance and simple definition. Therefore, the arias intensity I_h for the three earthquakes applied in the simulations were converted based on an empirical relation in [67] given by:

$$I_{mm} = 7.25 + 0.89 \log I_h \tag{5.5}$$

The I_{mm} values and GDIs for all three cases are shown in the table 5.2 and it could be said from this that since the building was already damaged during the Gorkha earthquake of 2015, there seemed to be a sudden collapse in all three cases as soon as the intensity changed to VIII from VII, which is also due to wide intervals in the Arias intensity and MMI scale conversion as shown in the figure 5.10. Also. there is a possibility of non estimation of intermediate damage states by the used damage index formulations, which is also mentioned in the literature [49].

Table 5.2: Global damage indices of B01 over MMI

MMI	Case 1	Case 2	Case 3
V	0.01	0.01	0.01
VI	0.02	0.01	0.02
VII	0.08	0.04	0.06
VIII	1.00	1.00	1.00
IX	1.00	1.00	1.00

5.7 Conclusions

5.7.1 Discussions and recommendations

- One of the major sources of uncertainties in this study is the estimation of masses and to handle it ideally a coefficient of variation with identification outcomes and the masses had to be done. In this case, to emphasise this importance, variation of masses had been done.

- In the modelling, the other strength related material properties and failure criteria had been approximated with engineering judgment but it has to be more realistic to identify the strength, non engineering defects related issues and failure criteria of materials have to be considered in detail.

- The mass in the frame actual comes from the walls, and in this case it has been modelled as rigid elements, which is a major source of inertial failure and the rigidity has been adjusted to avoid such failure. It is however recommended to model the walls with appropriate material models and interaction with concrete members.

- Finally, as the reliability of the outcomes are subject to modelling uncertainities, therefore it is recommended to develop a detailed model with brick elements with corresponding material models in the simualation, a probabilistic distribution of material properties in the numerical modelling, soil-structure interation with additional ground elements and use of other damage functions to cater for intermediate damage states.

5.7.2 Conclusions

Seismic capacity estimation based on damage index formulations on the outcomes of AEM simulations has been shown and it has been validated for an experimental frame. In the current study, it is intended to discuss the damage states of a vertical and horizontal members corresponding to its damage in terms of observed engineering parameters. In this study, the damage functions and definitions of members are used based on [43], which were modified accordingly for the requirement of ductile buildings. In addition to this, the building studied in Nepal has been verified with a numerical simulation by fusing with the properties of identification done in the previous chapter. In this context, a reasonable verification could be done for the frame

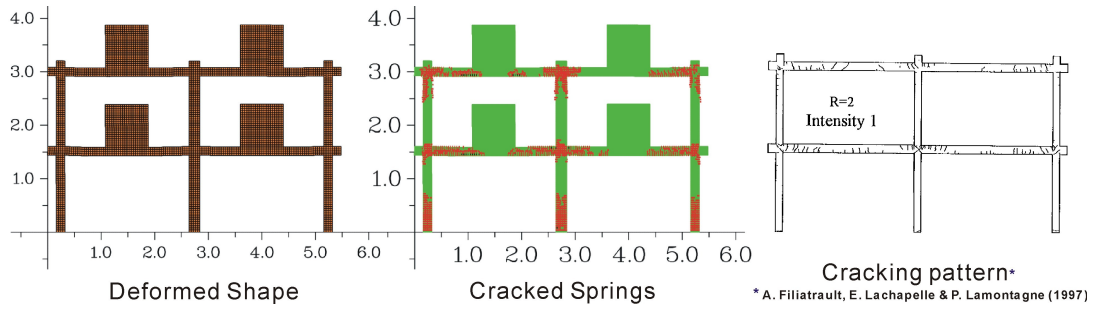

(a) After intensity 1

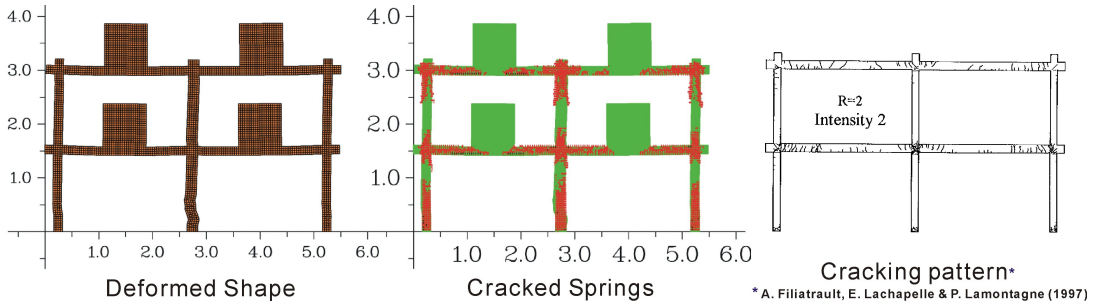

(b) After intensity 2

Figure 5.1: Visual states and cracked springs in the frame with experiment

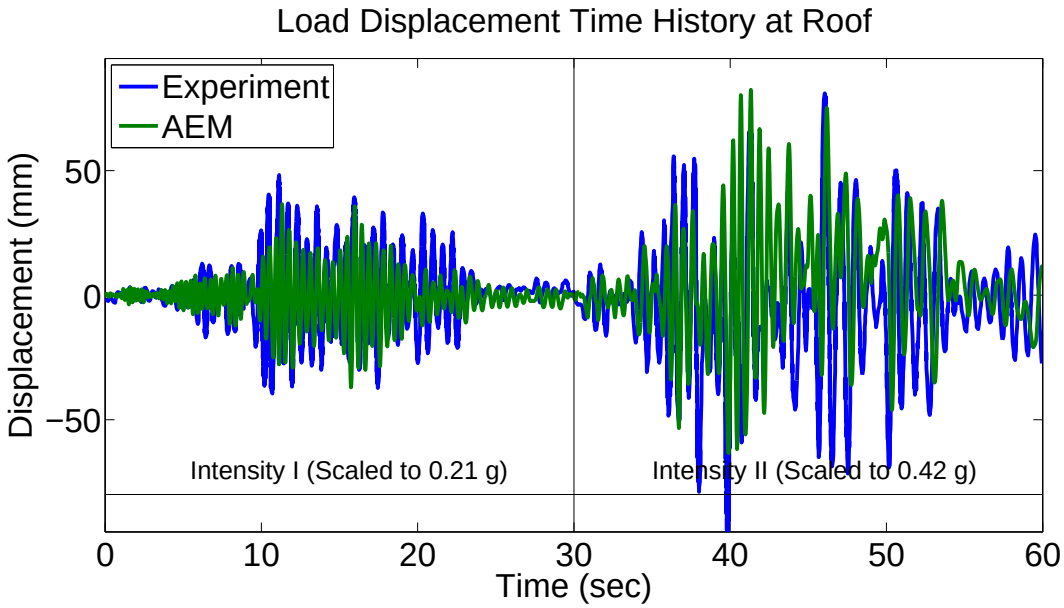

Figure 5.2: Response history of the frame F1 at the roof after both intensities

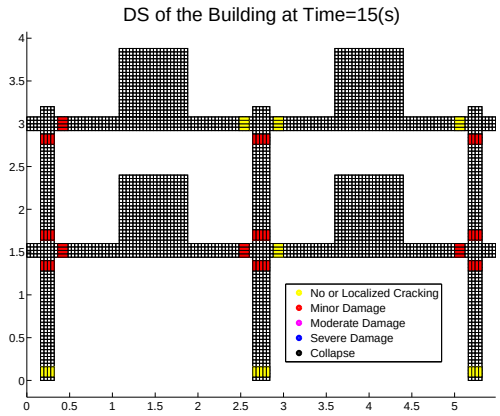

(a) Damage states of numerical frame after t=15s

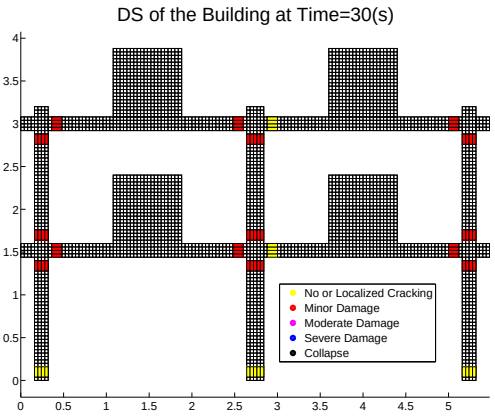

(b) Damage states of numerical frame after t=30s

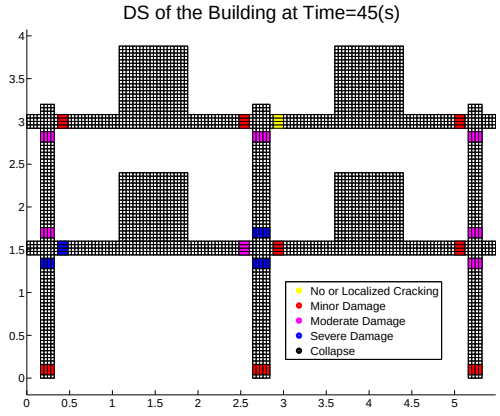

(c) Damage states of numerical frame after t=45s

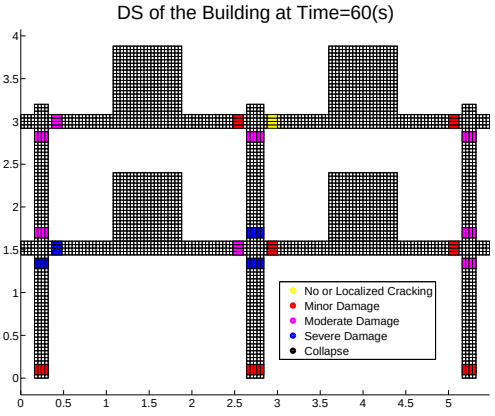

(d) Damage states of numerical frame after t=60s

Figure 5.3: Damage states of the building F01 based on damage indices at different time steps

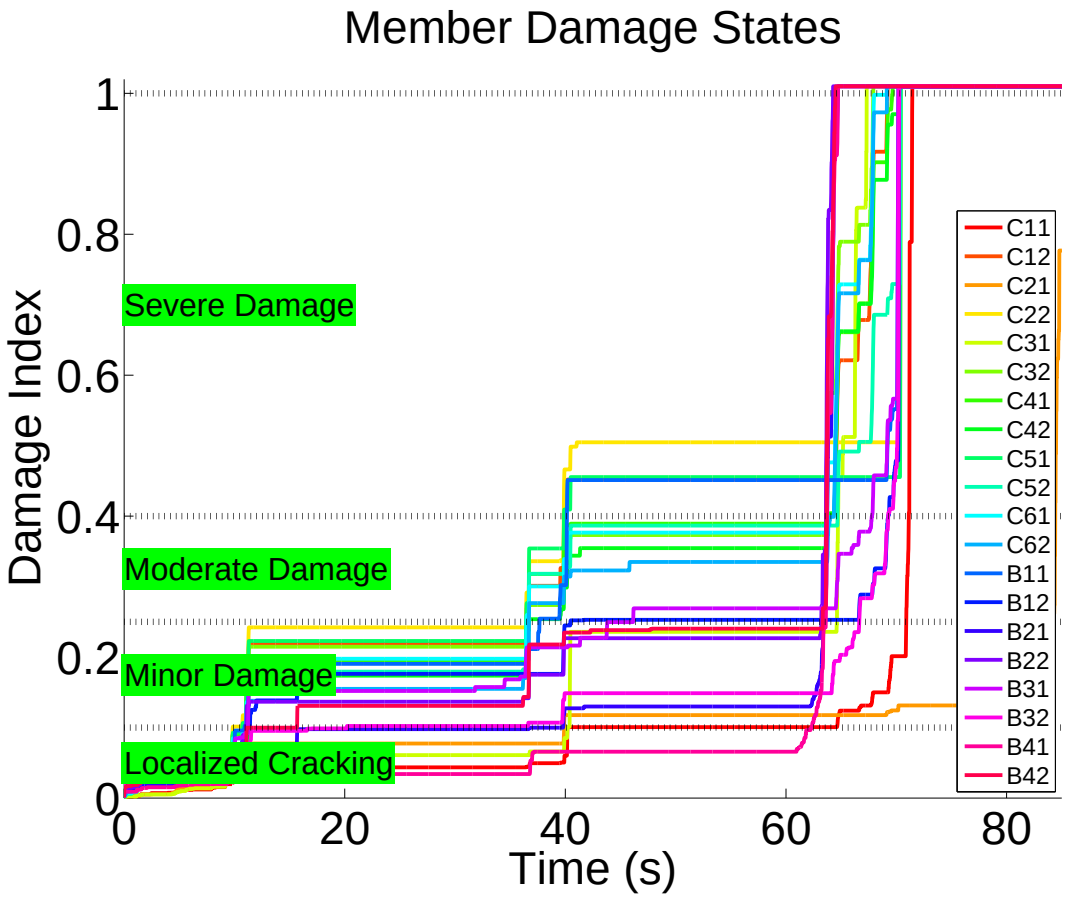

Figure 5.4: Damage states from simulation of F01 frame

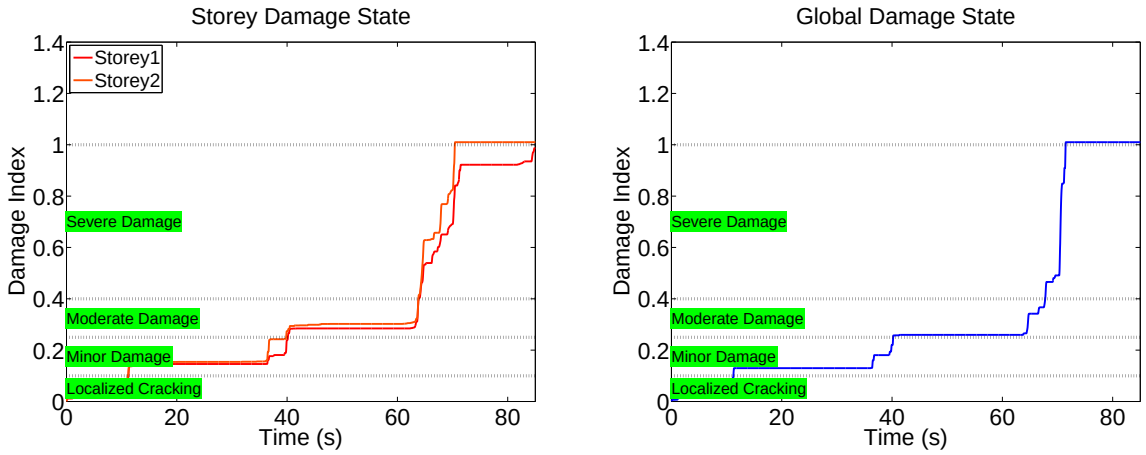

(a) Storey Damage Index

(b) Global Damage Index

Figure 5.5: LDI and SDI of F01 frame

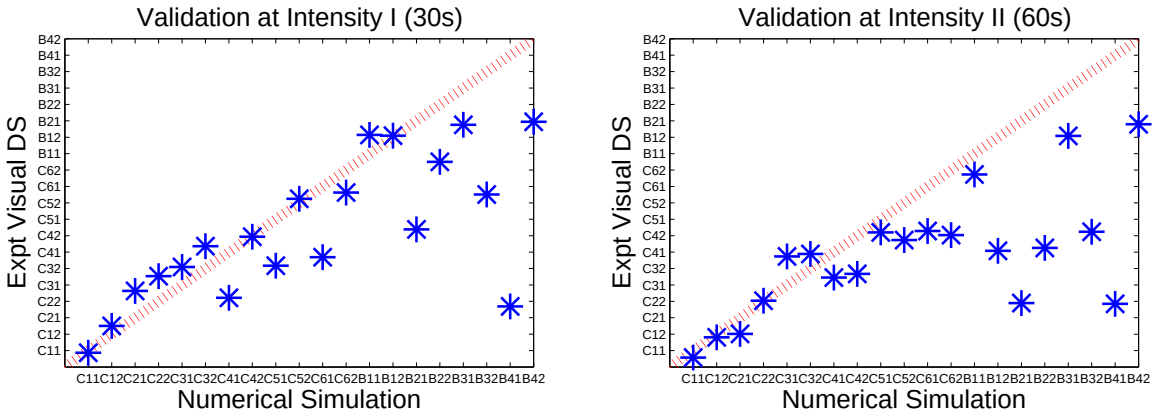

(a) Correlation after t=30s

(b) Correlation after t=30s

Figure 5.6: Correlation of visual and estimated damage states of F01

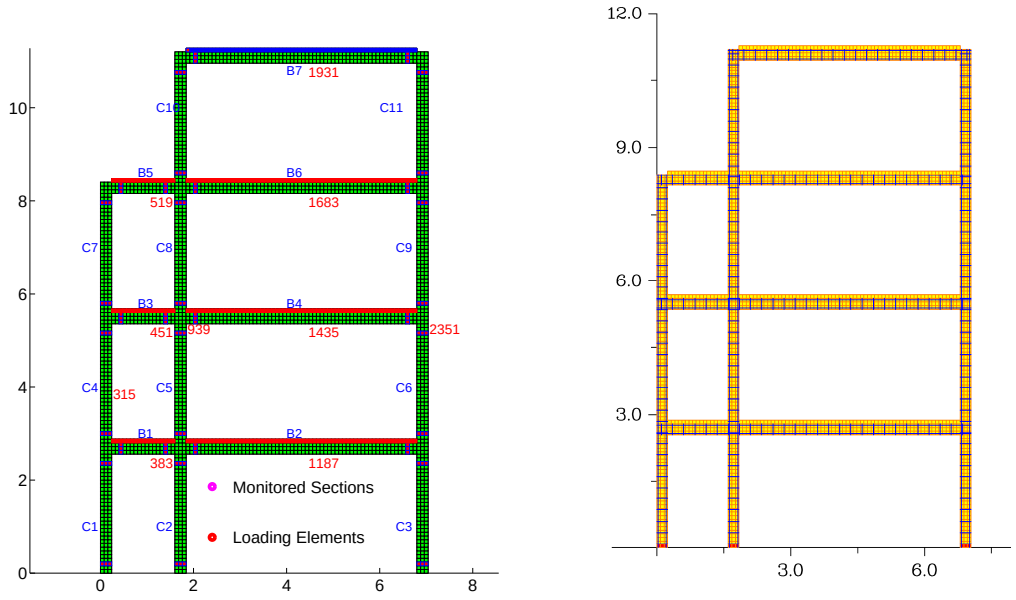

(a) Numerical model of B01

(b) AEM Model of B01 with discretization (All Cases)

Figure 5.7: AEM input model of B01 frame with loading elements and member numbering

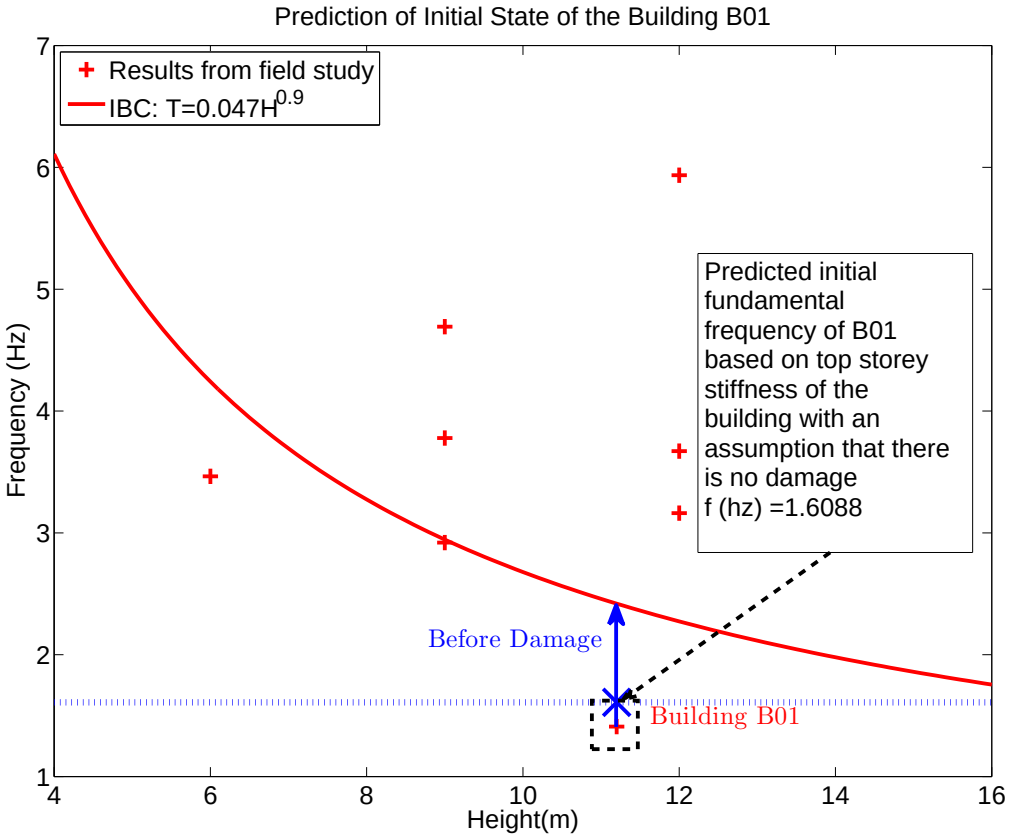

Figure 5.8: Prediction of initial state of building B01 based on top storey stiffness

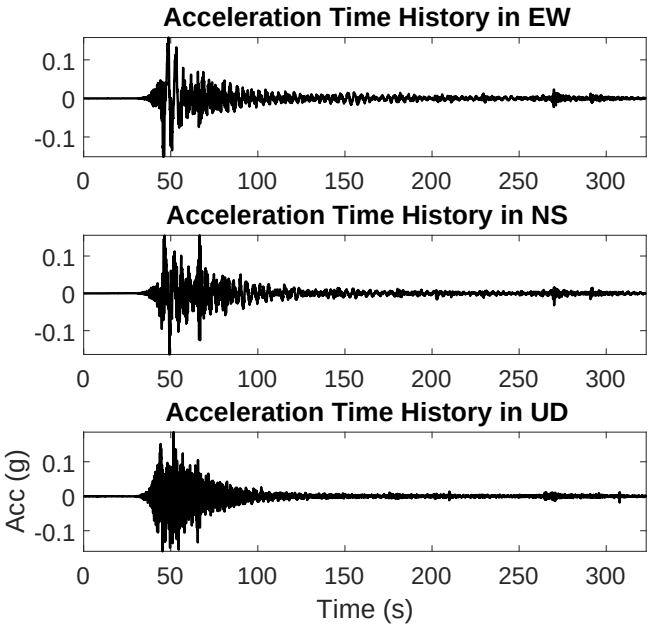

(a) Acceleration time histories

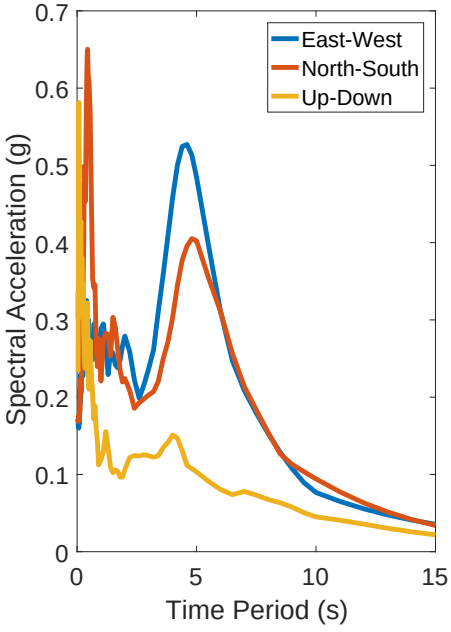

(b) Spectral acceleration

Figure 5.9: 2015 Gorkha earthquake ground motion parameters

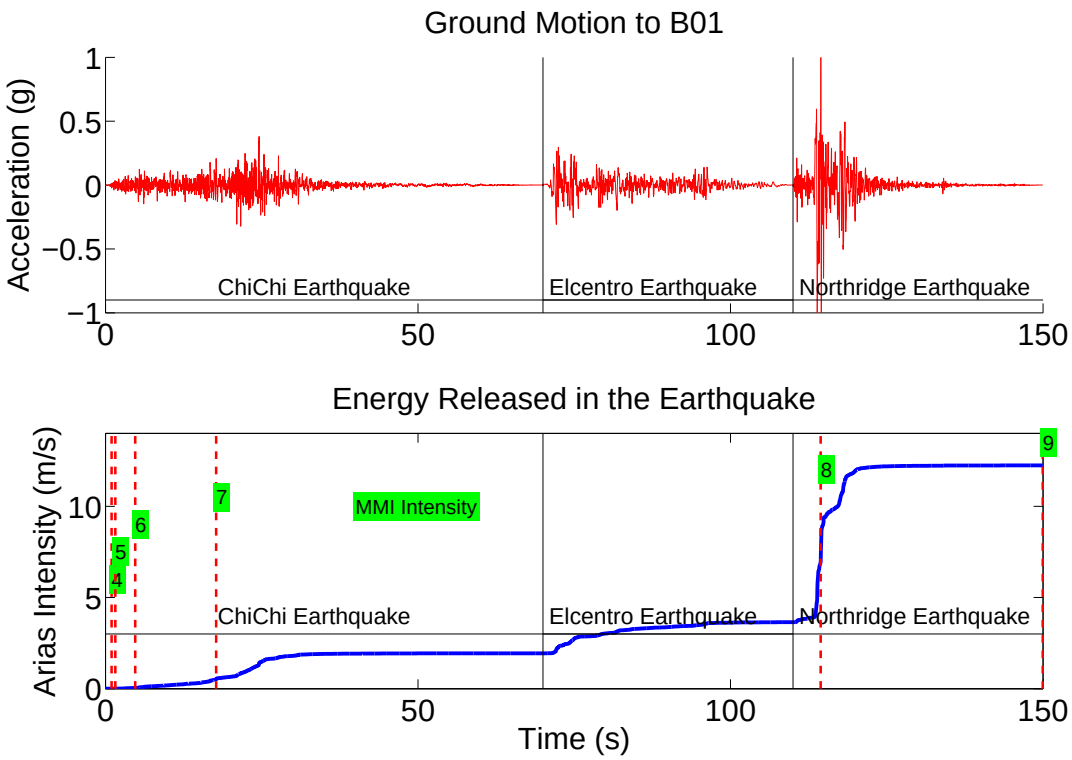

Figure 5.10: Earthquake ground motions applied to building B01

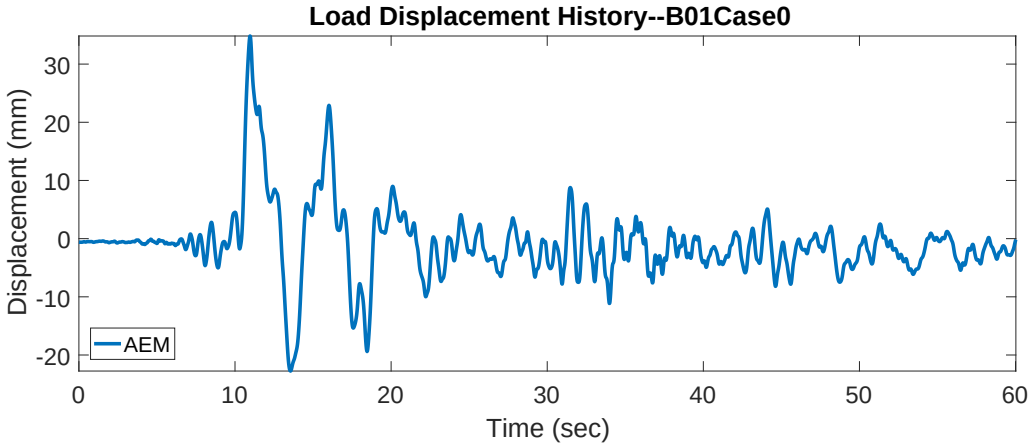

Figure 5.11: Roof displacement response time history of B01 case 0 due to Gorkha earthquake 2015

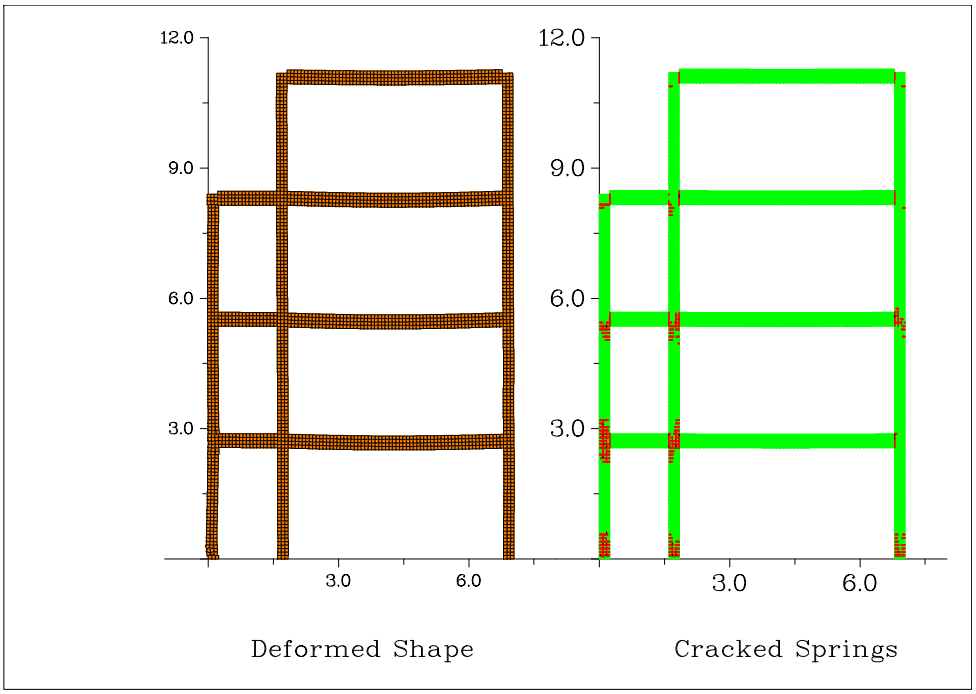

Figure 5.12: Building deformed shape and cracked springs on B01 case 0

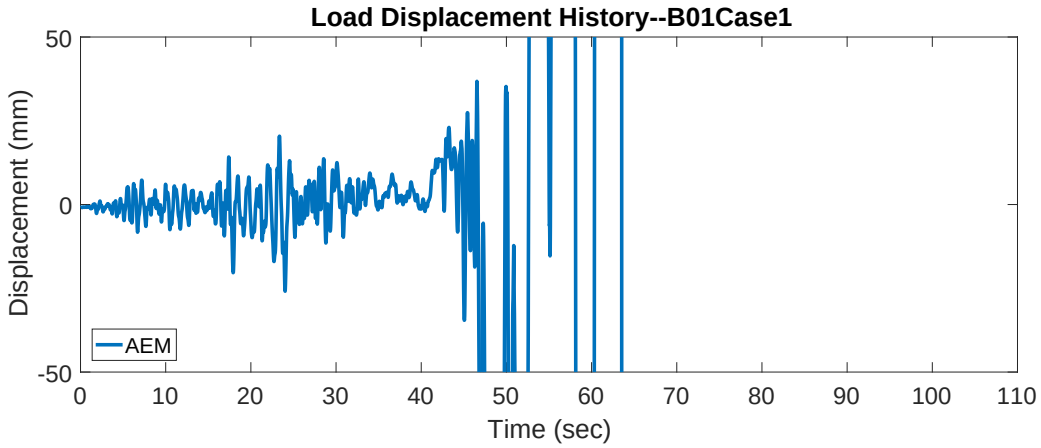

Figure 5.13: Response history of the frame B01 case 1 at the roof

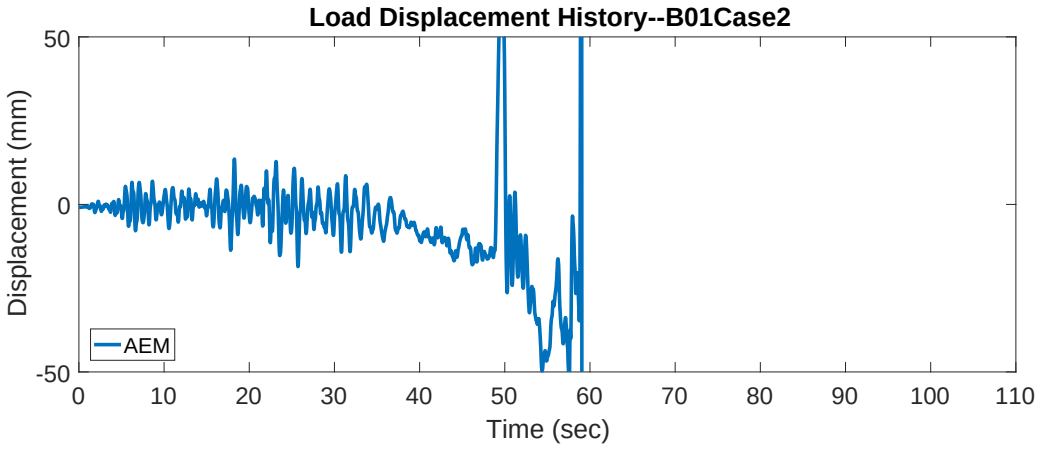

Figure 5.14: Response history of the frame B01 case 2 at the roof

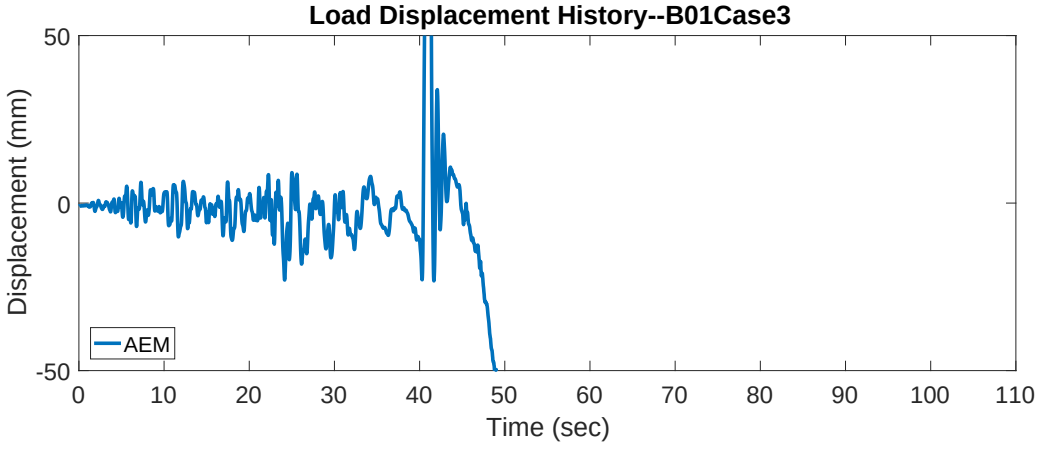

Figure 5.15: Response history of the frame B01 case 3 at the roof

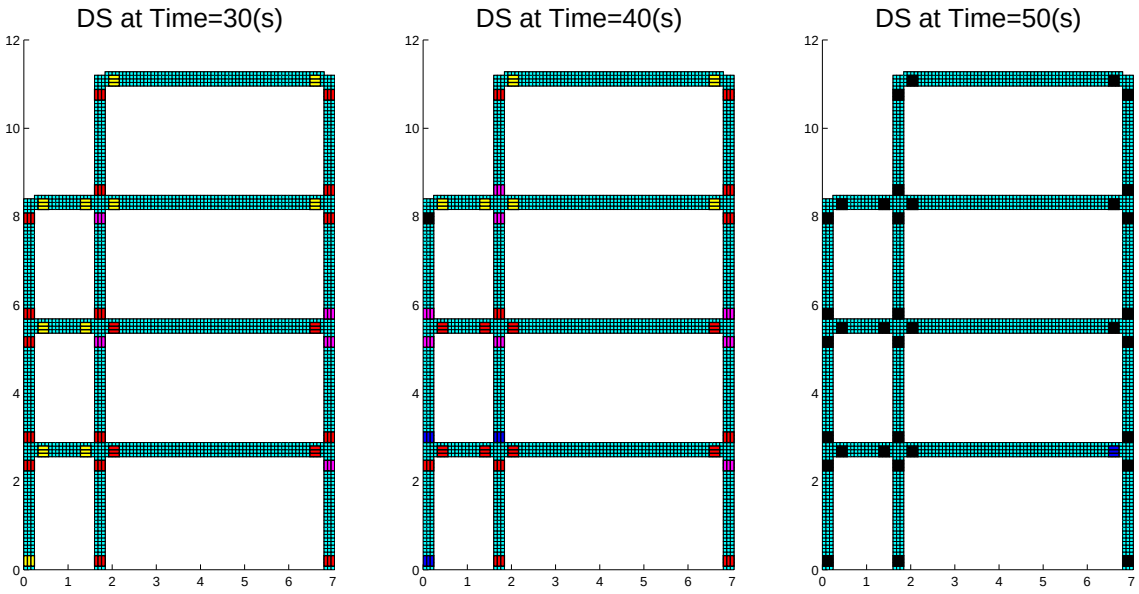

(a) Damage states after t=30s (b) Damage states after t=40s (c) Damage states after t=50s

Figure 5.16: Damage states of B01 case 1 based on damage indices at different time steps

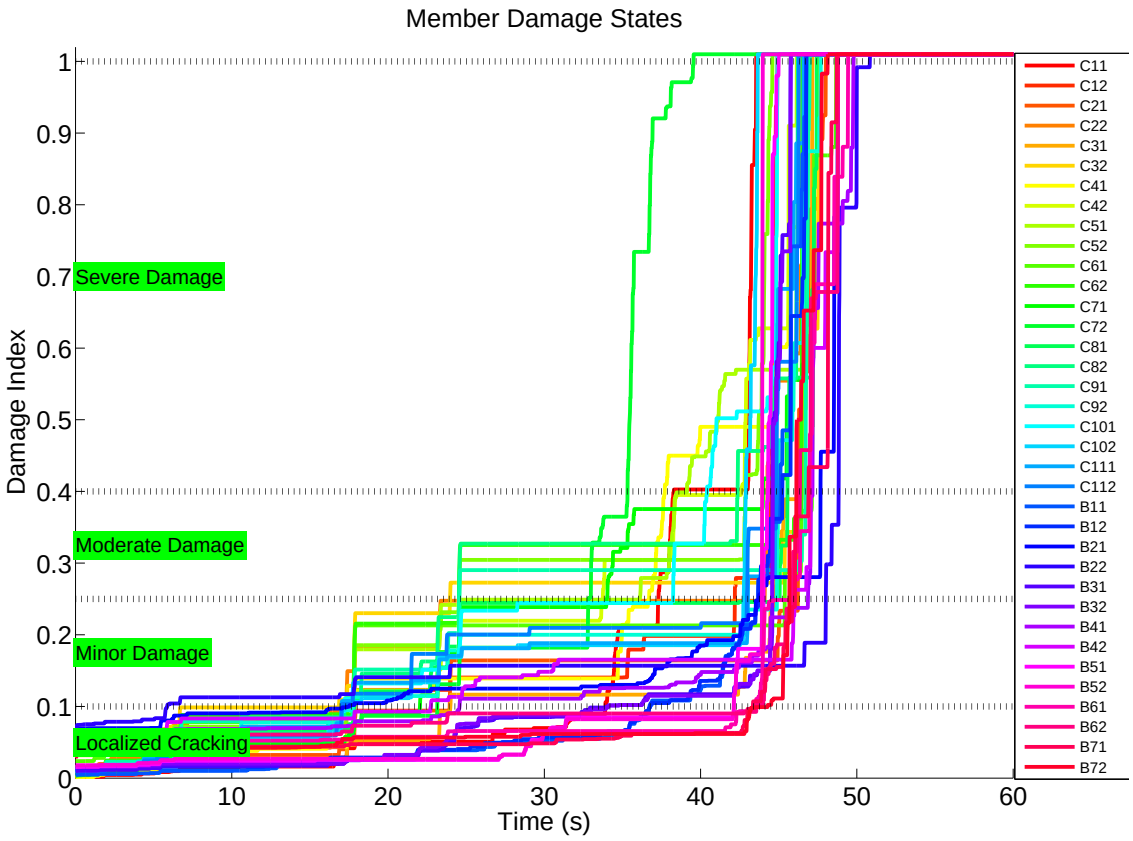

Figure 5.17: Damage states from simulation of B01 Case 1 frame

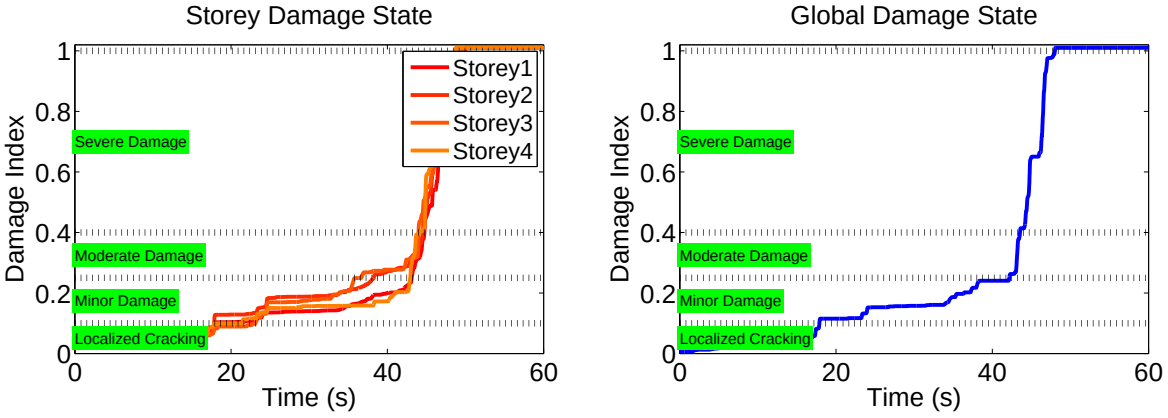

(a) Storey Damage Index

(b) Global Damage Index

Figure 5.18: LDI and SDI of B01 frame with case 1

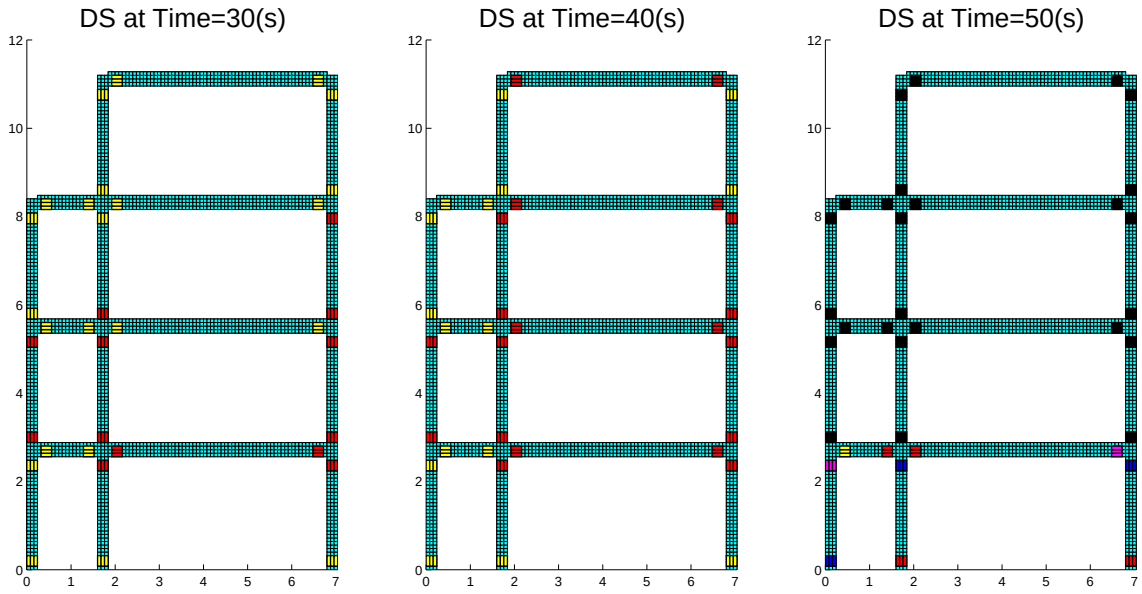

(a) Damage states after t=30s (b) Damage states after t=40s (c) Damage states after t=50s

Figure 5.19: Damage states of B01 case 2 based on damage indices at different time steps

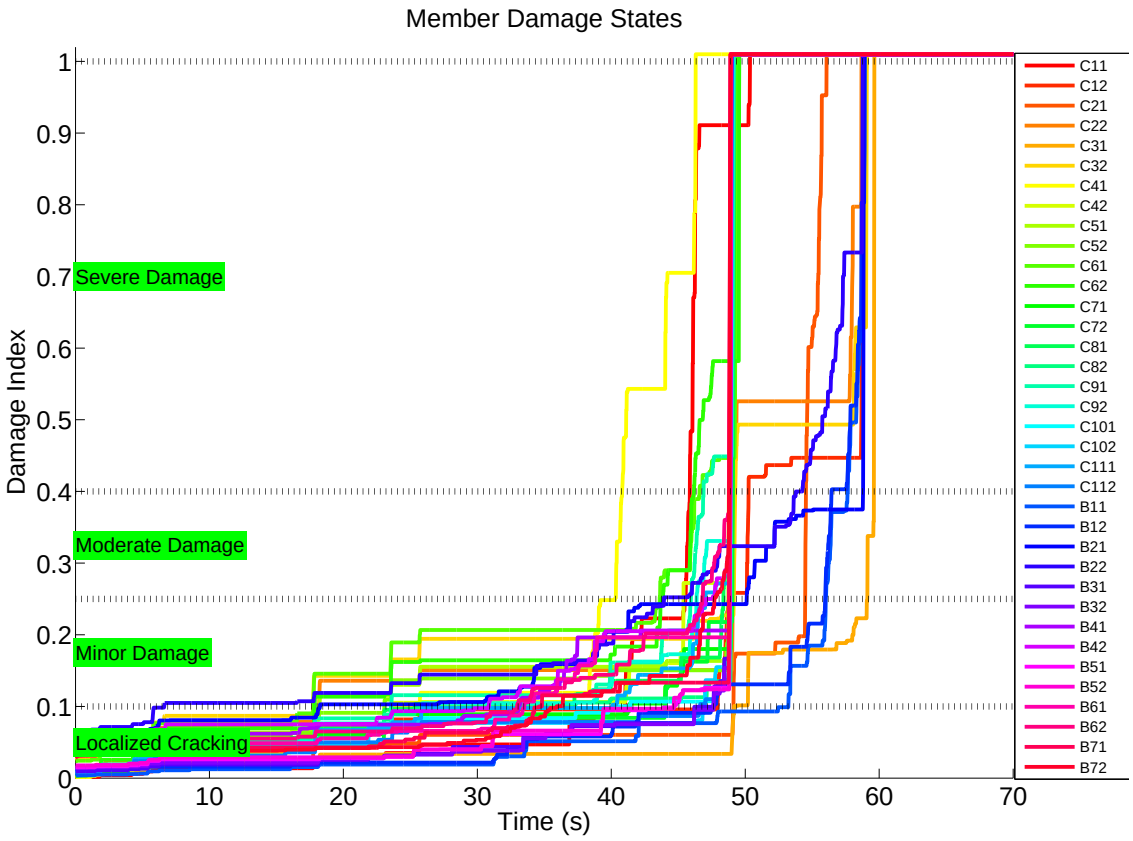

Figure 5.20: Damage states from simulation of B01 Case 2 frame

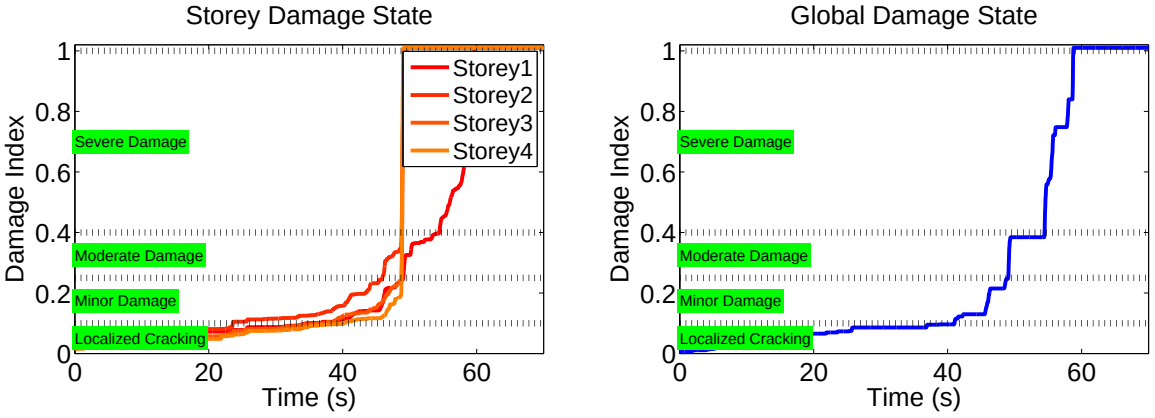

(a) Storey Damage Index

(b) Global Damage Index

Figure 5.21: LDI and SDI of B01 frame case 2

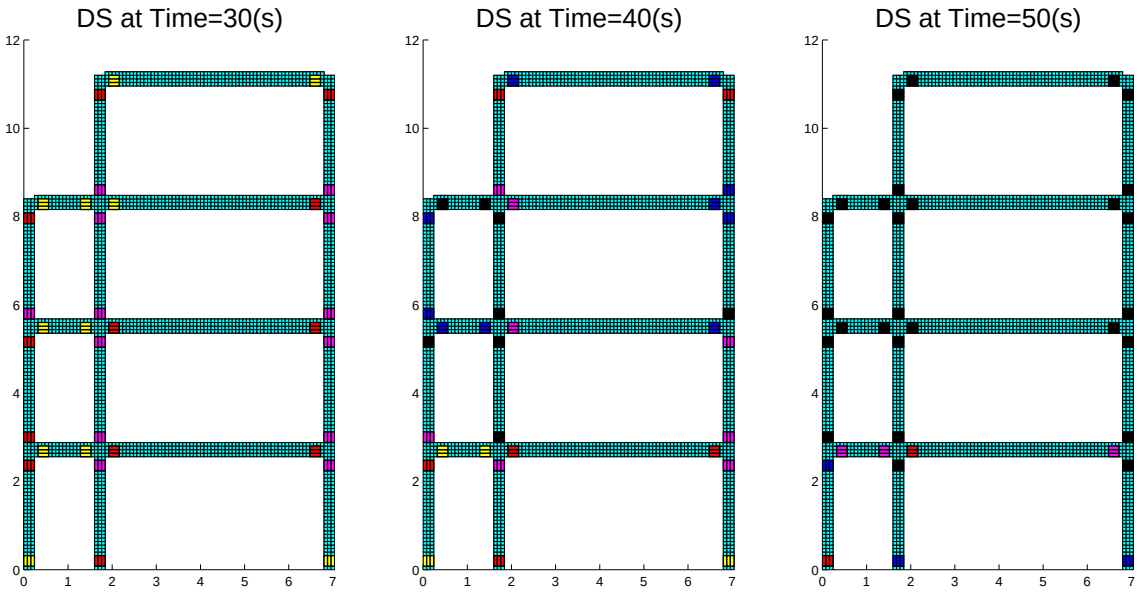

(a) Damage states after t=30s (b) Damage states after t=40s (c) Damage states after t=50s

Figure 5.22: Damage states of B01 case 3 based on damage indices at different time steps

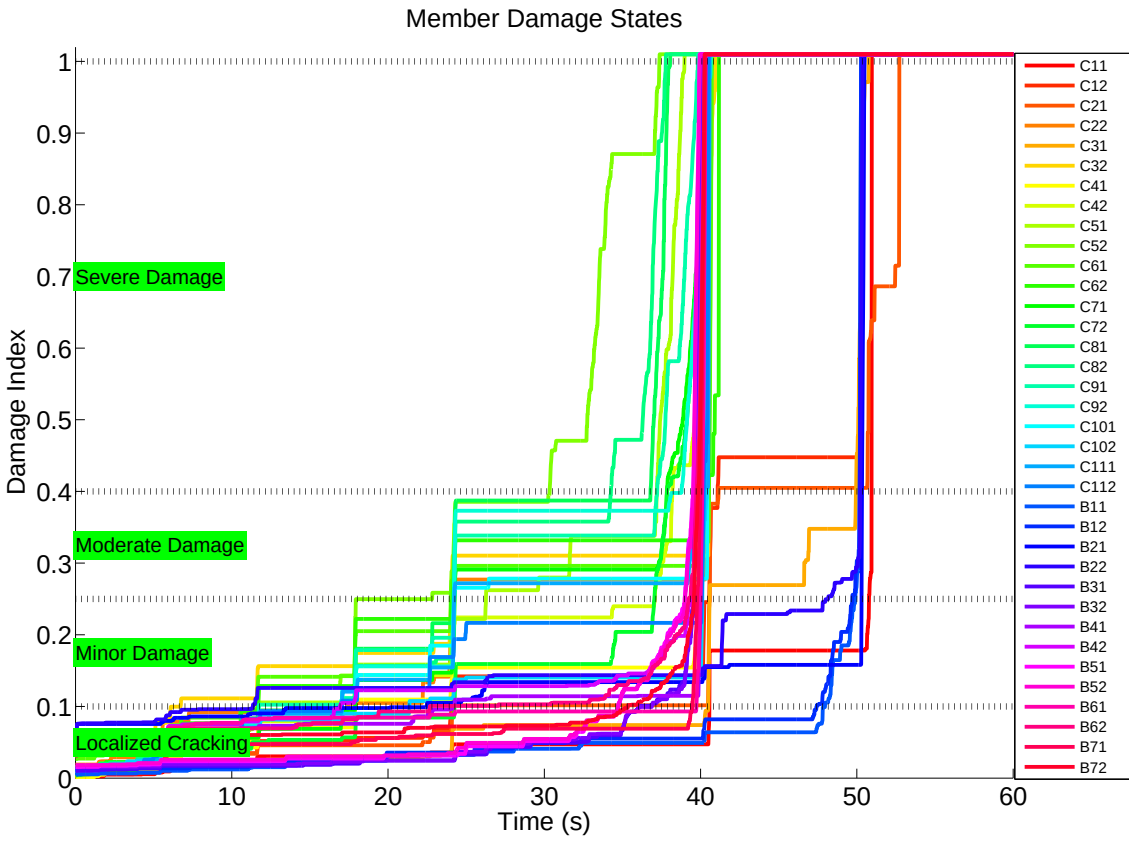

Figure 5.23: Damage states from simulation of B01 Case 3 frame

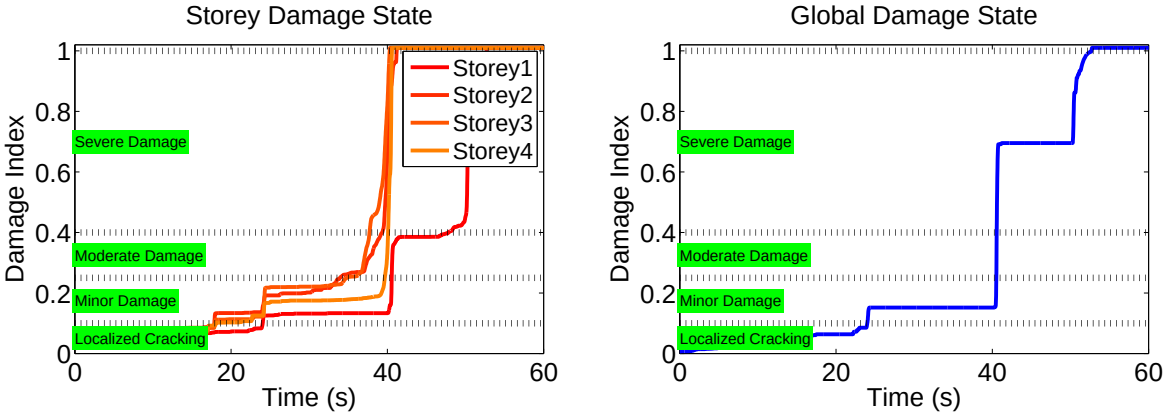

(a) Storey Damage Index

(b) Global Damage Index

Figure 5.24: LDI and SDI of B01 frame case 3

Chapter 6

Discussions and Conclusions

6.1 Summary

An improved methodology for carrying out seismic capacity has been demonstrated through this research. The main objective of this research was to make the numerical simulations of buildings against potential earthquakes more reliable by using the real parameters from the site to carry out non linear analysis of buildings and further discuss the capacity of the buildings. In this aspect, the research could be summarized as:

- A methodology for damage assessment has been introduced which can be more reliable than the existing methodologies in terms of its implementation, practicality, comprehensiveness and flexibility.

- In the perspective of this study, AEM had been validated and certain modifications were implemented for better non linear analysis of structures for obtaining seismic capacities.

- An iterative algorithm for estimating mass of a structure from a limited number of mode shapes is developed and it has proven to be invaluable in damage identification. Further, a 2-Step Identification methodology is introduced based on existing procedures for damage identification and material quantification. It is studied that these two procedures when connected with each other proves to be very useful in damage identification and material property updating.

  The changes of stiffness from the baseline can be identified including the location

of the damage. Further, an experimental evaluation was conducted to understand limitations and challenges of this study.

- A field study was conducted to understand various ground realities of a building and to understand carefully the various challenges, limitations and problems in the implementations of the method for real buildings especially those which are in developing countries. Also, a large amount of secondary data was collected in the course of this study for not only the numerical modelling but also to have engineering judgment on numerical simulations in terms of giving inputs as well as understanding the results.

- Seismic capacity is estimated using deformation based damage indices and is used for estimating the storey and global damage state of the building. These damage states were validated on an experimental frame from literature. A building was selected from the Nepal study for further evaluation, preliminary numerical model on AEM is developed based on the visually surveyed inputs and an incremental dynamic earthquake ground motion is applied to the frames and corresponding responses are extracted along with the damage indices and damage states.

6.2 Discussions

- This methodology is practical and easier to implement if a few uncertainties are clearly addressed.

- The outcomes of the analysis can be used in various situations which advocates to take a decision on weak buildings.

- In the same way, it has another very important advantage of carrying out reliability studies of existing buildings for strengthening against potential earthquakes.

- Building wise vulnerability assessment is a contemporary challenge and the vulnerability of each building can be used in seismic risk assessment of a society.

- Also, it can be used in post earthquake damage assessment of buildings during which the measures of strengthening/repair could be taken in addition to take a decision in occupancy.

6.2.1 Problems and Challenges

Estimating mass of a structure is a challenge This problem can be addressed by estimating the mass using engineering judgment and parametric study. Also, a coefficient of variation has to be introduced to have a higher confidence in the reliability of the results.

Mass can also be considered a parameter for update, but however it causes additional unknowns, for example in this study, an iterative algorithm to estimate mass is developed however, the strategy in monitoring is to be improved for the

Exact dimensions of the buildings The exact dimensions of a buildings is not known for many structures due to unavailability of blueprints but can be solved by detailed examination of the buildings

Insufficient Measurement Points The number of member properties which could be identified is proportional to number of measurement points

However, there are certain issues in assessing the properties of a building due to uncertainties in estimating the contributing mass, scaled mode-shapes, insufficient measurement points. Therefore, as an extension of this study, the methodology would be upgraded to be able to carry out seismic vulnerability assessment of Reinforced Concrete (RC) buildings using non-contact type vibration measurement system as multiple points in a structure could be measured using this method. To estimate the mass of the structure, better judgment and careful estimation of member dimensions and corresponding live loads is recommended. Also, through this study it is suggested to estimate the mass using an innovative iteration procedure which is independent from the actual iterative algorithm but it needs an accurate estimate of mode shapes, scaled to mass orthogonality. Therefore, it adds to another uncertainty of mode shapes, which could be solved by finding the modes from input loading, stochastic estimation or frequency shift technique.

Therefore, one of the most possible way for improving the identification technique in this methodology is to use a known input to the structure in monitoring to obtain scaled mode shapes. Though this is a conventional technique, it is important to note the fact that buildings are very complicated in its nature and an input has to be limited so as not to cause a damage to the building or any other disturbance but at the same time should promise sufficient accuracy in the estimation of scaled modes. Therefore, an improved

monitoring techniques by making use of a shaker and non contact type vibration measuring system to obtain scaled mode shapes from minimum number of excitation points. The overall method is described in this section.

6.2.2 Improvement in monitoring

A rational methodology was introduced in chapter 3 for the damage identification, localization and quantification which could be useful in material identification to be used for further analysis on AEM to obtain seismic capacity assessment. It was realized that these methods have strong dependency on a few parameters which were categorized into quantitative and qualitative parameters. Mainly, the initial objective was to have high quality mode shapes for damage identification and localization but due to compromise and problems is scaling with operational modal analysis, the mode shapes obtained through these are not scaled and the step-2 required higher confidence on obtaining mass matrix or the contributing mass for each node in a simple mass spring model of the structure. However and interesting mass matrix estimation method was developed but it had dependency on real mode shapes which are unit mass scaled or UMM. Therefore, the identification methodology introduced in chapter 3 would have been more powerful if either of these two parameters were estimated with higher accuracy. This section demonstrates a possible technique to improve the quality of mode shapes available for the buildings to be able to estimate the mass matrix in the first step. It is implicitly known that by increasing the quality and quantity parameters of identification, this method could be more practically applicable for use. An attempt to do this is by using a 'portable shaker', which is a device to provide known shaking force to a structure whereby combining with the operational modal analysis, can be used to extract good quality modes for real buildings.

To understand various parameters of this procedure in a more practical way, a theoretical example similar to the building considered in Nepal has been considered. In this study, the various implications and the various implications of this technique, and further how it could be used for detecting the damage and updating of parameters are studied in the following sections.

A sample four storey shear frame is considered for simplicity, the stiffness of each storey is calibrated to the estimated stiffness of building B01 as seen in chapter 4. This frame can also be visualized as a simple mass-spring-damper model for convenience in understand-

ing. The complete eigen analysis of the values could be done to extract the undamped natural frequencies and mode shapes of the structure.

Though damping are complicated parameters, for understanding purposes, they are assumed to be modal damping. A dynamic equation of motion is established with different cases of damping values and input forces. The damping values are based on general damping in the case of RC buildings and force parameters are governed mainly based on three values, namely the amplitude, duration and frequencies. The amplitude is expected to be as low as possible to get minimum number of modes for identification of properties, duration is dependent on the amount of other noise in the structure limiting the extraction of modal parameters and the frequencies shall have a lower and higher range to cater for exciting the required number of modes, which puts an emphasis on the using sine chirp, burst random sweep and broadband white noise with constant power spectral values. In this research, since the objective is to mainly to use a combination of using micro-tremor measurement and input based excitation is to mainly scale the mode shapes extracted through the other process, therefore, white noise is recommended to be the most suitable input for UMM scaling.

Procedure

The explanation of the procedure follows with a theoretical implementation on a four storey frame. The properties of the frame were calibrated to the actual building B01 as described chapter 4, also a modal damping of 5% is assumed in the process and therefore the natural frequencies and mode shapes from the undamped eigen value analysis is shown in the table 6.1. The overall methodology which has to be combined with U-Doppler is shown in figure 6.1. Firstly, a micro-tremor or U-Doppler test has to be conducted to estimate the natural frequencies and operational mode-shapes of the building, which would give a notable information on the modal state of the building such as the number of modes available, the frequency range, amplitudes of the response, etc. In the theoretical case, the analysis is done using a sample white noise as shown in figure 6.2. The displacement response of the frame is shown in figure 6.3 and the corresponding power spectrum and singular values of FDD are shown in figure 6.4. The extracted natural frequencies and operational mode shapes are tabulated in the table 6.2. It could be seen that the natural frequencies are reasonably accurate but the mode shapes are not scaled to the actual ones.

Therefore, now the next step is to scale the mode shapes to meet the UMM criteria and in order to do that an appropriate scaling procedure is needed. In this case, a portable shaker is intended to be used with varying frequencies of white noise to the structure with a particular maximum amplitude of shaking. However, the excitation force is meant to be limited as it should not cause any damage to the structure as well as this procedure has to be applicable on buildings which are not in sound state. There a minimum input is needed to be applied. In this case, the shaker is assumed to be placed at the top storey and the corresponding response is also estimated at the same location. Generally, the frequency response function (FRF) is extracted in the following way:

$$G_{YY} = HG_{YX} \tag{6.1}$$

$$\begin{Bmatrix} Y_1 \\ Y_2 \\ Y_3 \\ Y_4 \end{Bmatrix} = \begin{bmatrix} H_{11} & H_{12} & H_{13} & H_{14} \\ H_{21} & H_{22} & H_{23} & H_{24} \\ H_{31} & H_{32} & H_{33} & H_{34} \\ H_{41} & H_{42} & H_{43} & H_{44} \end{bmatrix} \begin{Bmatrix} 0 \\ 0 \\ 0 \\ X_4 \end{Bmatrix} \tag{6.2}$$

Here, the objective is to only scale the mode shapes, therefore only one value of FRF H_{44} is extracted, whose the corresponding FRF is shown in figure 6.6 and the scaling of mode shapes is done using curve fitting of FRF and extracting the imaginary amplitude of transfer function, frequency and modal damping of the structure. The curve fitting is done based on the following equation:

$$H(\omega) = \sum_{1}^{n} \frac{\phi_r {\phi_r}^T}{{\omega_r}^2 - \omega^2 + 2\zeta_r \omega_r i\omega} \tag{6.3}$$

At the first mode the equation gets transformed to

$$H(\omega_1) = \frac{{\phi_{41}}^2}{2\zeta_r \omega_1^2} \tag{6.4}$$

This scaled modal amplitude could be used for estimating scaled mode shapes from the operational modal analysis conducted earlier. However, this scaling has to be done for each mode independently where the damping is not uniform as in this case. In addition to this, further considerations are needed in understanding the practical implementation of this procedure.

Considerations in input to the structure

This scaling has to be done carefully without damaging the structure and exciting it to sufficient levels in estimating the scaling factors. The Nepal building B01 is considered

as a reference for knowing the excitation levels by calculating the RMS values of the amplitude, the corresponding top storey RMS was 8.3939. Another factor, which strongly influences the estimation of scaling factor is the duration of testing and various cases of estimates. In this study, various cases of durations and amplitudes are studied and its RMS ratio to Nepal building is tabulated in 6.3. All values below 1.0 suggests that the excitation is not sufficient for identification and the shaded region shows a possible area of excitation. In addition to this, error in scaling factors are shown in table 6.4 and it is to be concluded from this study that the accuracy is higher when the duration of input and monitoring is longer enough. The highlighted cells of the table gives an idea of required excitation for a building of the type B01 for estimating the scaling factors. A further detailed study is required to understand more information in the estimation of scaled mode shapes. The same modes are scaled and the mass update was applied to this case and the corresponding outcome after 1 million iterations with 2 modes as shown in the figure 6.7 and accuracy seemed to be good and it is possible to achieve higher accuracy with further improvements in the iterative algorithms.

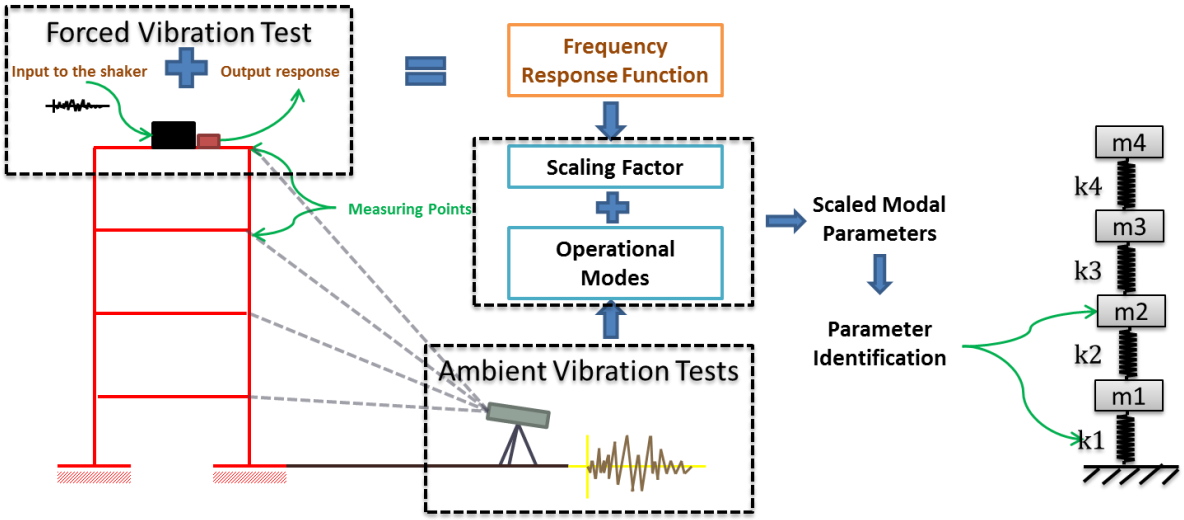

Figure 6.1: Complete scaling, modal analysis and parameter estimation

Table 6.1: Modal parameters as obtained from undamped eigen analysis

Undamped Eigen Frequencies and Mode Shapes				
	Mode 1	**Mode 2**	**Mode 3**	**Mode 4**
Frequencies (hz)	1.37	3.95	6.1	7.28
DOF 1	-0.0024	0.0052	0.0048	-0.0024
DOF 2	-0.0039	0.0036	-0.0037	0.0044
DOF 3	-0.0049	-0.0020	-0.0028	-0.0050
DOF 4	-0.0053	-0.0054	0.0054	0.0043

Table 6.2: Modal parameters as obtained from operational modal analysis

Identified Frequencies and Operational Mode Shapes			
	Mode 1	**Mode 2**	**Mode 3**
Frequencies (hz)	1.35	3.94	5.98
DOF 1	-0.2746	-0.5948	0.5203
DOF 2	-0.4512	0.4213	-0.3986
DOF 3	-0.5751	-0.2556	-0.4054
DOF 4	-0.6248	-0.6351	0.6372

Table 6.3: RMS ratio of different outputs to Nepal B01 ambient response

Time(s) Amp(N)	30	60	90	120	150	180	210	240	270	300	**Mean**
1	0.1	0.08	0.1	0.07	0.08	0.08	0.08	0.08	0.08	0.1	**0.09**
2	0.22	0.16	0.18	0.16	0.16	0.18	0.16	0.17	0.18	0.15	**0.17**
3	0.31	0.32	0.27	0.29	0.29	0.23	0.21	0.24	0.28	0.23	**0.27**
4	0.47	0.42	0.34	0.33	0.38	0.25	0.33	0.35	0.33	0.34	**0.35**
5	0.56	0.38	0.43	0.47	0.41	0.42	0.45	0.49	0.42	0.43	**0.45**
6	0.56	0.53	0.44	0.55	0.49	0.5	0.46	0.53	0.53	0.44	**0.5**
7	0.54	0.62	0.63	0.64	0.63	0.67	0.57	0.49	0.62	0.59	**0.6**
8	0.69	0.7	0.84	0.73	0.67	0.7	0.65	0.73	0.63	0.6	**0.69**
9	0.83	0.71	0.58	0.81	0.73	0.86	0.69	0.68	0.83	0.72	**0.74**
10	0.9	0.82	0.91	0.88	0.84	0.84	0.83	0.88	0.88	0.77	**0.85**
11	1.02	0.96	0.89	1.01	0.98	0.99	0.85	1.01	0.9	0.82	**0.94**
12	1.01	1.01	0.95	1.01	1.02	0.88	1.05	1.09	0.97	1.06	**1.01**
13	1.13	1.16	0.93	1.1	1.09	1.19	1.14	1.05	0.99	1.08	**1.09**
14	1.31	1.23	1.04	1.23	1.27	1.16	1.2	1.11	1.25	1.14	**1.19**
15	1.46	1.54	1.23	1.44	1.24	1.32	1.16	1.21	1.15	1.24	**1.3**
16	1.78	1.47	1.43	1.24	1.21	1.41	1.36	1.28	1.35	1.24	**1.38**
17	1.68	1.38	1.53	1.42	1.54	1.47	1.56	1.38	1.47	1.42	**1.48**
18	1.85	1.31	1.62	1.83	1.56	1.42	1.52	1.44	1.65	1.55	**1.58**
19	1.86	1.67	1.69	1.69	1.58	1.63	1.55	1.57	1.52	1.66	**1.64**
20	1.57	1.61	2.05	1.67	1.69	1.66	1.79	1.62	1.55	1.96	**1.72**
21	2.41	1.59	1.61	1.77	1.79	1.74	1.73	1.78	1.85	1.72	**1.8**
22	2.04	2.01	1.97	1.98	1.89	2.08	2	1.55	1.77	1.73	**1.9**
23	2.26	1.9	1.95	2.16	2.09	2.12	2.05	1.99	1.89	1.87	**2.03**
24	2.09	2	2.09	2.11	2.03	2.21	1.97	2.17	1.99	1.99	**2.07**
25	2.52	2.21	2.5	2.34	1.97	1.96	2.18	2.3	2.24	2.05	**2.23**

Table 6.4: Error in the estimation of scaling factor

Time(s) Amp(N)	**30**	**60**	**90**	**120**	**150**	**180**	**210**	**240**	**270**	**300**
1	30.84	8.4	6.24	8.86	8.14	0.71	6.45	1.12	0.04	0.72
2	23.52	9.51	6.43	2.8	0.43	1.16	1.7	0.23	1.73	0.8
3	13.92	6.53	6.3	2.69	1.27	3.54	1.65	1.6	0.17	0.39
4	19.27	10.94	3.41	8.87	1.71	0.78	1.3	0.85	1.09	0.16
5	47.85	18.39	4.93	1.88	2.45	2.66	1.81	1.28	0.2	0.19
6	28.96	9.53	3.67	3.3	1.12	0.87	2.24	1.39	1.31	0.91
7	32.86	9.57	8.79	0.58	4.3	3.45	1.43	1.87	0.94	1.87
8	18	15.15	2.35	2	2	1.85	0.29	0.89	2.71	1.73
9	17.92	2.56	5.64	3.95	2.85	1.02	1.96	0.14	1.12	0.14
10	27.62	12.59	11.81	1.41	1.4	0.23	1.3	2.81	0.01	1.84
11	22.89	13.84	8.49	2.77	2.35	0.74	4.2	1.19	1.81	2.29
12	13.13	6.61	6.66	2.14	5.28	1.3	1.43	0.56	0.57	0.14
13	20.68	12.19	4.67	4.03	0.58	1.82	0.83	0.72	0.35	0.24
14	28.74	21.93	3.04	6.26	2.4	2.61	0.97	0.1	0.97	1.61
15	19.13	10.44	1.97	5.56	4.45	3.43	0.35	2.81	0.6	0.1
16	25.15	11.9	4.63	2.76	4.23	0.65	0.67	1.86	0.06	0.84
17	26.22	4.77	3.24	2.04	4.82	1.48	1.02	0.34	0.49	0.78
18	25.56	6.74	6.9	2.65	0.2	2.42	0.41	0.19	1.95	1.19
19	19.07	10.49	13.2	4.6	0.29	1.63	1.49	1.97	2.26	1.01
20	23.88	9.86	4.34	2.68	0.02	1.54	1.21	0.59	0.96	0.24
21	12.74	18.56	5.53	2.96	6.17	0.87	0.12	0.21	1.09	0.26
22	37.16	15.84	12.75	3.59	3.72	0.61	2.49	0.83	0.51	0.36
23	11.61	3.85	8.39	0.08	2.17	1.54	2.58	3.49	0.17	0.08
24	9.46	16.67	4.25	2.77	4.85	3.95	2.27	1.35	0.18	0.25
25	37.38	7.73	4.72	1.49	0.89	0.82	1.31	0.04	0.52	0.06
Mean	**23.74**	**10.98**	**6.09**	**3.31**	**2.72**	**1.67**	**1.66**	**1.14**	**0.87**	**0.73**

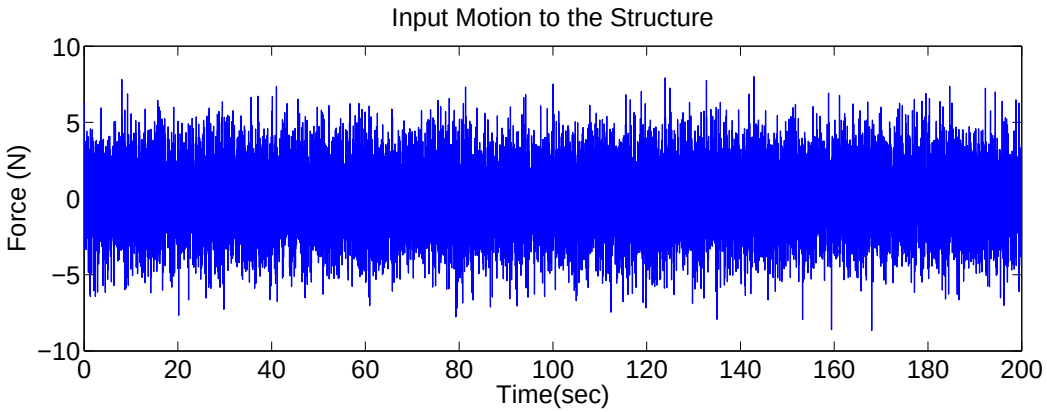

Figure 6.2: Input motion applied using an external shaker equivalent to general white noise from ambience

6.3 Future Work

This are some unsubstantiated components of this work which will have to be completed to have this methodology in practice and these are some of the components where attention is expected in future:

- **Implementation of shaker based EMA**

  The shaker based implementation has to be verified with a miniature frame and a real building on site and confirm the applicability of this method in the presence of noise and other factors which could plausibly affect the outcomes.

- **Experimental validation with RC frames**

  This methodology for assessment of damage and condition of the structure against potential earthquakes, has shown its applicability already on the structures in the field. As an interest in the scientific community, for better understanding of the methodology a thorough validation on RC buildings are needed. A full scaled RC building constructed in controlled condition would an ideal case for experimental validation, but since carrying out an experiment at such a scale is practically inconvenient and therefore it is recommended to conduct a scaled testing of RC building in controlled conditions.

- **Extension of identification algorithm** Further modifications/extension is needed in the 2-step identification methodology to be able to incorporate operational mode shapes also.

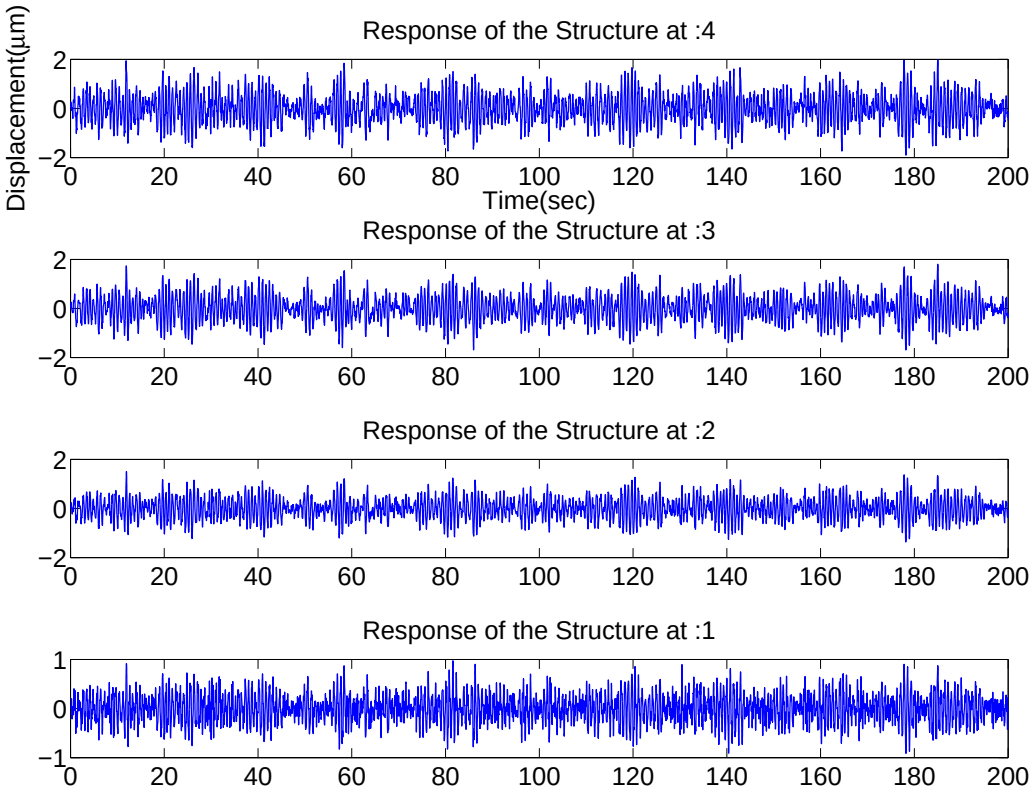

Figure 6.3: Displacement response of the example frame

- **Required improvements in AEM** Extend AEM for modelling non-engineering and poor construction practices and incorporate identification algorithm in the routines. In addition to this, a 3D modelling would be more appropriate for this study as the modal analysis could be carried out in all direction.

- **Improve optimization schemes** More optimization parameters such as mass, geometry, etc. can be included to be able to discuss the capacity of the structure. Include other optimization schemes such as Baysian updating and Nelder Mead simplex methods to address uncertain issues such as noise in the system.

- **Damage database**

  Compilation of a damage database by changing the input parameters and ground motion with reference to the mode shapes and fundamental frequencies to estimate seismic capacity of the system.

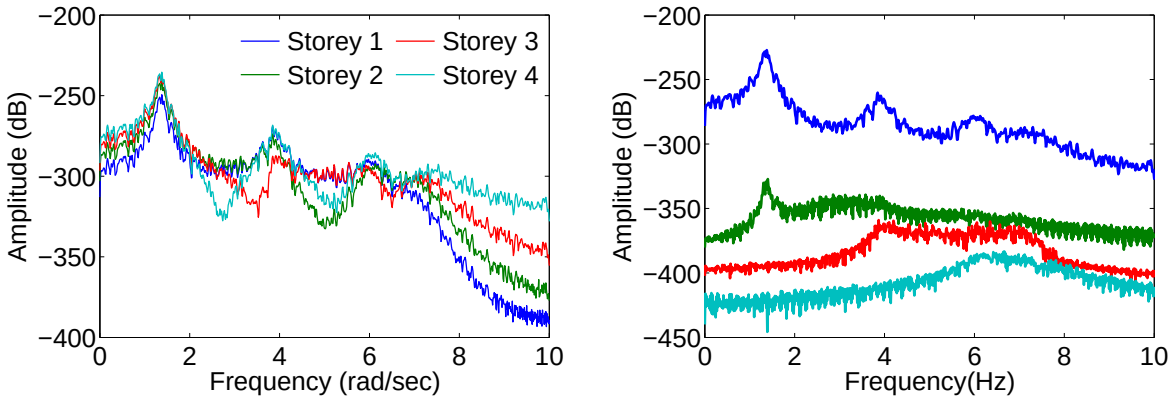

(a) Power-spectrum of response at each floor (b) Singular values of PSD matrix

Figure 6.4: Operational modal analysis of the example frame

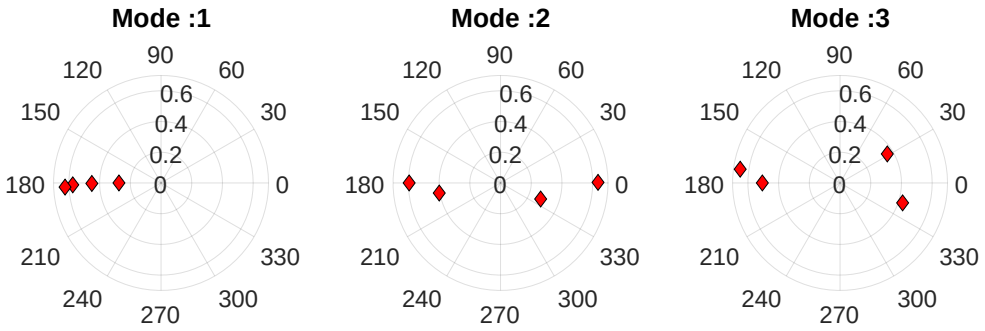

Figure 6.5: Mode shapes with imaginary components from output only analysis

6.4 Conclusions

- A new post peak softening model has been developed for uniaxial compression behavior of concrete, which had been validated with static and dynamic case of loadings
- In this research and algorithm is developed based on Topole and Stubbs damage index method and an optimization extension to it for material identification
- An innovative mass estimation model has been developed based on Berman optimum mass update. Here, an iterative algorithm is substantiated to achieve convergence to actual values.
- Theoretically, these methods seemed to have strong significance as had been very accurate even with limited number of modes in underdetermined systems, but however, a strong demand on the input parameters, scaled mode shapes and masses

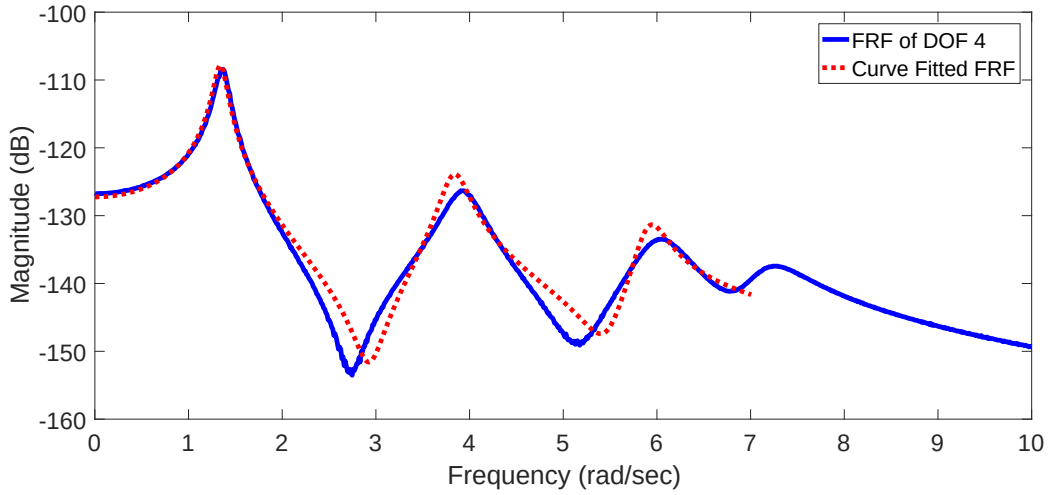

Figure 6.6: Frequency response function at top floor due to input shaker and curve fit to extract modal parameters

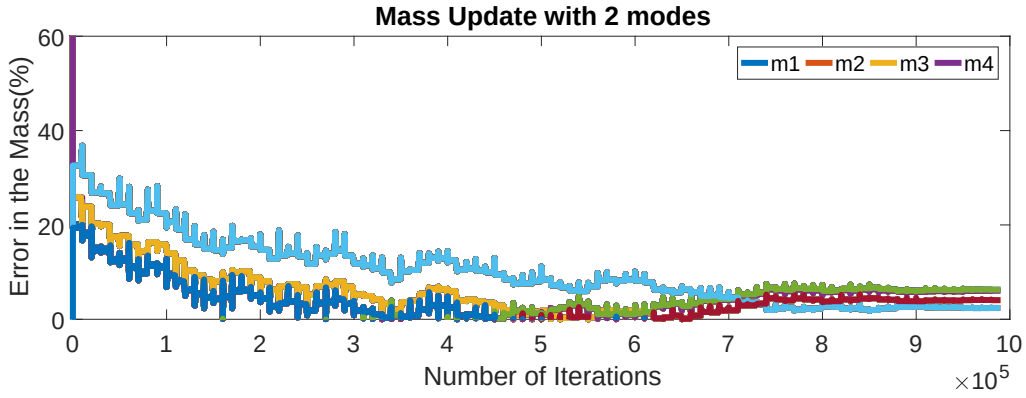

Figure 6.7: Iterative mass update on the example frame

make the method uncertain. This indeed was confirmed with experiments and a field study was conducted to find out other parameters affecting material parameter identification for buildings. This method was implemented on a building studied in the field by changing the optimization parameters to have higher weightage for frequencies than modes. This is also a source of uncertainty but could give some information on the material properties of the structure.

- Deformation based damage indices are used in the seismic capacity estimation. A lot of parameters have been compromised due to the use of preliminary analysis in this research, however the damage indices have been validated for an experimental frame. The global damage states of the buildings could give an insight of failure

of the buildings and compilation of this method over multiple buildings could give more realistic fragility functions of a building stock in a region.

- Finally, a method to scale the mode shapes using a combination of operational modal analysis and shaker base experimental modal analysis with limited amplitude and measurement points is proposed. The theoretical validation has been investigated and presented. This method has a strong potential of obtaining scaled mode shapes and can be used in the contributing masses with higher accuracies. This can possibly be useful in detecting the material properties and location of damage in structures.

Bibliography

[1] Minimizing measurement uncertainty in calibration and use of accelerometers. Technical Report TP-299, 2010.

[2] *Seismic Vulnerability Assessment Of Building Types In India*. Technical Document (Tech-Doc) On Typology Of Buildings In India, 2013.

[3] *Seismic Vulnerability Assessment Of Building Types In India*. Technical Document (Tech-Doc) On Typology Of Buildings In India, 2013.

[4] Federal Emergency Management Agency. *Rapid Visual Screening of Buildings for Potential Seismic Hazards: A Handbook*. FEMA, 1988.

[5] Sinan Akkar, Haluk Sucuoğlu, and Ahmet Yakut. Displacement-based fragility functions for low- And mid-rise ordinary concrete buildings. *Earthquake Spectra*, 21(4):901–927, 2005.

[6] Anand S Arya. Non-engineered construction in developing countries-an approach toward earthquake risk prediction. *Bulletin of the New Zealand Society for Earthquake Engineering*, 33(3):187–208, 2000.

[7] AS Arya. Rapid visual screening of buildings in various seismic zones in india. *Prepared under GoI-UNDP disaster risk management programme. National Disaster Management Division, New Delhi*, 2003.

[8] Z Bazant and B Oh. Crack band theory of concrete. *Materials and Structures*, 16:155–177, 1983.

[9] A Berman. Mass matrix correction using an incomplete set of measured modes. *AIAA Journal*, 17(October):1147–1148, 1979.

[10] A. Berman and E. J. Nagy. Improvement of a large analytical model using test data. *AIAA journal*, 21(8):1168–1173, 1983.

[11] R De Borst. Some recent developments in computational modelling of concrete fracture. *International journal of fracture*, (1980):5–36, 1997.

[12] Rune Brincker, Lingmi Zhang, and Palle Andersen. Modal identification of output-only systems using frequency domain decomposition. *Smart Materials and Structures*, 10(3):441–445, 2001.

[13] G Michele Calvi, Rui Pinho, Guido Magenes, Julian J Bommer, L Fernando Restrepo-Vélez, and Helen Crowley. Development of seismic vulnerability assessment methodologies over the past 30 years. *ISET journal of Earthquake Technology*, 43(3):75–104, 2006.

[14] J Cervenka and V Cervenka. On finite element modeling of compressive failure in brittle materials. *Computational Modelling of Concrete Structures*, page 273, 2014.

[15] J Cervenka, V Cervenka, R Eligehausen, and Zdeněk P Bažant. Fracture-plastic material model for concrete, application to analysis of powder actuated anchors. In *Proc. FRAMCOS*, volume 3, pages 1107–1116, 1998.

[16] D D'ayala, A Meslem, D Vamvatsikos, K Porter, T Rossetto, H Crowley, and V Silva. Guidelines for analytical vulnerability assessment of low/mid-rise buildings: Methodology. vulnerability global component project, 2014.

[17] André Filiatrault, Éric Lachapelle, and Patrick Lamontagne. Seismic performance of ductile and nominally ductile reinforced concrete moment resisting frames. I. Experimental study. *Canadian Journal of Civil Engineering*, 25(2):331–341, 1998.

[18] R L Fox and M P Kapoor. Rates of Change of Eigenvalues and Eigenvectors. *Aiaa J.*, 6(12):2426–2429, 1968.

[19] Sigmund A Freeman. Review of the Development of the Capacity Spectrum Method. *ISET Journal of Earthquake Technology*, 41(1):113, 2004.

[20] Augusto Gansser. Geology of the himalayas. 1964.

[21] R Guragain, A Dixit, and K Meguro. Development of fragility functions for low strength masonry buildings in nepal using applied element methods. In *15th world conference of earthquake engineering, Lisbon, Portugal*, 2012.

[22] Ahmed F Hassan and Mete A Sozen. Seismic vulnerability assessment of low-rise buildings in regions with infrequent earthquakes. *ACI Structural Journal*, 94(1):31–39, 1997.

[23] MHMR HAZUS and FEMA NIBS. Multi-Hazard Loss Estimation Methodology. *FEMA http://www. fema. gov*, 690, 2003.

[24] Mahmood Hosseini and Mohammad Reza Imagh-E-Naiini. Quick method for estimating the lateral stiffness of building systems. *Structural Design of Tall Buildings*, 8(3):247–260, 1999.

[25] Alireza Irani and Abdolrahim Jalali. Seismic Vulnerability Assessment of Reinforced. pages 6–8, 2012.

[26] Daniel C. Jansen and Surendra P. Shah. Effect of Length on Compressive Strain Softening of Concrete. *Journal of Engineering Mechanics*, 123(1):25–35, 1997.

[27] A Kappos, K Pitilakis, K Stylianidis, K Morfidis, and D Asimakopoulos. Cost-benefit analysis for the seismic rehabilitation of buildings in thessaloniki, based on a hybrid method of vulnerability assessment. In *Proceedings of the 5th international conference on seismic zonation, Nice*, volume 1, pages 406–413, 1995.

[28] AJ Kappos, KC Stylianidis, and K Pitilakis. Development of seismic risk scenarios based on a hybrid method of vulnerability assessment. *Natural Hazards*, 17(2):177–192, 1998.

[29] Andreas J. Kappos. Seismic damage indices for RC buildings: evaluation of concepts and procedures. *Progress in Structural Engineering and Materials*, 1:78–87, 1997.

[30] Andreas J. Kappos, Georgios Panagopoulos, Christos Panagiotopoulos, and Gregorios Penelis. A hybrid method for the vulnerability assessment of R/C and URM buildings. *Bulletin of Earthquake Engineering*, 4(4):391–413, 2006.

[31] S. K. Kunnath, a. M. Reinhorn, and R. F. Lobo. IDARC Version 3.0: A Program for the Inelastic Damage Analysis of Reinforced Concrete Structures. Technical Report NCEER-92-0022, 1992.

[32] K Lang. Seismic Vulnerability of Existing Buildings. *Meteorological Society*, 12(12):1309 – 1313, 1982.

[33] Torsak Lertsrisakulrat, Ken Watanabe, Maki Matsuo, and Junichiro Niwa. Experimental Study on parameters in Localizaistion of Concrete Subjected to Compression., 2001.

[34] Koichi Maekawa, Hajime Okamura, and Amorn Pimanmas. *Non-linear mechanics of reinforced concrete*. CRC Press, 2003.

[35] M G Mahoney. FEMA P58 : Next-Generation Building Seismic Performance Assessment Methodology. 10, 2010.

[36] Gro Markeset and Arne Hillerborg. Softening of concrete in compression — Localization and size effects. *Cement and Concrete Research*, 25(4):702–708, 1995.

[37] Aydan Menderes, Arzu Erener, and Gülcan Sarp. Automatic detection of damaged buildings after earthquake hazard by using remote sensing and information technologies. *Procedia Earth and Planetary Science*, 15:257–262, 2015.

[38] John E. Mottershead, Michael Link, and Michael I. Friswell. The sensitivity method in finite element model updating: A tutorial. *Mechanical Systems and Signal Processing*, 25(7):2275–2296, 2011.

[39] Hikaru Nakamura and Takeshi Higai. Compressive fracture energy and fracture zone length of concrete. *Modeling of inelastic behavior of RC structures under seismic loads*, pages 471–487, 2001.

[40] Y. Nakano, M. Maeda, H. Kuramoto, and M. Murakami. Guideline for post-earthquake damage evaluation and rehabilitation of buildings in Japan. In *13th World Conference on Earthquake Engineering, Vancouver, Canada*, number 124, 2004.

[41] Masamichi Ohkubo. *Current Japanese system on seismic capacity and retrofit in techniques for existing reinforced concrete buildings and post-earthquake damage inspection and restoration techniques*, volume 91. Dept. of Applied Mechanics & Engineering Sciences, University of California, San Diego, 1991.

[42] T. B Panagiotakos and M. N. Fardis. Deformation of reinforced concrete at yielding and untimate. *ACI Structural Journal*, 98(2):135–147, 2001.

[43] Y. Park, A. Ang, and Y. Wen. Seismic Damage Analysis of Reinforced Concrete Buildings. *Journal of Structural Engineering*, 111(4):740–757, 1985.

[44] T. Paulay and N. Priestley. *Seismic design of reinforced concrete and masonry buildings*. 1992.

[45] K Pitilakis, H Crowley, a M Kaynia, and Critical Facilities. *SYNER-G : Typology Defi nition and Fragility Functions for Physical Elements at Seismic Risk*, volume 11. 100.

[46] Kyriazis Pitilakis, Paolo Franchin, Bijan Khazai, and Helmut Wenzel. *SYNER-G: Systemic Seismic Vulnerability and Risk Assessment of Complex Urban, Utility, Lifeline Systems and Critical Facilities: Methodology and Applications*, volume 31. Springer, 2014.

[47] Mustapha Remki. Seismic Vulnerability Functions of Strategic Buildings in the City of Algiers. (July):4–6, 2011.

[48] Tiziana Rossetto and Amr Elnashai. A new analytical procedure for the derivation of displacement-based vulnerability curves for populations of RC structures. *Engineering Structures*, 27(3):397–409, 2005.

[49] S R Shiradhonkar. *Seismic damage categorisation and {Damage} {Index} for {Reinforced} {Concrete} {Buildings}*. {PhD} Thesis, Department of Civil Engineering, {IIT} Bombay, Mumbai, India, aug 2016.

[50] Ajay Singhal and Anne S Kiremidjian. Method for probabilistic evaluation of seismic structural damage. *Journal of Structural Engineering*, 122(12):1459–1467, 1996.

[51] Ravi Sinha and Alok Goyal. A national policy for seismic vulnerability assessment of buildings and procedure for rapid visual screening of buildings for potential seismic vulnerability. *Department of Civil Engineering, Indian Institute of Technology, Bombay, India*, 2004.

[52] Ravi Sinha and Saurabh Shiradhonkar. Validation of Seismic Damage States for Reinforced Concrete Buildings, 2014.

[53] MR Tabeshpour, A Bakhshi, and AA Golafshani. Vulnerability and Damage Analysis of Existing Buildings. *proc. of 13th World ...*, (1261), 2004.

[54] Hatem Tagel-Din. A new efficient method for nonlinear, large deformation and collapse analysis of structures, 1998.

[55] H Tanaka. *Effect of lateral confining reinforcement on the ductile behaviour of reinforced concrete columns*. PhD thesis, University of Canterbury, 1990.

[56] Klaus Gregor Topole and Norris Stubbs. Non-destructive damage evaluation of a structure from limited modal parameters. *Earthquake Engineering & Structural Dynamics*, 24(11):1427–1436, 1995.

[57] N V Tue and N\DJ Tung. A new model for concrete in compression considering the growth of the damage zone. In *Proceedings of the Thirteenth East Asia-Pacific Conference on Structural Engineering and Construction (EASEC-13)*, pages B—-6. The Thirteenth East Asia-Pacific Conference on Structural Engineering and Construction (EASEC-13), 2013.

[58] Fumiaki Uehan. Development of the u-doppler non-contact vibration measuring system for diagnosis of railway structures. *Quarterly Report of RTRI*, 49(3):178–183, 2008.

[59] Fumiaki Uehan and Kimiro Meguro. Assessment of seismic damage to railway structures using applied element method and microtremor measurement. In *13th World Conference on Earthquake Engineering Vancouver, BC, Canada August*, pages 1–6, 2004.

[60] William P. Vafakos, Frank Romano, Joseph Kempner, Bernd Caesar, and Joerg Peter. Direct update of dynamic mathematical models from modal test data. *AIAA Journal*, 25(11):1494–1499, 1987.

[61] J B M Van Mier. Strain-softening of Concrete under Multiaxial Loading Conditions, PhD thesis. pages 1–244, 1984.

[62] Jan G M Van Mier. Multiaxial strain-softening of concrete - Part I: Fracture. *Materials and Structures*, 19(3):179–190, 1986.

[63] C E Ventura, H G L Prion, C Black, K M Rezai, and V Latendresse. Modal properties of a steel frame used for seismic evaluation studies. *Proceedings of the International Modal Analysis Conference - IMAC*, 2:1885–1891, 1997.

[64] RA René Vonk. Softening of concrete loaded in compression. 1992.

[65] Liang Wang and Tommy HT Chan. Review of vibration-based damage detection and condition assessment of bridge structures using structural health monitoring. QUT Conference Proceedings, 2009.

[66] Benedikt Weber and Patrick Paultre. Damage Identification in a Truss Tower by Regularized Model Updating. *Journal of Structural Engineering, ASCE*, 136(3):307–316, 2010.

[67] Raymond C Wilson. Relation of Arias intensity to magnitude and distance in California. Technical Report September, US Geological Survey,, 1993.

[68] A Yin, CS Dubey, TK Kelty, George E Gehrels, CY Chou, M Grove, and O Lovera. Structural evolution of the arunachal himalaya and implications for asymmetric development of the himalayan orogen. *Current Science*, 90(2):195–200, 2006.

[69] Jinjiang Zhang, M Santosh, Xiaoxian Wang, Lei Guo, Xiongying Yang, and Bo Zhang. Tectonics of the northern himalaya since the india–asia collision. *Gondwana Research*, 21(4):939–960, 2012.

Appendices

Appendix A

Compression Size Effects on Concrete Cube

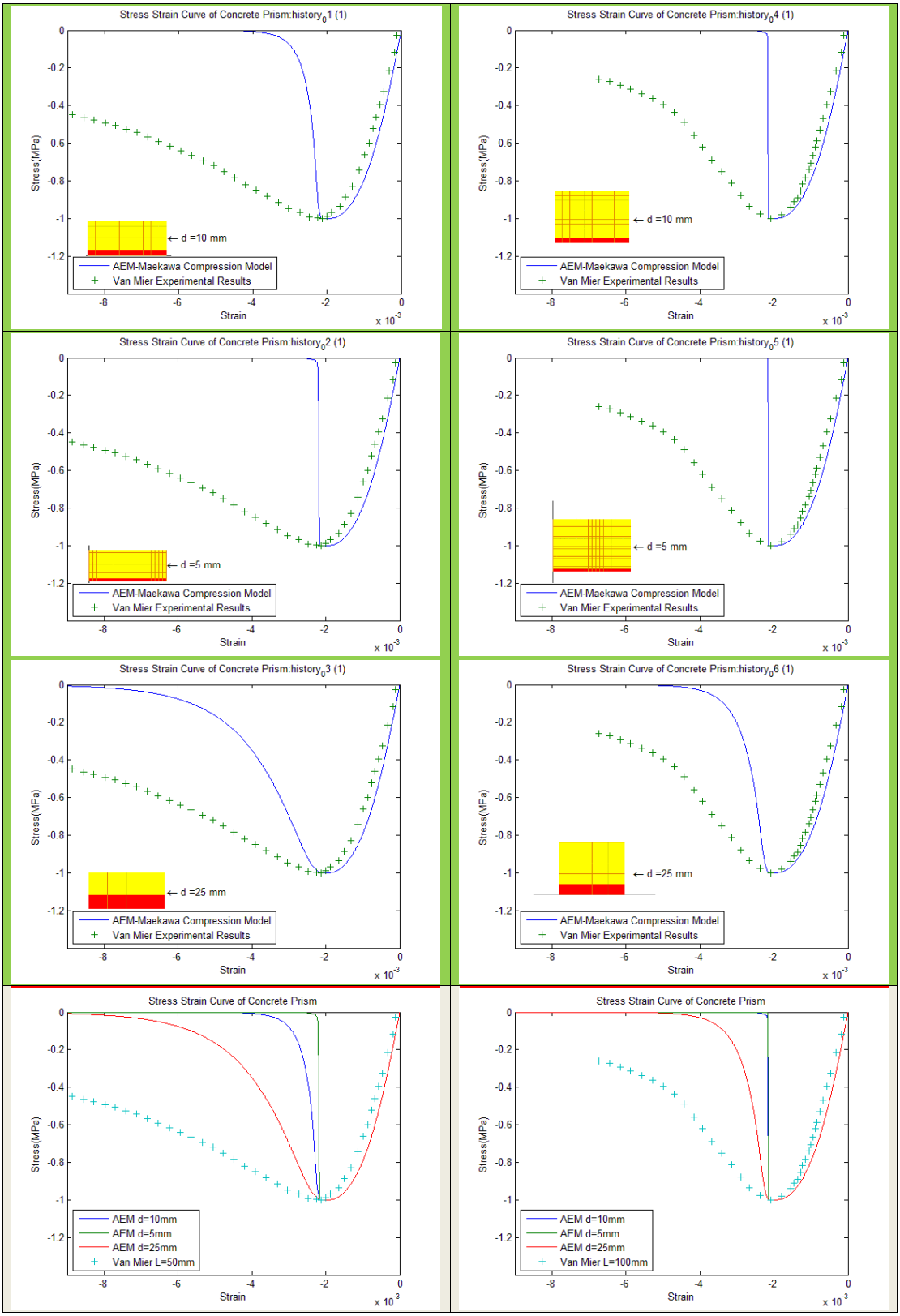

Figure A.1: Concrete cube compression modelling with Maekawa [34] material model part 1

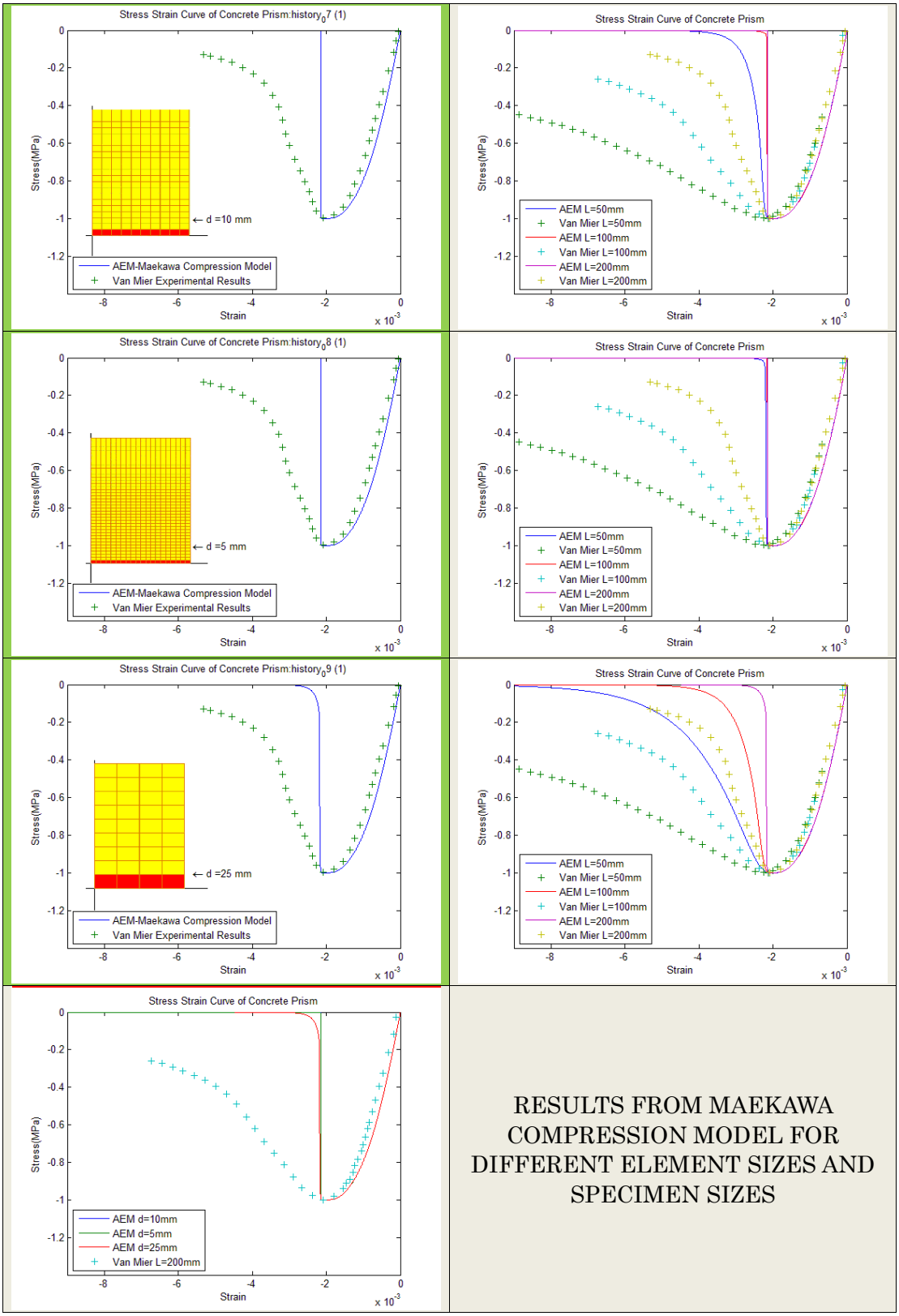

Figure A.2: Concrete cube compression modelling with Maekawa [34] material model part 2

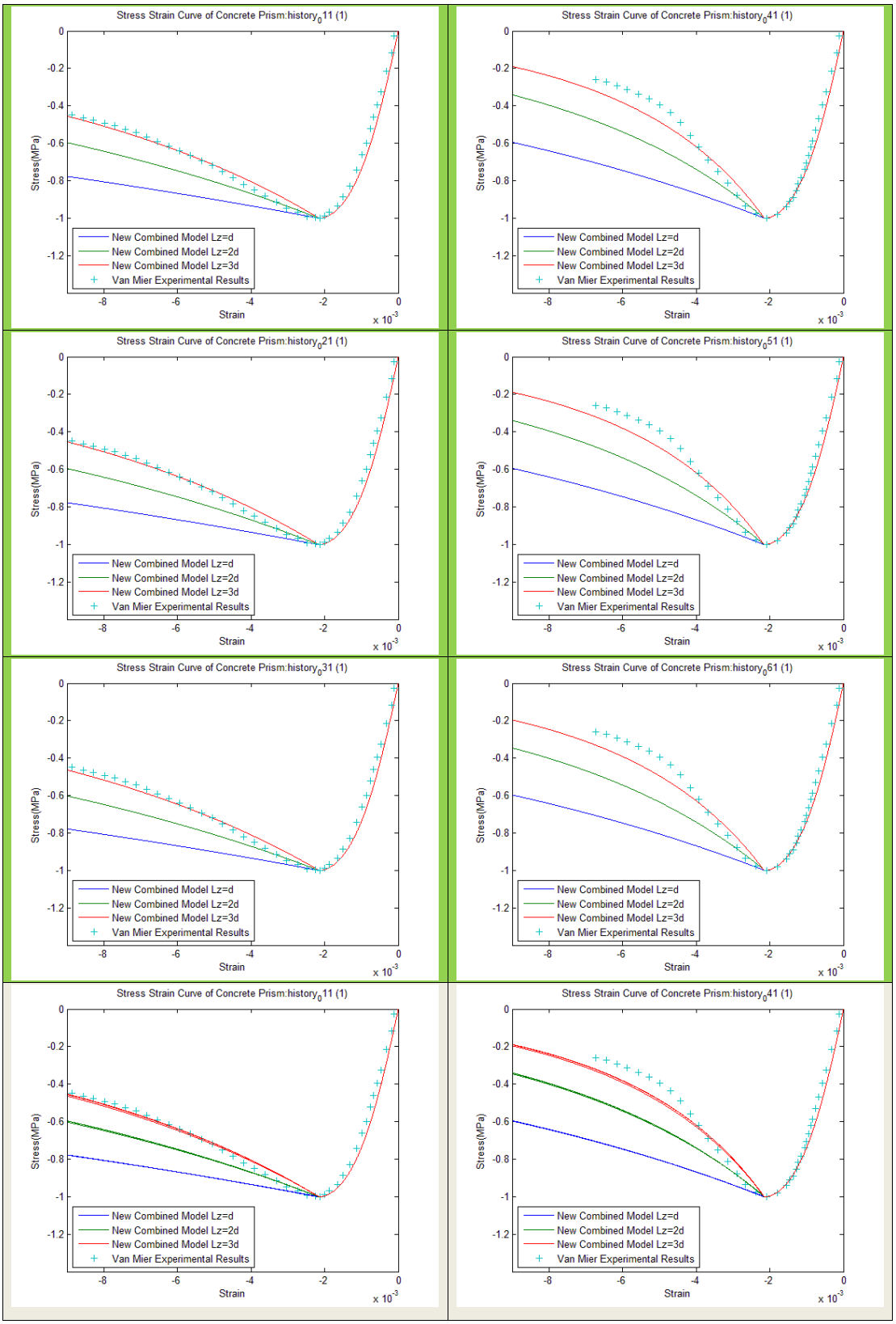

Figure A.3: Concrete cube compression modelling with combined material model part 1

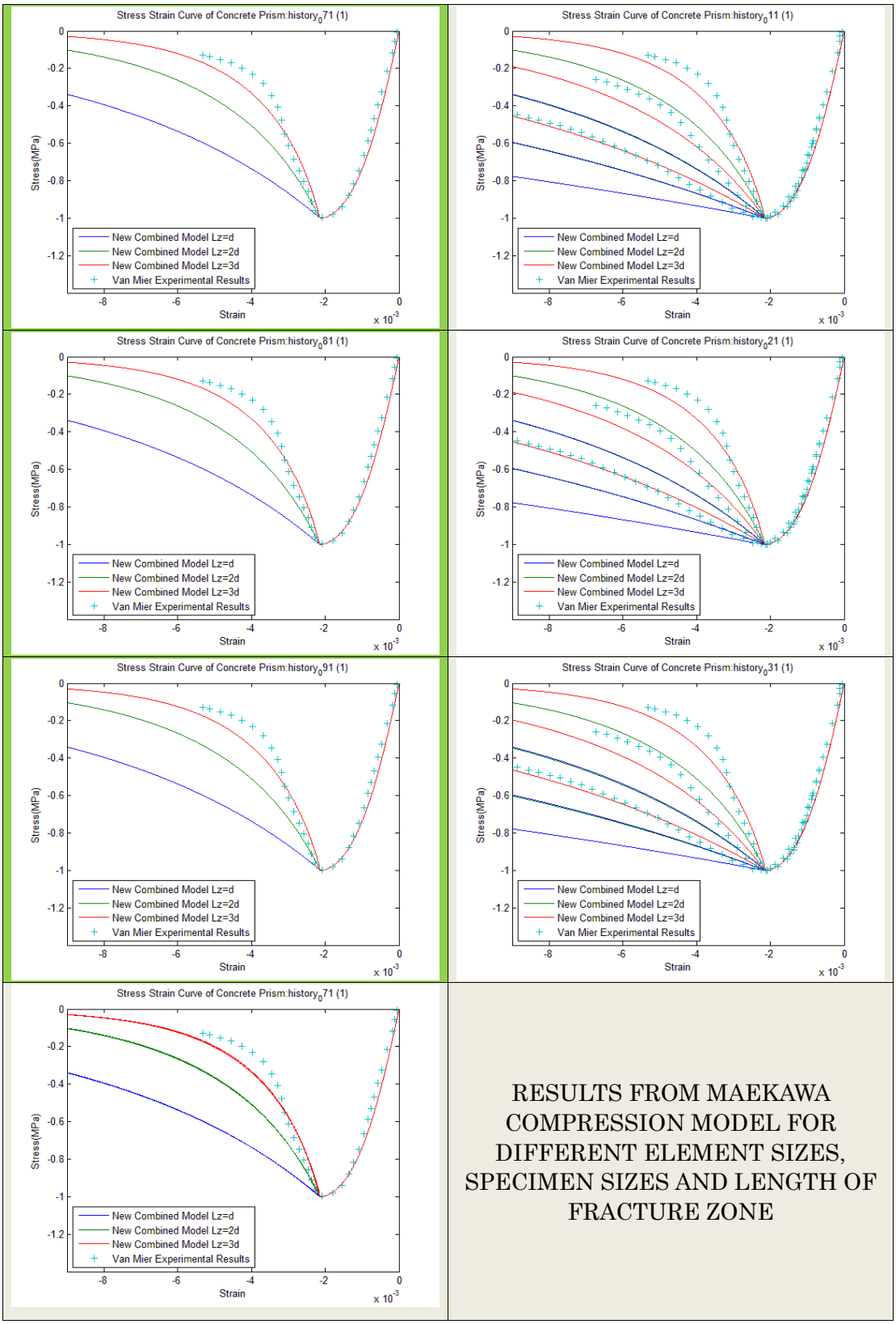

Figure A.4: Concrete cube compression modelling with combined material model part 2

Appendix B

Glossary

B.1 Definitions

Fracture Energy In this research, it is the amount of energy required or released in causing a failure in tension or compression zone in concrete.

Experimental Modal Analysis (EMA) Modal analysis is the process of extracting the dynamic characteristics (Natural Frequencies, Mode Shapes, Damping) of a vibrating system from frequency response function.

Modal Identification It is the process of identification of natural frequencies and modes shapes in a system using experimental or operational modal analysis techniques.

Material Identification It is the process of identification of material properties, damage or reduction of stiffness from the initial state of the structure.

System Identification The field of system identification uses statistical methods to build mathematical models of dynamical systems from measured data.

Aliasing This is an error associated due to the misinterpretation of wrong frequencies due to slow sampling rate.

Leakage Error in Fourier Transform of incomplete signals. This is corrected by applying windowing techniques.

Offset It is an error in acceleration readings due to zero correction or improper calibration.

Transfer Function The transfer function is defined as the ratio of the Laplace transform of the output to the input of the system.

Frequency Response Function (FRF) It is a special case of transfer function in frequency domain. It is obtained by taking the ratio of Fourier transform of output and input.

Fast Fourier Transform (FFT) It is an algorithm to compute Discrete Fourier Transform. There are many algorithms to compute, but an algorithm named 'Coley-Tookey Algorithm' is used in this study

Power Spectral Density (PSD) PSD shows the strength of variations (energy) of a signal over time. Mathematically, PSD is the Fourier Transform of autocorrelation function. Units: Energy/Frequency

Singular Value Decomposition(SVD) It is the factorization of a matrix of the form: A=U*S*V . Here S is similar to eigen value and U is similar to eigen vector in real or complex domain.

Calibration Constant The calibration constant is the coefficient used to convert the strain value acquired by a strain gauge transducer due to a physical quantity

Band-Stop Filter In signal processing, a filter removes unwanted component from a signal. A band-stop filter rejects some particular frequencies.

White Noise or Broadband Random In signal processing, white noise is a random signal with a constant power spectral density.

Appendix C

Nepal Field Study

(a) Building 2 and its corresponding damaged state in the field study conducted in Nepal

(b) Building 7 and its corresponding damaged state in the field study conducted in Nepal

Building2 Building 2 was a school building and a corner column was selected for monitoring in it. It is a two storey frame with masonry infill and the construction is still in progress.

Building7 Building 7 was significantly damaged locations in this building was surveyed.

(a) Building 9 and its corresponding damaged state in the field study conducted in Nepal

(b) Building 11 and its corresponding damaged state in the field study conducted in Nepal

Building9 Building 9, residential building surveyed at the central location

Building11 Building 11 belonged to NSET office in Dolkha, the building had a few mild cracks in the masonry column connections. There were few cosmetic cracks as well

Building12 Building 12 had many cracks on the basement storey over the non structural components such as walls

Building13 Building 13 had mild cracks on the masonry portion of it and the building was extremely weak and had many non engineered components in the building. This building looked very soft.

Building17 Building 17 belonged to a structural engineer from NSET (organization for seismic safety in Nepal), and it had good compliance with the code.

(a) Building 12 and its corresponding damaged state in the field study conducted in Nepal

(b) Building 13 and its corresponding damaged state in the field study conducted in Nepal

Figure C.4: Building 17 and its corresponding damaged state in the field study conducted in Nepal